Mid-to-Late Holocene Climate and Ecological Changes over Europe

A Dissertation

Submitted in Partial Fulfilment of the

Requirements for the Degree of Doctor rerum naturalium (Dr. rer. nat.)

to the Department of Earth Sciences

of the Freie Universität of Berlin

by

Emmanuele Russo

Berlin, September 2016

Supervisor: Prof. Dr. Ulrich Cubasch
Institut für Meteorologie
Freie Universität Berlin
Second examiner: Prof. Dr. Wiebke Bebermeier
Institut für Geographische Wissenschaften
Freie Universität Berlin

Date of the viva voce/defense: 14.12.2016

Publications

Large portion of Chapter 3, 4 and 5 have been published in the following paper:

- Mid-to-late Holocene Temperature Evolution and Atmospheric Dynamics over Europe in Regional Model Simulations. **E. Russo**, U. Cubasch.
  Climate of the Past, 12, 1645-1662, doi:10.5194/cp-12-1645-2016, 2016.

The contents of Chapter 7 are adapted from the following paper:

- Eneolitic Textile Production and Climate Change in Southern East Europe. A. Grabundzija., **E. Russo**.
  Documenta Prehistorica, 43, 301-326, doi:10.4312/dp.43.15, 2016.

Additionally, the results of the thesis have contributed to the following works:

- Notes for a Political Ecology of Non-Sedentary People. R. Bernbeck, U. Cubasch, A. Gass, E. Kaiser, H. Parzinger, S. Pollock, J. Rowland, **E. Russo**, W. Schier, G. Tassie.
  e-TOPOI. Journal for Ancient Studies, Special Volume 6: Space and Knowledge, 45-73, 2016.

- Towards modeling the regional rainfall changes over Iran due to the climate forcing of the past 6000 years. B. Fallah, S. Soudoudi, **E. Russo**, U. Cubasch, I. Kirchner.
  Quaternary International, doi:10.1016/j.quaint.2015.09.061, 2015.

Abstract

In recent years interest has increased concerning the possible consequences of human-induced climate change. In order to produce more reliable predictions of future changes and their possible effects, with the aim of designing successful mitigation and adaptation policies, the study of the past is of fundamental importance.

In this thesis, climate and ecological changes that characterized Europe during the mid-to-late Holocene (from 6000 years before present to the pre-industrial period) are investigated. For this purpose, an experimental framework, consisting of regional and global climate models, vegetation models and proxy records, is developed. Beside investigating natural past climate variability, one of the main goals of the research is the study of possible consequences that such changes had on the civilizations inhabiting the European region. Knowing the impact of climate changes on past civilizations, and the way they reacted to it, constitutes an important reference for the future.

In the first part of the thesis, several simulations with three climate models at different spatial resolutions are designed. Particular attention is paid to the description and reconstruction of the mid-to-late Holocene natural climate forcings.

Then the importance of highly resolved simulations for the investigation of past climate change is investigated. Results show that, for certain parameters, such as near surface temperature, the advantages of the use of Regional Climate Models (RCMs) are noticeable.

Consequently, the research focuses on the study of the evolution of seasonal temperature values during the mid-to-late Holocene, as simulated by an RCM and as derived from proxy-reconstructions. Results show that the model is able to reproduce the winter temperature trend reconstructed from proxy-data over part of the domain. However, no significant trend is evident over northern Europe in the model results, while reconstructions show progressively cooling conditions. The reason for the mismatch is a wrong representation of changes in atmospheric circulation by the model. More specifically, proxies suggest a more positive phase of the North Atlantic Oscillation (NAO) at the mid-Holocene, which the model fails to reproduce. In summer, model results show an uniform decreasing trend over the entire European domain, as a direct response to changes in insolation. Proxies, while presenting a similar behaviour over northern Europe, are characterized by an opposite increasing trend over southern Europe. Analyses show that, in this case, the reason for the mismatch is a wrong representation of soil-atmosphere interaction in the model.

Successively, the results of the RCM simulations are used as input for a bio-equilibrium vegetation model, in order to investigate changes in the distribution of European vegetation during the mid-to-late Holocene. In this manner, a different perspective for the evaluation of the climate simulations is considered. The main feature arising in this case is a spread of dry vegetation over southern Europe at the mid-Holocene, not evident in proxy reconstructions. This is consistent with generally warmer conditions simulated by the RCM over the area.

Finally, the results of the different model simulations are used for their application in archaeological case studies. The advantage of the developed framework is that the outcomes of the different models can be selected and used according to the specific research question addressed. A study on the influence of climate changes on the prehistoric textile revolution in the Pannonian Plain, a region of Central Europe, is presented here. Employing the results of a transient continuous simulation with a coupled Atmosphere Ocean General Circulation Model (AOGCM), possible correlations between changes in the textile production of the populations inhabiting the area, and changes in seasonal climate and ecological conditions, are presented.

This work represents not only a valuable example of multidisciplinary research, but also a robust reference for further investigations, providing at the same time a significant contribution to the debate on the climate and ecological changes that characterized Europe during the mid-to-late Holocene.

Abstrakt

In den vergangenen Jahrzehnten ist das Interesse daran gestiegen, die möglichen Auswirkungen des anthropogenen Klimawandel auf den Menschen genauer zu untersuchen. Um zuverlässigere Vorhersagen zukünftiger Veränderungen und ihrer Auswirkungen mit dem Ziel zu untersuchen, erfolgreiche Minderungs- und Anpassungsmaßnahmen durchzuführen, ist die Erforschung der vergangener Klimaänderungen von grundlegender Bedeutung.

In dieser Arbeit werden klimatologische und ökologische Veränderungen untersucht, die den Europäischen Raum während des mittleren bis späten Holozäns (von vor 6000 Jahren bis zum vorindustriellen Zeitalter) kennzeichnen. Zu diesem Zweck wird eine Modellkette berechnet, bestehend aus regionalen und globalen Klimamodellen, Vegetationsmodellen und Proxy-Aufzeichnungen. Neben der Untersuchung der natürlichen Klimavariablilität in der Vergangenheit, ist eines der Hauptziele die Untersuchung der möglichen Konsequenzen, die solche Veränderungen auf die Zivilisationen im Europäischen Raum. Die Kenntnis der Auswirkungen von Klimaänderungen auf vergangene Zivilisationen und die Art, wie diese darauf reagierten, stellt eine wichtige Referenz für die Zukunft dar.

Im ersten Teil der Arbeit werden Simulationen mit drei Klimamodellen mit unterschiedlichen räumlichen Auflösungen untersucht. Besondere Aufmerksamkeit wird der Rekonstruktion des externen Strahlungsantrieb im mittleren bis späten Holozäns gewidmet.

Die Ergebnisse von Simulationen mit regionalen Klimamodellen (RCMs) zeigen, dass für bestimmte Parameter wie beispielsweise bodennahe Temperatur die Vorteile der Verwendung von hochaufgelösten Modellen deutlich sichtbar sind.

Der darauf folgende Teil der Arbeit konzentriert sich auf die Untersuchung der Entwicklung von saisonalen Mitteltemperaturen während des mittleren bis späten Holozäns, wobei RCM-Simulationen und Proxy-Rekonstruktionen miteinander verglichen werden. Die Ergebnisse zeigen, dass das RCM in der Lage ist, die Temperaturtrends im Winter in den Proxy-Daten in Teilen des Modellgebiets zu reproduzieren. Über Nordeuropa sind jedoch im RCM keine signifikanten Trends sichtbar, während die Rekonstruktionen eine Abkühlung zeigen. Der Grund für die Diskrepanz ist eine fehlerhafte Darstellung von Veränderungen der atmosphärischen Zirkulationsmuster durch das Modell. Proxydaten deuten auf eine positivere Phase der Nordatlantischen Oszillation in der Mitte des Holozäns hin, die das Modell nicht reproduziert. Im Sommer zeigen die Modellergebnisse einen einheitlich negativen Trend im gesamten europäischen Modellgebiet als eine direkte Reaktion auf die veränderte Einstrahlung. Während die Proxydaten ein ähnliches Verhalten über Nordeu-

ropa zeigen, sind sie durch einen entgegengesetzten positiven Trend über Südeuropa gekennzeichnet. Analysen zeigen, dass in diesem Fall der Grund für die Unterschiedlichen Trends in Modell- und Proxydaten eine fehlerhafte Darstellung von Boden-Atmosphäre-Wechselwirkungen im Modell ist.

Im nächsten Schritt werden die Ergebnisse der RCM-Simulationen als Antrieb für ein Vegetationsmodell verwendet, um Veränderungen in der räumlichen Verteilung der Vegetation in Europa während des mittleren bis späten Holozäns zu untersuchen. Das Hauptmerkmal der Ergebnisse ist eine Ausbreitung der trockenen Vegetation in Südeuropa in der Mitte des Holozäns, die in den Proxydaten jedoch nicht ersichtlich ist. Die trockenere Vegetation ist im Einklang mit den eher wärmeren Bedingungen die im RCM in dem Bereich simuliert werden.

Im letzten Schritt werden die Ergebnisse der verschiedenen Modellsimulationen in archäologischen Fallstudien angewendet. Der Vorteil des entwickelten Modell-Frameworks ist, dass die Ergebnisse der verschiedenen Modelle entsprechend der spezifischen Fragestellung ausgewählt und verwendet werden können. Hier wird eine Studie über den Einfluss von Klimaänderungen auf die prähistorische Textil-Revolution in der Pannonischen Tiefebene, einer Region Zentraleuropa, vorgestellt. Die Ergebnisse einer transienten kontinuierlichen Simulation mit einem gekoppelten Ozean-Atmosphäre-Zirkulationsmodell zeigen eine mögliche Korrelation zwischen Veränderungen in der Textilproduktion der Bevölkerung, die das Gebiet besiedeltes und Veränderungen im saisonalen Klima und den vorherrschenden ökologischen Bedingungen.

Insgesamt ist diese Arbeit ist nicht nur ein wertvolles Beispiel für multidisziplinäre Forschung, sondern auch eine robuste Referenz für weitere Untersuchungen. Die Ergebnisse sind ein wichtiger Beitrag zur Debatte über die klimatologischen und ökologischen Veränderungen, die Europa während des mittleren bis späten Holozäns kennzeichneten.

Contents

Title Page **i**

Abstract **v**

Table of Contents **ix**

1 Introduction **1**

2 The Climate of the Past: a Key for the Future **7**
2.1 Introduction 7
2.2 Climate Forcings and their Changes during the Holocene . . . 8
2.2.1 Orbital Forcings 8
2.2.2 Solar Activity 10
2.2.3 Greenhouse Gases 12
2.2.4 Volcanic Eruptions 14
2.3 Climate Models as a Tool for Paleoclimate Reconstructions . . 16
2.4 The Time Slice Technique and Dynamical Downscaling 17

3 Paleoclimate Simulations **19**
3.1 Introduction 19
3.2 The ECHO-G and a Continuous Transient Paleo-Simulation . 20
3.3 ECHAM5 Simulations 22
3.4 Comparison and Validation of Global Simulations 23
3.5 Setup of the Regional Climate Model
CCLM for Paleoclimate Studies 24
3.5.1 Parameterizations and Initial Conditions 24
3.5.2 Climate Forcings 28
3.5.3 Performance of the Regional Simulations and Validation of the Results 30
3.6 Conclusions 33

4 The Added-Value of a Regional Climate Model for Paleoclimate Studies 39
4.1 Introduction . . . 39
4.2 Added Value, RCMs and Climate Change . . . 40
4.3 Pollen-Based Reconstructions . . . 42
4.4 Models-Proxies Comparison . . . 44
4.4.1 Qualitative Analysis . . . 44
4.4.2 Quantitative Analysis . . . 47
4.5 Conclusions . . . 50

5 Mid-to-Late Holocene Temperature Evolution and Atmospheric Dynamics over Europe in Regional Simulations 53
5.1 Introduction . . . 53
5.2 Changes in Insolation and Temperature Evolution . . . 54
5.3 Methods . . . 56
5.4 Model and Proxies Behaviour . . . 57
5.5 Changes in Atmospheric Circulation . . . 61
5.6 Other Modelling Studies . . . 66
5.7 Conclusions . . . 68

6 Mid-to-Late Holocene European Vegetation Changes 69
6.1 Introduction . . . 69
6.2 Biomes and Plant Functional Types . . . 70
6.3 Reconstructions of the Mid-to-Late Holocene European Vegetation . . . 71
6.3.1 Reconstructed Patterns . . . 73
6.3.2 Human Impact . . . 74
6.4 The BIOME4 Model . . . 75
6.4.1 Model Structure and Development . . . 75
6.4.2 Experimental Setup . . . 77
6.5 Results . . . 81
6.5.1 Present Day . . . 81
6.5.2 Mid-to-Late Holocene . . . 81
6.6 Conclusions . . . 85

7 A Case Study: Climate Trends Changing Threads in the Prehistoric Pannonian Plain 87
7.1 Introduction . . . 87
7.2 Scope of the Study . . . 88
7.3 Flax Fibres and Early Wool: Prehistorical Evidences for Their Use and Development in the Context of Textile Production . . . 90

7.4 Methodology 92
7.4.1 Spindle-Whorls 92
7.4.2 Climate Simulations 96
7.5 Results 96
7.5.1 Adapting Technologies 96
7.5.2 Climate Conditioning 100
7.6 Discussion and Conclusions 103

8 Conclusions and Outlook **107**
8.1 Conclusions 107
8.2 Perspectives and Future Work 110

Dedicated to
my grandmother Maria, lijepa moja dušiza

Chapter 1

Introduction

"we find no vestige of a beginning, no prospect of an end"
- James Hutton -

Climate has a direct effect on all living organisms and so has always, and always will have an influence on human life (Riede, 2014; Weiss and Bradley, 2001; Wigley et al., 1985). From antiquity to present day human life and civilization have been affected by the availability of natural resources such as water, food, construction material, etc. In this way the flourish or the collapse of a society has often been related with the impact of climate change. Changes in climate are at least partly responsible for the rise and fall of many ancient civilizations (Cullen et al., 2000; Fagan, 2008; Haug et al., 2003; Weiss, 1997; Wigley et al., 1985; Zhang et al., 2007). When analysing the course of economic, social and political changes in past times, the impact of climatic fluctuations and changes has been recognised as one of the factors that requires particular consideration, though there has always been dispute about just how much attention needs to be paid to this variable (Brooke, 2014; Van de Noort, 2011; Wigley et al., 1985). In general, the real issue is not whether climate has had an influence, but just what that influence was and whether it was of any real significance. Any historical interpretation that denies the potential of individuals, or groups of individuals, to influence history, is surrealistic. Nevertheless, such influences occur within the context of geography and climate, and any denial of the consequences of this are equally insupportable (Brooke, 2014; Wigley et al., 1985). In this context, paleoclimatology, by investigating the distribution in space and time of the climates of the past, has indeed a relevant part to play.

In the present work, we attempt to add to the physical understanding of natural climate and ecological variability during the mid-to-late Holocene, the period that goes from 6000 years Before Present (BP) to the beginning of

the anthropocene[1] (ca. 200 years ago), a study of its possible consequences on the development of European civilization and history, focusing on particular case studies. Even though Europe is the main area of research, the results allowed, in some cases, to focus also on other regions.

Research Questions

Earth history is ruled by glacial-interglacial cycles with different returning periods. Changes in insolation distribution due to variations in the Earth's orbit around the Sun are considered the dominant drivers of glacial-interglacial cycles throughout the Quaternary (i.e. the current ice age, covering the last 2.8 million years) (Hays et al., 1976; Imbrie et al., 1992; Milanković, 1941). The last glacial period had his peak around 21000 years BP. Then, changes in the orbital configuration of the Earth's around the Sun led to the end of the glacial period and to the beginning of the current interglacial, known as the Holocene, at approximately 11500 BP.

During the Early Holocene, between roughly 11500 and 9000 BP, the exposure of the poles to the Sun due to the Earth's tilt was the maximum possible. Exactly at the same time the orbital precession led the Earth in summer to the closest possible distance from the Sun. This represented the maximum of the Earth's solar exposure in the postglacial period, followed a few millennia later by the peak of the interglacial warmth, also known as *mid-Holocene thermal optimum* ($\sim$ 7000 BP) (Brooke, 2014). The high values of the tilt of the Earth's led to an extreme seasonal variability to the northern latitudes during the early Holocene, with particularly warm summers and cold and stormy winters in the Northern Hemisphere (NH). During the same period summer mega-monsoons watered north Africa, Arabia, the eastern Mediterranean, the Indian subcontinent, and southern China. Additionally, with the warm-up of the early Holocene, the North Atlantic Oscillation (NAO) shifted toward a strongly positive mode, causing warmer winter temperatures and moisture advection to northern Europe (Brooke, 2014).

Successively, during the mid-to-late Holocene (from approximately 7000 BP to present days), the Earth changed its precessional seasonality and wobble. Summer insolation progressively declined in the NH, with the regions along the 60^o north latitude line receiving today about seven percent less solar radiation during the summer than they would have 10000 years ago (Brooke, 2014). Conversely, insolation rose in the Southern Hemisphere (SH), leading

[1]Historical period when human activities began to have a significant global impact on Earth's geology and ecosystems.

to a southward shift of the entire array of climate systems, and ending the Early Holocene epoch of mega-monsoons (Brooke, 2014).

Particular importance during the mid-to-late Holocene is gained by Europe, both climatologically, due to the mentioned changes, and historically, since starting from 7000 years BP Europe has seen the blooming of different cultures and races that have played a fundamental role in the development of modern civilizations. With the goal of investigating possible changes in European climate during the mid-to-late Holocene and gaining further insights on the drivers of such changes, in the first part of our research we developed an experimental framework consisting of global and regional climate models at different resolutions.

Other studies have employed climate models in order to investigate European climate changes during the mid-to-late Holocene (Bonfils et al., 2004; Braconnot et al., 2007a,b; Fischer and Jungclaus, 2011; Masson et al., 1999). In many cases, unfortunately, the spatial resolution of these models was not high enough in order to understand the impact of simulated data on a regional scale. The improvement in resolution of climate models has always been mentioned as one of the most important factors when investigating past climatic conditions, especially in order to evaluate and compare the results against proxy data. Despite this, only a few studies have tried to directly estimate the possible advantages of highly resolved simulations for the study of past climate change.

Motivated by such considerations, we pose the following research question:

1. How do climate models perform in comparison with proxy reconstructions, according to their spatial resolution? Based on this comparison, what are the possible advantages of the use of a regional climate model for paleoclimate studies?

During the mid-to-late Holocene, over northern latitudes in general, as a consequence of significant changes in the seasonal cycle of insolation, relevant variations in the seasonal values of surface variables would have been expected. However, evidence has shown that reconstructed climatic parameters, such as surface temperature, over Europe, did not always follow directly the astronomical forcings (Bonfils et al., 2004; Braconnot et al., 2007a; Cheddadi et al., 1996; Davis et al., 2003; Mauri et al., 2014). Their signal seems to have also been influenced by other complex processes such as atmospheric circulation, geography, or land-surface interactions with the atmosphere. Using a compilation of European reconstructions (Mauri et al., 2014) and focusing our attention on near surface temperature and the regional climate model results, we additionally pose the following research questions:

2. What is the development of the mid-to-late Holocene European seasonal temperature cycle towards present day conditions? Which processes is it related to?

3. What is the main behaviour of the simulated mid-to-late Holocene temperature over Europe? What are the reasons for possible mismatches with reconstructions?

The climatic changes that interested Europe during the mid-to-late Holocene had a direct effect on every component of the biosphere. In particular, the vegetation distribution and composition changed in time. The profound modifications in the climatic conditions, the retreat of the ice sheets and the changes in temperature and in precipitation patterns had a strong impact on different areas and led to a radical modification of the land cover. Aware of these effects, we focus our attention on another research question:

4. What were the changes in vegetation distribution during the mid-to-late Holocene in Europe? How is the developed experimental framework able to reproduce such changes?

Knowing the relationship between specific climate conditions and the growth of different species of plants for present times, we use a bioecological equilibrium model in order to obtain the distribution of different plant functional types during the mid-to-late Holocene, according to the simulated climate conditions.

Climate and ecological changes are frequently used as an explanation for events in the archaeological record. Events such as the abandonment of a region previously occupied, the occupation of a region presently uninhabitable, the sudden changes in population size, and the introduction of new agricultural crops or techniques, may be related to local environmental changes and ultimately to changes in climate. The data reconstructed by the employment of climate and vegetation models can be an useful tool in order to evaluate whether changes in climatic and ecological conditions had any influence on the development of different past societies. For this reason, the question that we raise at the end of our research is:

5. Are there any relationships between the mid-to-late Holocene climate change and societal changes over Europe?

Evidence provides little support for a climatic interpretation of the general course of European history. Research may be more usefully directed to the analysis of the effects of changing climate upon particular regions, and of the

nature and costs of nature shock (Wigley et al., 1985). Under these considerations, we focus our investigations on a specific case study. Archaeological evidence suggests that the cultures inhabiting the region of the Pannonian Plain between the late 7th millennium BP and the end of the 5th millennium BP, undertook a technological revolution in the textile production, probably triggered by changing climatic conditions. Using a multidisciplinary approach, joining together climate reconstructions, climate model results, and archaeological evidence, possible explanations in support of the latest hypothesis are proposed.

This thesis is organized into five main chapters. In Chapter 2 details on paleoclimate and paleoclimate modelling are given. Chapter 3 provides a technical description of the climate models setup and their evaluation. In Chapter 4 the results of global and regional climate model simulations for the mid-to-late Holocene are compared against proxy reconstructions. The main goal is to determine the possible added value of regional climate models for their application in paleoclimate studies. Chapter 5 includes the analysis of European mid-to-late Holocene temperature evolution and investigation of possible driving processes. In Chapter 6 changes in the distribution of the mid-to-late Holocene European vegetation are investigated. Successively, Chapter 7 presents the results of the considered archaeological case study. Finally, Chapter 8 is dedicated to conclusions and an outlook of possible future research.

Chapter 2

The Climate of the Past: a Key for the Future

"We must respect the past, and mistrust the present, if we wish to provide for the safety of the future."
- Joseph Joubert -

2.1 Introduction

In recent decades, in the media, attention has increased concerning future climate change, and its possible effects on human beings and on the life on Earth in general. Nowadays, one of the most discussed topics is the estimation of the possible effects of such changes in the near future, and the discrimination of the anthropogenic component. In this context, particular importance is gained by the knowledge of the variability of the climate in the past due to the effects of natural forcings. In fact, without knowing which processes have driven the climate of the past on different time scales, it would be impossible to attempt to predict the climate of the future. With this respect we can affirm that the past is the key for the future.

In this chapter, we provide specific details on the main natural drivers of climate changes, and their evolution during the entire Holocene. In particular, we describe their reconstruction techniques and their possible effects on the climate system. Then, a general overview is given on the importance of climate models for the study of the climate of the past and their contribution to its understanding. Finally, different modelling techniques are introduced.

2.2 Climate Forcings and their Changes during the Holocene

The climate system is a dynamic system in transient balance (McGuffie and Henderson-Sellers, 2005). It counts five main components that are: the atmosphere, the hydrosphere, the cryosphere, the biosphere and the lithosphere and the ensemble of their mutual interactions (Masson-Delmotte et al., 2013). Any factor that causes a sustained change to the amount of incoming/outgoing energy of the climate system is defined as a *climate forcing* and can lead to climate changes. Following the definition of McGuffie and Henderson-Sellers (2005), "a climate forcing is a change imposed on the planetary energy balance that, typically, causes a change in global temperature" .

Climate forcings can be divided into *internal forcings*, including all natural mechanisms within the climate system itself, or *external forcings*, that can either be natural or anthropogenic, like, for example, greenhouse gases emissions related to human activities. For the study of the climate of the past, particular attention needs to be paid to natural forcings (Masson-Delmotte et al., 2013; Wanner et al., 2008).

2.2.1 Orbital Forcings

The main changes in the climate system related to natural forcings are supposed to be related to changes in the Earth's orbit, also known as *Milankovitch cycle*. The main drivers of ice age cycles are thought to be the changes in the seasonal distribution of Sun's radiation reaching the Earth and of its distribution across the globe, due to slight variations in the Earth's orbit (Jansen et al., 2007; Masson-Delmotte et al., 2013; Wanner et al., 2008). These orbital variations have different periods and are three: the changes in the orbital precession, the changes in the tilt of the Earth's axis of rotation and the variation in the Earth's orbit eccentricity (Fig. 2.1).

Earth's orbit around the Sun has the shape of an ellipse of which the Sun occupies one of the foci. Due to gravitational interaction with the other planets, primarily Jupiter, the ecliptic, and consequently the perihelion (the closest point of the Earth's orbit to the Sun) are moved around in space. This *orbital precession* causes a progressive change in the time of the equinoxes, with two main apparent periodicities of 23000 years and 18800 years. This change does not affect the total radiation received by the Earth, but its temporal and spatial distribution (McGuffie and Henderson-Sellers, 2005).

The *obliquity* of the Earth's axis of rotation varies in time from about 22^o

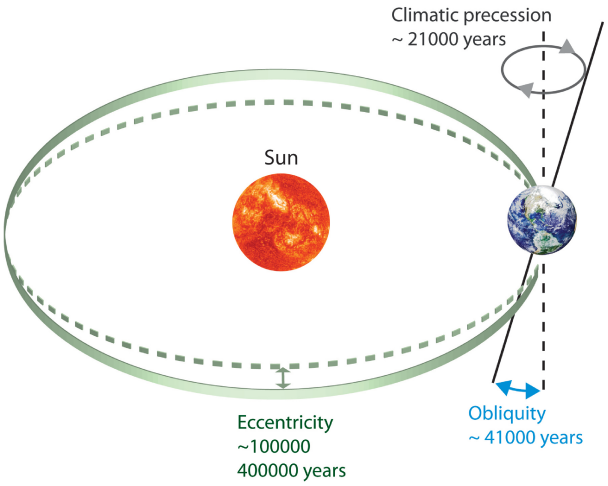

Figure 2.1: *Scheme of the three main Earth's astronomical cycles: the* precession of the equinoxes*, the changes in the* obliquity *of the Earth's axis of rotation and the variation of the orbit's* eccentricity*. Picture adapted from:* http://biocycle.atmos.colostate.edu/shiny/Milankovitch/.

to 24.5^o, with a period of about 40000 years. The current value is 23.5^o. As for the orbital precession, changes in the obliquity do not alter the total received radiation but the range of seasonality and spatial distribution (McGuffie and Henderson-Sellers, 2005).

Changes in the Earth's orbit *eccentricity* represent its third astronomical forcing. The Earth's orbit varies between a more eccentric and a more circular state in a quasi-cyclic way, completing the cycle in about 110000 years. The eccentricity of the orbit has a main influence on the mean annual incident flux. In the last 5 million years, the eccentricity has varied from 0.000483 to 0.060791, resulting in changes in the incident flux of +0.014% to −0.170% from the current value ($\sim +0.19 W/m^2$ and $\sim -2.3 W/m^2$ respectively).

While the Milankovitch forcings can be considered as the drivers of long-term, cyclic climatic changes, the energy distributions within spectral analyses of climate and of orbital variations are different (McGuffie and Henderson-Sellers, 2005). Almost certainly, these external changes trigger large feedback effects in the climate system which are yet to be fully understood (Flückiger et al., 2002; Jouzel et al., 2001; Masson-Delmotte et al., 2013).

Interglacial periods seem to take place in phases with more intense summer solar radiation in the NH (Fig. 2.2). Since the middle Quaternary ($\sim$ 800000 years BP), these glacial-interglacial cycles have had a frequency of approximately 100000 years, occuring only about every fifth peak in the precession cycle (Fig. 2.2) (Masson-Delmotte et al., 2013). Additionally, the five

more recent glacial-interglacial cycles were characterized by more remarkable changes in temperature than the previous ones. The full explanation for this phenomena is still an active area of research. Non-linear processes such as positive feedbacks within the climate system must also be very important in determining when glacial and interglacial periods occur.

The current interglacial, the Holocene, started approximately 12000 years ago. After the last glacial peak around 21000 years BP, insolation started to rise again due to changes in the orbital parameters, reaching its maximum during the early Holocene, approximately 9000 years BP, for then decreasing again. At present we are almost at a relative minimum, but predictions show as probably no glaciation will be triggered before the next 50000 years as a combined effect of human Greenhouse Gases (GHGs) emission and orbital parameters (Berger and Loutre, 2002). This would make the Holocene the longest interglacial of the Quaternary, the period of Earth's history characterized by the onset of NH glaciations approximately 2.8 million years ago (Loutre and Berger, 2003).

2.2.2 Solar Activity

Changes in solar activity are considered to be the second natural driver of climate changes. The Sun activity varies on different timescales. For example, the Sun emitted only 70% of its actual radiation around 4 billion years ago. If we focus on smaller timescales, different cycles characterize the Sun activity, between which the most famous is the 11-year sunspot cycle. Other cycles have periods of 88 (*Gleissberg* cycle), 211 (*Suess* cycle) and 2100 years (*Hallstattzeit* cycle). These cycles show inherent correlation with the number of sunspots, but the reasons are not totally understood at present. The number of sunspots can be reconstructed through analyses of the content of ^{14}C in three ring cellulose (Solanki et al., 2004). In periods of major solar activity (and more sunspots) the stronger solar winds alllow less cosmic rays to reach the Earth atmosphere. Knowing the flux of incoming cosmic rays in the past, it would be possible to reconstruct the solar activity for the same period. The ^{14}C is a radioactive isotope normally used for datation of archaeological samples or proxy data. Its mean-life is approximately 5730 years, and its concentration on Earth should be expected to decrease in a thousand years. Instead, it is mantained almost constant by its continuous production as cosmic rays generate neutrons that in the lower stratosphere and in the upper troposphere in turn create ^{14}C when they strike ^{14}N atoms. Once formed, the ^{14}C reacts with the ozone of the atmosphere creating CO_2 then dissolved in the ocean and taken up by plants via photosynthesis. Knowing the content of ^{14}C in three cellulose and his mean-life,

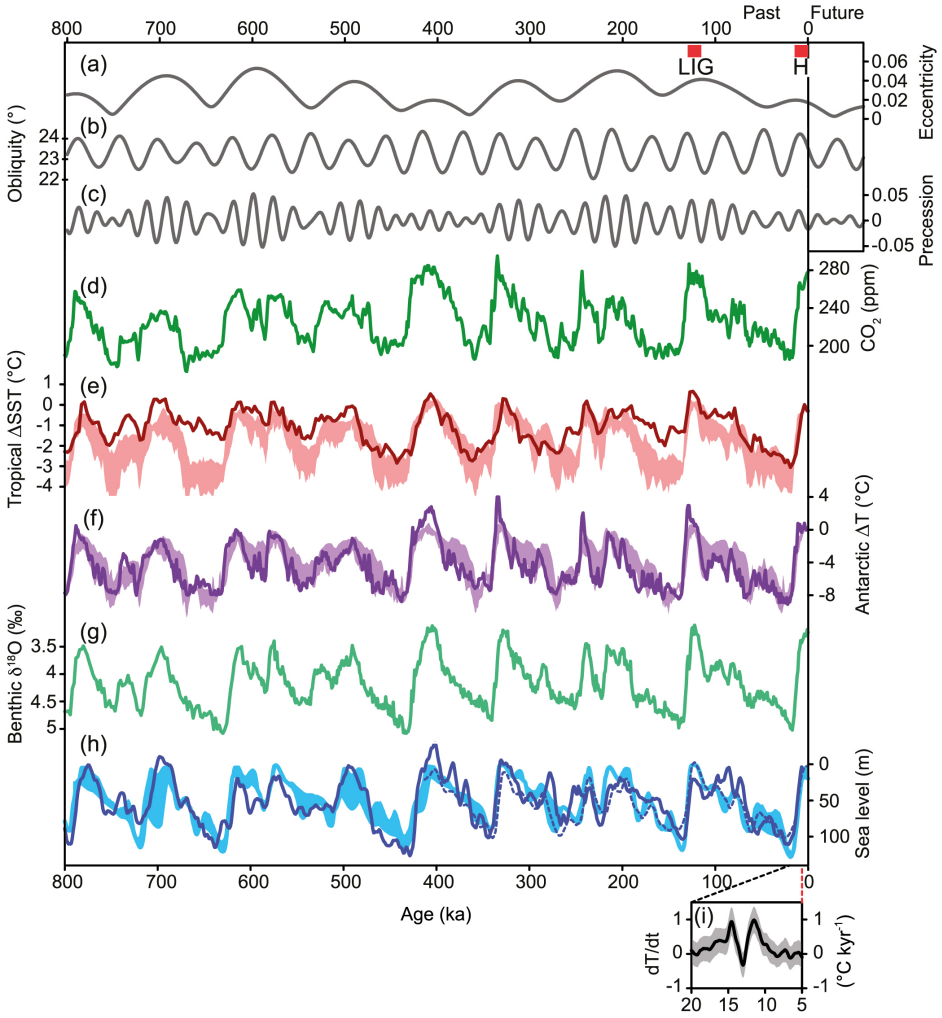

Figure 2.2: *Orbital parameters and proxy records over the past 800000 years. a) Eccentricity. b) Obliquity. c) Precessional parameter (Berger and Loutre, 1991). d) Atmospheric concentration of CO_2 from Antarctic ice cores (Ahn and Brook, 2008; Lüthi et al., 2008; Petit et al., 1999; Siegenthaler et al., 2005). e) Tropical Sea Surface Temperature (Herbert et al., 2010). f) Antarctic temperature based on up to seven different ice cores (Barbante et al., 2006; Blunier and Brook, 2001; Jouzel et al., 2007; Petit et al., 1999; Stenni et al., 2011; Watanabe et al., 2003). g) Benthic $\delta^{18}O$, a proxy for global ice volume and deep-ocean temperature (Lisiecki and Raymo, 2005). h) Reconstructed sea level (dashed line: Rohling et al. (2010); solid line: Elderfield et al. (2012)). Lines represent orbital forcing and proxy records, shaded areas represent the range of simulations with climate models (GENIE-1, Holden and Edwards (2010); Bern3D, Ritz et al. (2011)), climate-ice sheet models of intermediate complexity (CLIMBER-2, Ganopolski and Calov (2011)) and an ice sheet model (IcIES, Abe-Ouchi et al. (2007)) forced by variations of the orbital parameters and the atmospheric concentrations of the major GHGs. i) Rate of changes of global mean temperature during Termination I based on Shakun et al. (2012). Figure from Masson-Delmotte et al. (2013).*

Solanki et al. (2004) reconstructed the Sun activity during the last 11000 years. Damon and Jirikowic (1992) conjectured that in the periods of minor solar activity, like for example the Maunder minimum ($\sim$ 600 years ago), the Sun apparent radius expanded, causing a slight decrease in temperature. For Martin-Puertas et al. (2012), the atmospheric circulation reacted abruptly during past solar minima, and the changes in atmospheric circulation amplified the solar signal causing abrupt climate change (Martin-Puertas et al., 2012). Based on correlations between solar variability and meteorological variables, weaker westerly winds have been observed in winters with a less active Sun, for example at the minimum phase of the 11-year sunspot cycle (Ineson et al., 2011). According to the analysis of their results, Ineson et al. (2011) concluded that low solar activity most likely drives cold winters in northern Europe and the United States, and mild winters over southern Europe and Canada, with little direct change in globally averaged temperature. Based on the correlation between changes in cosmogenic isotopes, solar activity and climate proxy records, different authors supported the idea that solar activity constitutes a possible driver for centennial and millennial variability (Bond et al., 2001; Fleitmann et al., 2003; Karlén and Kuylenstierna, 1996; Wang et al., 2005). The current lack of consistency between various datasets makes it difficult, based on current knowledge, to estimate the real effect of solar variability on millennial time-scale climate variations (Jansen et al., 2007; Wanner et al., 2008).

2.2.3 Greenhouse Gases

Another main natural forcing that during recent days has acquired particular importance, due to the increasing emission trend of the industrial era and its consequences on the climate system, is the concentration of Greenhouse Gases (GHGs) in the atmosphere.

The main part of the solar electromagnetic spectrum is composed of low wavelength radiation, mainly visible and near-visible light (e.g. ultraviolet). One third of the solar radiation that reaches the top of the Earth's atmosphere is reflected back to the space. The remaining is absorbed by the surface and partly by the atmosphere. The Earth behaves as a black body and reemits the absorbed energy at longer wavelengths, primarily in the infrared part of the spectrum. Much of this energy is then absorbed by the atmosphere, causing a warming gradient in the troposphere. This phenomena is called Greenhouse Effect (GE). Carbon dioxide (CO_2), Methane (CH_4) and Nitrous Oxide (N_2O) are the principle GHGs in the atmosphere after the water vapor. Concentration of GHGs in the atmosphere has varied widely during the entire Earth's History. Reconstructed concentration of GHGs from Antarctic ice

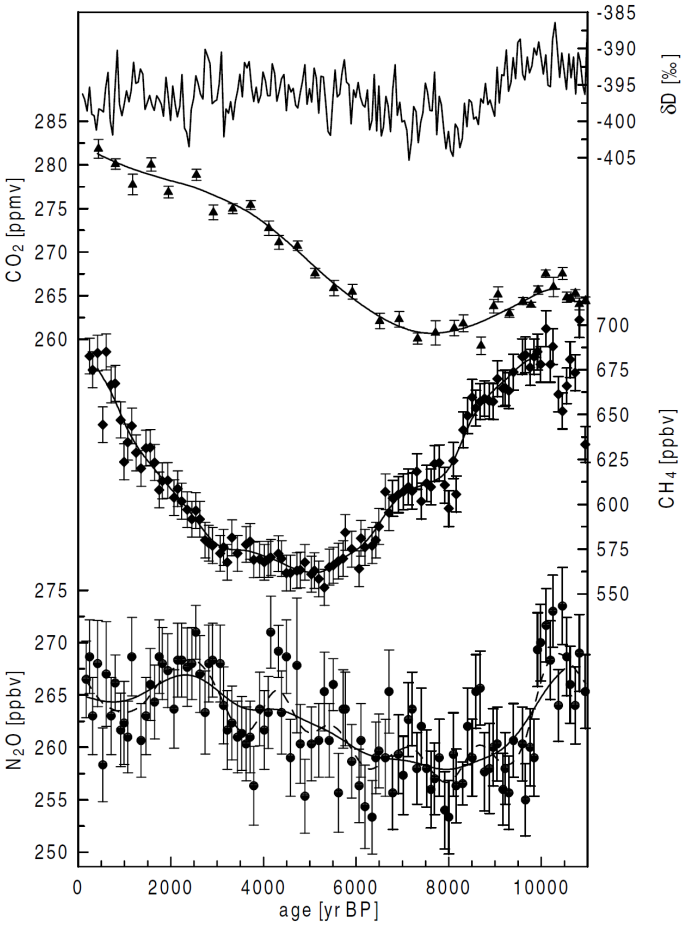

Figure 2.3: *CO_2 (triangles), CH_4 (diamonds), N_2O (circles) records from Flückiger et al. (2002), and deuterium (top trace) records from Jouzel et al. (2001) for the Holocene time period. Figure from: Flückiger et al. (2002).*

cores (Fig. 2.3) has shown that, during the Holocene, variations were small when compared, for example, to glacial-interglacial periods (Flückiger et al., 2002). All the three main GHGs show a concentration decrease in the first part of the Holocene, followed by an increase during pre-industrial time. The lowest value of CO_2 and N_2O is evident between 8000 and 6000 BP , while, for CH_4, the minimum of concentration is between 6000 and 3000 BP (Fig. 2.3) (Wanner et al., 2008).

One of the possible explanations for such trend was proposed by Ruddiman (2003), affirming that anthropogenic land use caused a GHGs anomaly over the last 8000 years.

2.2.4 Volcanic Eruptions

Volcanoes influence climate by injecting large quantities of particulates and gases into the atmosphere, increasing the Earth's albedo, or reflectivity, and cooling the climate. Volcanic eruptions can thereby produce significant temperature anomalies of at least a few tenths of a degree.

Most eruptions inject particulates into the troposphere at heights between 5 and 8 km. These are rapidly removed either by gravitational or rain processes and their effect on climate is in this case minimal. Conversely, debris expelled during more violent eruptions are able to reach the upper troposphere or even the lower stratosphere (15-25 km) (e.g. Mount Agung in 1963, El Chichón in 1982 and Mount Pinatubo in 1991 (Bluth et al., 1992; McGuffie and Henderson-Sellers, 2005; Rampino and Self, 1982; Varekamp et al., 1984)). Even though such eruptions are much less frequent, their effects on climate are likely to be more significant (McGuffie and Henderson-Sellers, 2005).

Large volcanic eruptions, such as the eruption of Mt. Pinatubo in 1991, can cool the surface by around 0.1°C to 0.3°C for up to three years (Bluth et al., 1992; Stothers, 2009). One of the most important volcanic eruptions that affected European Holocene history is the Thera eruption. The Island of Thera, part of the Santorini island group, is situated in the Eastern Mediterranean, 110 kilometres north of Crete. The Island of Thera is what remains of a large volcano that erupted more than 3,600 years ago. This eruption is probably one of the most severe volcanic explosions of the Holocene, and had a strong impact on the course of history of the entire Mediterranean and Europe. The effects of this explosion were noticeable: it caused a drop in global temperature, the production of tnunamis up 12 meters tall, the spread of ashes as far as Asia, and the death of more than 40000 people (Foster et al., 1996; Pearson et al., 2009). As a consequence of such explosion, the powerful Minoan civilization inhabiting the nearby island of Crete declined suddenly soon after Thera erupted: Tsunamis produced by the eruption destroyed its naval fleet and coastal villages (McCoy et al., 2000; Minoura et al., 2000; Pichler and Schiering, 1977); additionally, the successive drop in temperatures caused by the massive amounts of sulphur dioxide ejected into the atmosphere led to several years of cold, wet summers in the region, ruining harvests. The combination of these effects was lethal for the well-developed Minoan culture (Doumas, 1983; Driessen, 2002; Grattan, 2006).

Another important case study is represented by a set of volcanic explosions that took place, almost simultaneously, at the end of the 13th century CE (Common Era). These events are thought to have triggered the cold climatic spell known with the name of Little Ice Age (LIA). In a recent study

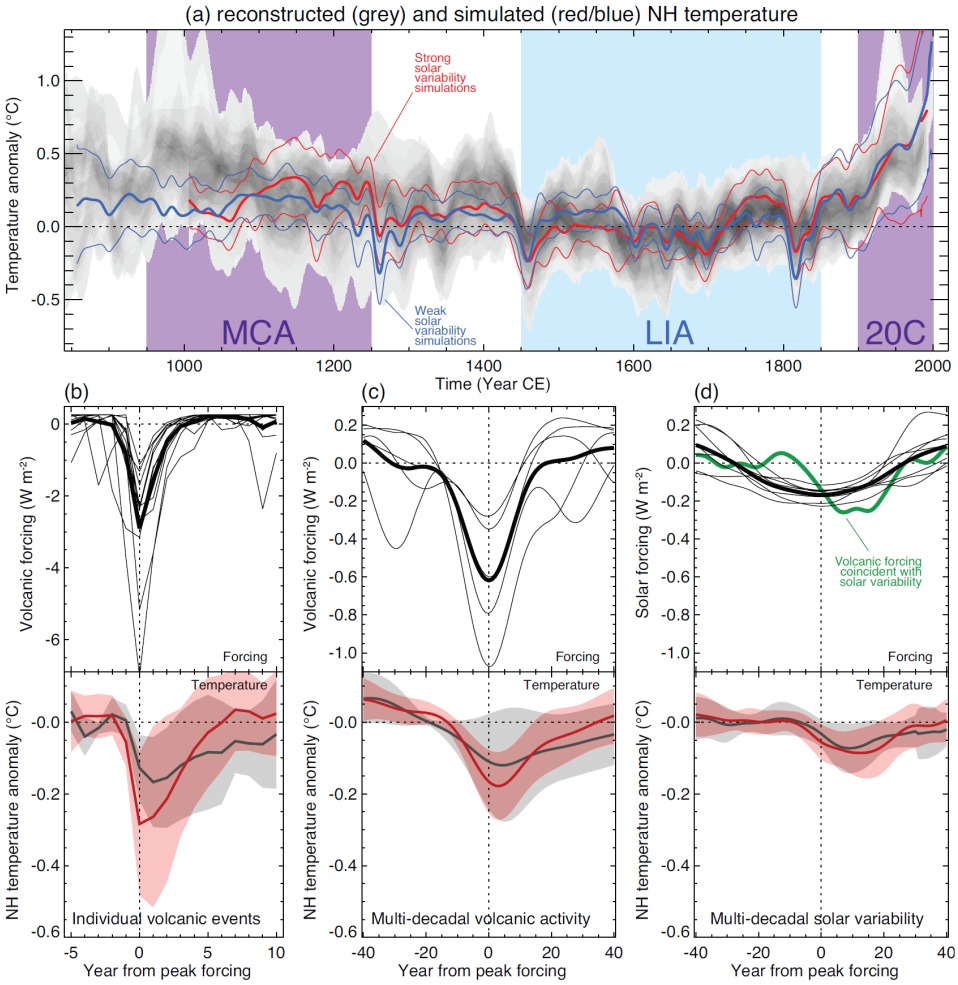

Figure 2.4: *Comparisons of simulated and reconstructed NH temperature changes. a) Changes over the last millennium. b) Response to individual volcanic events. c) Response to multi-decadal periods of volcanic activity. d) Response to multi-decadal variations in solar activity. Some reconstructions represent a smaller spatial domain than the full NH or a specific season, while annual temperatures for the full NH mean are shown for the simulations. a) Simulations shown by coloured lines (thick lines: multi-model-mean; thin lines: multi-model 90% range; red/blue lines: models forced by stronger/weaker solar variability); overlap of reconstructed temperatures shown by grey shading; all data are expressed as anomalies from their 1500-1850 mean and smoothed with a 30-year filter. Superposed composites of the forcing and temperature response to: b) 12 of the strongest individual volcanic forcing events after 1400 CE (data not smoothed); c) multi-decadal changes in volcanic activity; d) multi-decadal changes in solar irradiance. Upper panels show volcanic or solar forcing for the individual selected periods together with the composite mean (thick line); in d), the composite mean of volcanic forcing (green) during the solar composite is also shown. Lower panels show the NH temperature composite means and 90% range of spread between simulations (red line, pink shading) or reconstructions (grey line and shading), with overlap indicated by darker shading. Figure from Masson-Delmotte et al. (2013).*

Miller et al. (2012) sustained that "if the climate system is hit again and again by cold conditions over a relatively short period (e.g. volcanic eruptions) there appears to be a cumulative cooling effect". They showed, with the support of a climate model, that explosive volcanism must have triggered a considerable self-sustaining positive feedback. Repeated explosive volcanism might have led to a persistent expansion of sea ice during the LIA, prompting a period of colder than average conditions (Fig. 2.4).

2.3 Climate Models as a Tool for Paleoclimate Reconstructions

The importance of paleoclimate relies on the necessity to better understand the physical processes that drove the climate system on different time periods of the past, in order to produce more reliable predictions for the future. As affirmed by Masson-Delmotte et al. (2013): "developing a quantitative understanding of mechanisms is the most effective way to learn from past climate for the future".
Information on the climate of the past can be obtained with proxy reconstructions and climate models. Proxy reconstructions are preserved physical characteristics of the environment derived from natural recorders of climate variability such as tree rings, pollen, ice cores, corals, etc. With the use of proxies scientists can extend our understanding of the climate system far beyond the instrumental records. Climate models can be defined as mathematical representations of the climate system based on well-established physical principles (Randall et al., 2007). They allow to better understand the mechanisms of past climate changes that led to the information derived from proxy records. Climate models are of fundamental importance in order to quantitatively test physical hypotheses, such as the Milankovitch theory, allowing to investigate the linkage between cause and effect in past climate change. Additionally, the application of climate models to paleoclimate studies represents a concrete opportunity to test models sensitivity to changes in the climate forcings.

Indeed, the importance of palaeoclimate modelling can be summarized in the following two points:

- Test our understanding of the climate system on the range of reconstructed past climate changes.
- Evaluate the ability of climate models to simulate realistic climate change.

The importance of the use of climate models in paleoclimate studies has been highlighted by Jiang and Zhang (2006), affirming that modelling past climate conditions and consequently improving our understanding of climate changes over different timescales is a prerequisite necessary for a confident forecast of near-future climates involving both natural and anthropogenic factors. If models could be able to successfully reproduce major climate changes during different historical and geological periods, the confidence in predicting future climate changes will certainly increase. At the same time, investigating models responses to changes in the climate forcings in the past can help to interpret proxy records, giving a substantial contribution to the advancement of the whole geosciences (Jiang and Zhang, 2006).

2.4 The Time Slice Technique and Dynamical Downscaling

Different models are developed for each component of the climate system. Often these models, for a minor cost in terms of computational time and resources, are used in a stand-alone version, but they can also be used coupled the one to the others, in order to include the feedback of each component. The so-called Atmospheric Ocean Global Circulation Models (AOGCMs) represent the atmosphere and the ocean and are one of the most employed example of coupled climate models. In general the number of parameters and physical processes involved in a coupled AOGCM makes it really difficult, in terms of computational time and resources, to perform transient climate simulations for long periods of time at a high-resolution, important for regional and local scale information and impact studies. To overcome these difficulties, four types of downscaling techniques have been proposed in recent times (Leung et al., 2003):

1. High-resolution global time-slice experiments (Cubasch et al., 1995; Körper et al., 2009; May and Roeckner, 2001).
2. Variable resolution global time-slice experiments (Déqué et al., 1998).
3. Nested regional climate models (Denis et al., 2002; Giorgi, 2006; Giorgi et al., 1998; Leung et al., 2003; Maurer et al., 2007).
4. Statistical downscaling (Benestad et al., 2008; Wilby et al., 1998, 2004).

Each of these techniques has its own advantages or disatvantages. The time slice technique consists in running *time slice* or *snapshot* experiments

in which an Atmospheric Global Circulation Model (AGCM) is forced by the Sea Surface Temperature (SST) and Sea Ice Cover (SIC) calculated in a transient simulation with a coarser resolution coupled AOGCM (Cubasch, 1992; Stephenson and Held, 1993). The advantage of this method is that the model can be integrated for several decades around the time of interest with a high resolution. On the other hand, the lack of feedbacks of the atmospheric fluxes on the SST is the price paid for saving computer time (Déqué et al., 1998).

Statistical methods are generally based on the assumption that statistical relationships found for present-day climate will remain valid for future climate. Nevertheless, due to their limited need in computing resources, they are relatively easy to implement.

Dynamical downscaling by means of a Regional Climate Model (RCM) forced at its lateral boundaries by an AOGCM or an AGCM, is probably the most common technique. Its main limitation is the lack of atmospheric feedbacks from the regional to the global scale (Douville, 2005). On the other hand, the reproductioon of the non-linear interactions and processes with those scales that are not resolved at the low resolutions, make it a powerful tool in climate research (Dimri, 2009; Feser et al., 2011; Gao et al., 2011; Lee and Hong, 2014; May and Roeckner, 2001; Mayer et al., 2015).

In this work an approach consisting of a combination of two of the mentioned downscaling techniques, the time-slice technique and dynamical downscaling, is adoperated. In the next chapter, more insights on the experimental framework, on the models employed and on their technical tuning and setup will be specified.

Chapter 3

Paleoclimate Simulations

"Get your facts first, then you can distort them as you please."
- Mark Twain -

3.1 Introduction

In this work we perform a set of climate simulations covering the mid-to-late Holocene, employing models at different resolution. The modus operandi consists of three parts and is based on the so-called time-slice technique (Cubasch et al., 1995; Körper et al., 2009; May and Roeckner, 2001). First, a transient continuous simulation covering the entire mid-to-late Holocene is performed with a coupled AOGCM. Successively, seven different time slices are selected, at a temporal distance of approximately 1000 years from each other, from 6000 years ago down to the pre-industrial period, 200 years before present. For every time slice a simulation is conducted, covering a 30-year period, with an high-resolution AGCM, using prescribed SIC and SSTs derived from the transient run. Finally, the AGCM outputs are further downscaled with an RCM. The area considered in our analysis covers the entire Europe and part of Northern Africa.

In this chapter, the employed climate models and their main characteristics are described. The experimental setup and the technical configuration of each simulation are illustrated and the results are finally evaluated. First, consistency between the two GCMs simulations is verified. Then, the RCM performance is evaluated through a present-day test run. Results are consistent with the outcomes of other studies and constitute a valuable benchmark for the interpretation of the mid-to-late Holocene simulations.

3.2 The ECHO-G and a Continuous Transient Paleo-Simulation

The first component of our experimental framework is represented by the ECHO-G (Legutke et al., 1999), a coupled AOGCM developed at the Max Planck Institute of Meteorology in Hamburg, consisting of the atmospheric model ECHAM4 (Rockner et al., 1996) and the oceanic model HOPE-G (Wolff et al., 1997). The atmospheric part has an horizontal resolution of T30 ($\sim 3.75^o \times 3.75^o$) and 19 vertical levels, while its oceanic component, the ocean model HOPE-G, presents an horizontal resolution of approximately $2.8^o \times 2.8^o$ with 20 vertical levels (Wagner et al., 2007).

The results of a mid-to-late Holocene ECHO-G transient continuous simulation carried out by Wagner et al. (2007) are used in our study. The simulation was initialised at the end of a 500-year spin-up control run with constant forcings for 7000 BP. The experiment was performed using different climate forcings for the mid-to-late Holocene. Variations in the orbital parameters between 7000 BP and the preindustrial period were derived from Berger (1978) (Fig. 3.1). Solar forcing was reconstructed based on produc-

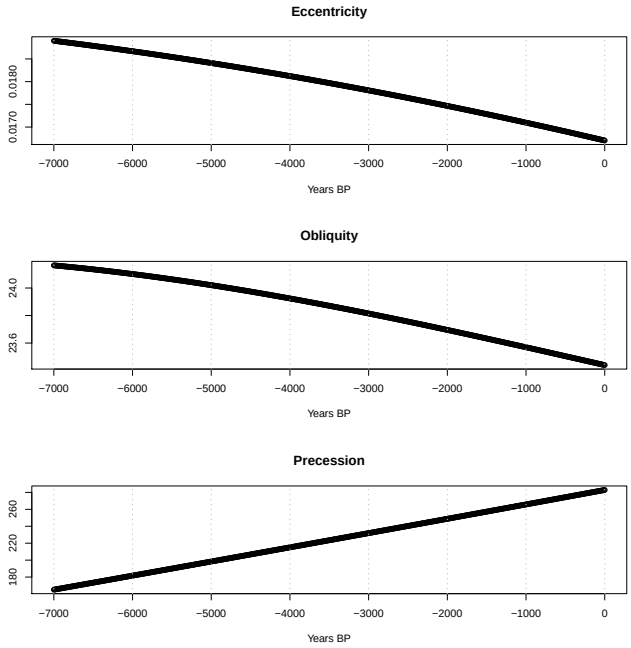

Figure 3.1: *Changes in the orbital parameters during the mid-to-late Holocene as calculated in Berger (1978). From up to bottom: Eccentricity, Obliquity and Precession values.*

tion estimates of $\Delta^{14}C$ from Solanki et al. (2004) (Fig. 3.2a). Values of GHGs were deduced from air trapped in Antarctic ice cores as calculated in Flückiger et al. (2002) (Fig. 3.2b). Volcanic forcing was not included in the experiment due to the high uncertainty in the reconstructions of the volcanic activity during the mid-to-late Holocene (Wagner et al., 2007). Fixed prescribed (pre-industrial) vegetation was used. SIC was interactively calculated with a sea-ice model. No mid-Holocene sea-ice initial conditions were prescribed. Wagner et al. (2007) assume that during the 500 year spin-up simulation, the sea ice has adapted to the mid-Holocene conditions at 7000 BP. Additionally, the experiment was performed with constant values of stratospheric ozone distribution. Several studies have highlighted the importance of the interactions between ozone and the incoming solar radiation (Wagner et al., 2007). For example, Fröhlich and Lean (2004) suggested that the creation and distruction of stratospheric ozone is controlled by variations in the solar output, which are most pronounced in the short wavelengths. Therefore using spectrally resolved rather than total irradiance variations could be more indicated (Lean et al., 2005). Unfortunately, for the mid-to-late Holocene, spectrally resolved information on solar irradiance is not available. The interaction between shortwave radiation and stratospheric ozone also influences tropospheric temperatures and circulation. For example, according to Rind et al. (2004), during the Maunder minimum stratospheric temperature changes related to stratospheric ozone dynamics led to a negative phase

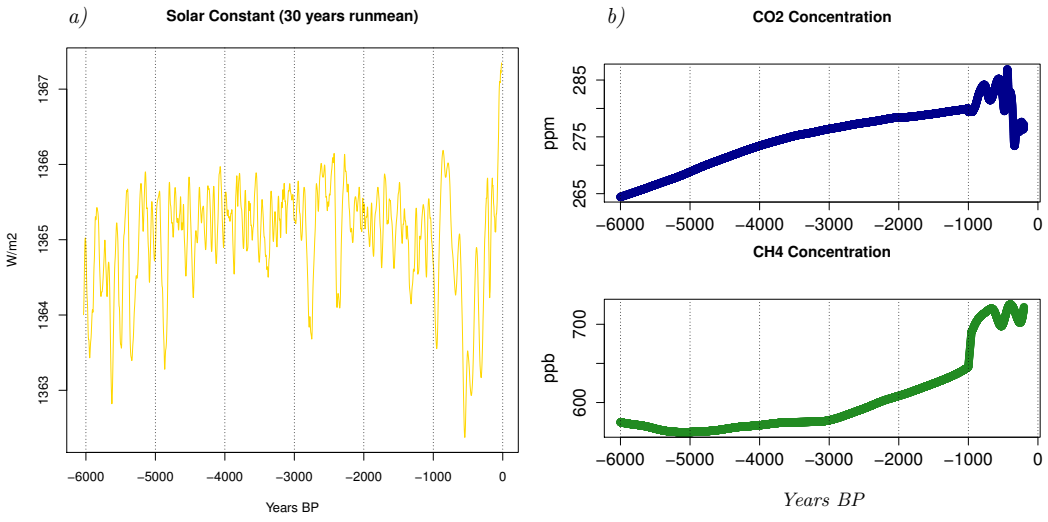

Figure 3.2: *a) 30 years running mean of solar activity derived from the reconstructions of Solanki et al. (2004). b) concentration values of CO_2 and CH_4 during the mid-to-late Holocene as reconstructed in Flückiger et al. (2002).*

of the Atlantic Oscillation (AO). Because of the lack of a dynamical ozone module in ECHO-G, the ozone-related effects on tropospheric temperatures and circulation are not present in the considered simulations.

3.3 ECHAM5 Simulations

The ECHAM5 is an AGCM developed by the Max Planck Institute for Meteorology of Hamburg, Germany. ECHAM5 employs a spectral dynamical core. Vorticity, divergence, temperature and the logarithm of surface pressure are represented in the horizontal dimension by a truncated series of spherical harmonics. The general form of the corresponding equations follows that of the early multi-level spectral models (Hoskins and Simmons, 1975). Triangular truncation is used at wavenumbers 21, 31, 42, 63, 85, 106 or 159. The model utilizes a semi-implicit leapfrog time differencing scheme (Roeckner et al., 2003). We employed the ECHAM5 for the performance of a set of simulations for seven different time intervals of the mid-to-late Holocene, each one covering 30-year periods and taken approximately at a distance of 1000 years one from the other. Five years spin-up time has been considered in each case. Prescribed SIC and SSTs from the transient continuous ECHO-G simulation have been used. In the interpolation procedure a method similar to the Cressman scan analysis procedure (Cressman, 1959) suggested by the Atmospheric Model Intercomparison Project phase 2 (AMIP2) has been used. In order to have smooth transitions at the coastline, a mask with more ocean points than in reality is used, covering also part of the land. In this way, in the interpolation process, the SST will have more influence at land/sea boundary. For time interpolation, the method suggested by the AMIP2 has not been employed. Daily values are obtained by linearly interpolating between monthly mean original values. In such a way, the monthly average is not preserved and also the seasonal cycle and the interannual variance are less accurately represented. Future work would consist in the performance of the same simulations with an upgraded method for interpolation. Changes in the climate forcings have been implemented into the model accordingly to the ones used for the ECHO-G simulation.

Table 3.1 shows the different values of precession of perihelion, obliquity and eccentricity for each time slice of the mid-to-late Holocene.

Table 3.1: *Values of orbital parameters for each of the mid-to-late Holocene time slices, as computed by Berger (1978).*

Year(BP)	**Prec.**	**Obliq.**	**Eccent.**
200	278.66	23.47	0.0170
1000	265.75	23.57	0.0171
2000	248.82	23.70	0.0175
3000	231.12	23.82	0.0178
4000	214.30	23.93	0.0181
5000	197.57	24.03	0.0184
6000	180.88	24.11	0.0187

3.4 Comparison and Validation of Global Simulations

The ECHAM5 time-slice simulations have been conducted in different periods of the project. In order to test their consistency, the ECHO-G and ECHAM5 results are compared, both globally and for Europe, for a set of standard variables. A similar behaviour of the two models would indicate a correct execution of the ECHAM5 simulations, each one with respect to the others. Analysis focuses on near surface temperature (T 2M) and total precipitation (TOT PREC) yearly values. The main differences between the two datasets are most likely due to their different spatial resolution (Fig. 3.3): higher resolution leads to a better representation of the orography, the coastline and to the parameterization of physical processes that take place on a smaller scale. Considerable changes are expected for the two variables into consideration and for their spatial distribution when switching from a model with a lower resolution to a higher resoluted one.

Global means of near surface temperature are in good agreement and follow the same temporal evolution in all the cases (Fig. 3.4). For precipitation, even if the trends of the two datasets are comfortably similar (Fig. 3.4) there is a remarkable bias between the ECHO-G and the ECHAM5 data. This is likely due to the improvement in the representation of global orography. Interestingly, even on the regional scale, the trends in the two realizations are, for all the variables, comparable (Fig. 3.5). ECHAM5 values of temperature, in particular, fall in all the cases within one sigma from the ECHO-G ones. Consequently, we can affirm that all the ECHAM5 simulations have been performed consistently the one with the others.

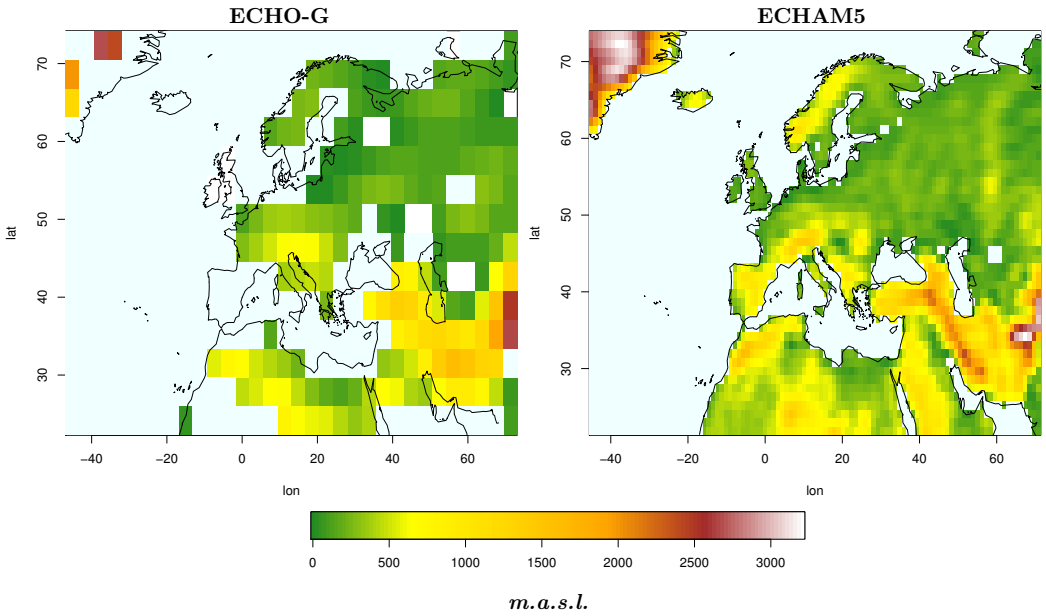

Figure 3.3: *Orography and sea-land mask of the ECHO-G (left) and ECHAM5 grids (right) for Europe.*

3.5 Setup of the Regional Climate Model CCLM for Paleoclimate Studies

Once the consistency of the ECHAM5 simulations has been tested, the results are used as boundary and initial conditions for the performance of a set of simulations with the COSMO model in CLimate Mode (CCLM) for the same time slices. The CCLM is a non-hydrostatic regional climate model with rotated geographical coordinates and a terrain following height coordinate (Rockel and Geyer, 2008), developed from the Local Model (LM) of the German weather service (Doms and Schättler, 2003). Here, version 4.8_clm19 of the model at an horizontal resolution of 0.44 longitude degrees and 40 vertical levels is used.

3.5.1 Parameterizations and Initial Conditions

The setup of the CCLM adopted in this study is based upon the work of Hollweg et al. (2008) within the Euro-CORDEX downscaling experiment (Jacob et al., 2014). A more detailed description of the model configuration used is provided in Tab. 3.2.

For this study the model has been employed coupled to a Soil Atmosphere Vegetation Transfer scheme (SVAT), the TERRA ML, a multi-layer model

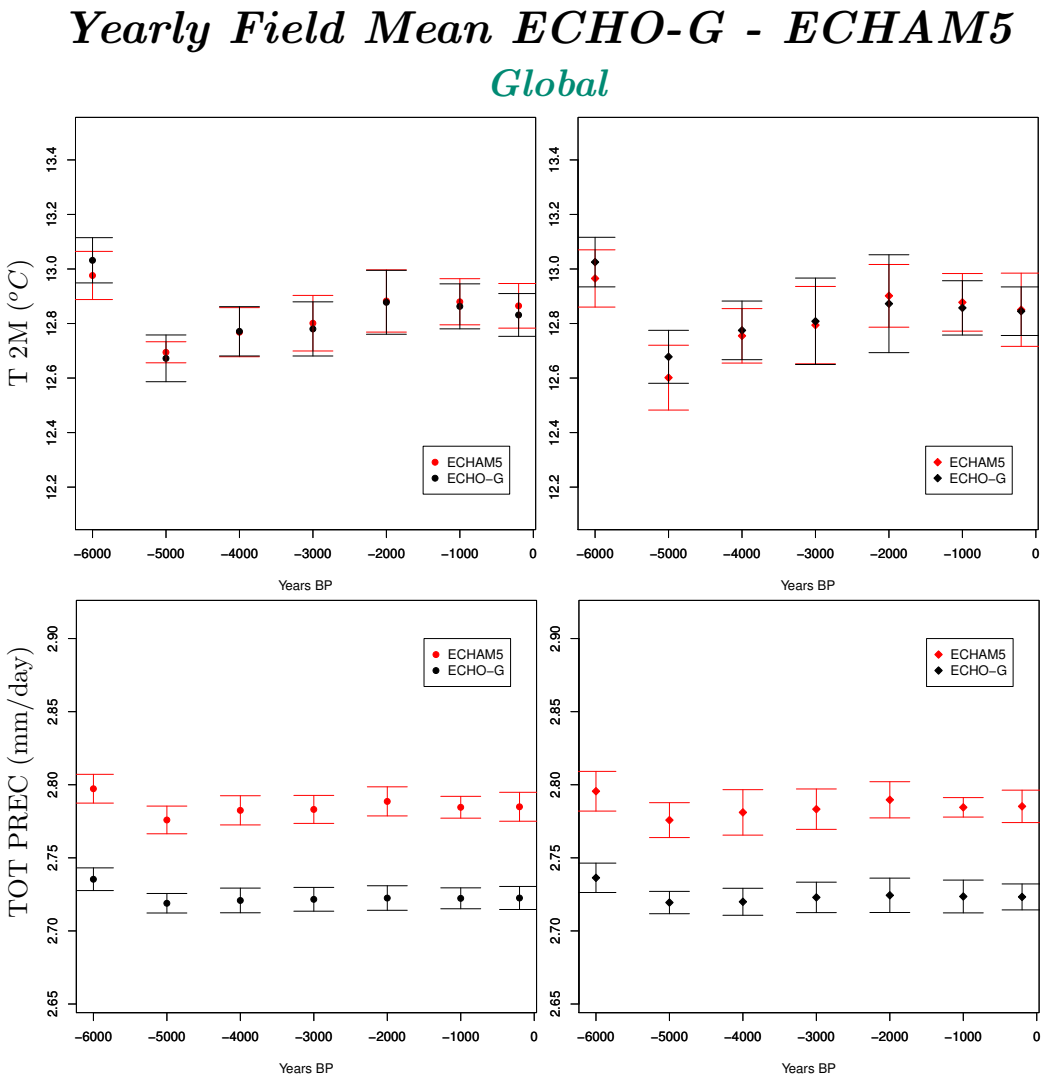

Figure 3.4: *Comparison Maps of the global mean of near surface temperature (top) and total precipitation (bottom) yearly regional values between the ECHO-G and the ECHAM5 simulations. In the left column mean values and relative standard deviations, calculated for each time-slice, are presented. In the right column the median (right) and the corresponding interquantile range, calculated for the same periods, are shown.*

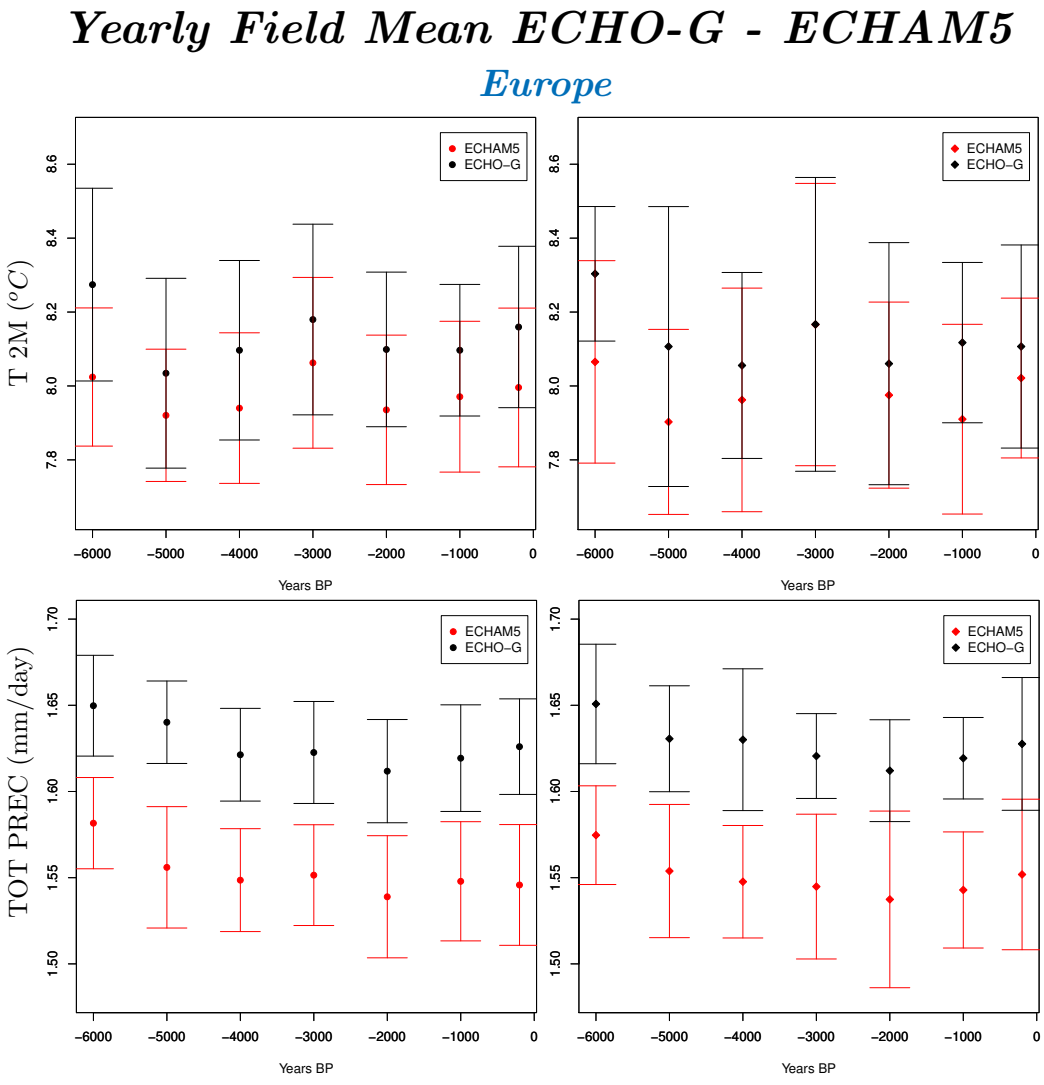

Figure 3.5: *Comparison Maps of the European mean of near surface temperature (top) and total precipitation (bottom) yearly regional values between the ECHO-G and the ECHAM5 simulations. In the left column mean values and relative standard deviations, calculated for each time-slice, are presented. In the right column the median (right) and the corresponding interquantile range, calculated for the same periods, are shown.*

Table 3.2: *CCLM main model configuration parameters.*

Convection	Tiedtke (Tiedtke, 1989)
Time Integration	Runge-Kutta, ΔT=240s
Robert-Aselin time filter (alphaas)	0.53
Lateral Relaxation Layer	500Km
Radiation	Ritter and Geleyn (Ritter and Geleyn, 1992)
Turbulence	Implicit treatment of vertical diff. using Neumann boundary conditions
Rayleigh Damping Layer (rdheight)	11Km
Soil Active Layers	9
Active Soil Depth	5.74m

with a constant temperature lower boundary condition that allows to reproduce the fluxes of heat, water and momentum between the soil-surface and the atmosphere (Grasselt et al., 2008). These surface fluxes constitute the lower boundary conditions for the atmospheric part of the model. Their calculation requires the knowledge of the temperature and the specific humidity at the ground. The task of the soil model is to predict these quantities by the simultaneous solution of a separate set of equations which describes various thermal and hydrological processes within the soil. The multi-layer concept avoids the dependence of layer thicknesses on the soil type. Additionally, it avoids the use of different layer structures for the thermal and the hydrological section of the model. In total, five different types of soil are distinguished: sand, sandy loam, loam, loamy-clay and clay. Three additional special soil types are also considered: ice, rock and peat. Hydrological processes in the ground are not considered for ice and rock. The soil model consists of two parts. In the first part the computation of bare soil evaporation and plant transpiration is performed. In the second, the equation of heat conduction and the Richards equation are solved (Grasselt et al., 2008). Recent data of the physical parameters of the Earth's surface (e.g., orography, land use, vegetation fraction, and land-sea mask) are employed for the simulations. Some of these parameters are generally constant in time (e.g. orography). Other fields depend on the time of the year (e.g. plant characteristics). For these, the actual values are computed by interpolation in time between maximum and minimum values, provided as constant fields.

The use of a climate model coupled to a SVAT, makes it necessary to consider a longer spin-up time. In fact, for atmospheric only climate models,

due to the fast response-time of the processes involved in the atmosphere, this time is considerably short, going from days to months (Hansen et al., 1984; Liou, 1992). Conversely, soil and land processes have a slower response-time. Indeed, when these processes are simulated, a longer spin-up time of the order of years is necessary. In our case five years are considered. This choice has been made according to bibliographic evidence (Christensen, 1999; Li et al., 2011; Zhao, 2013) and to the results of different tests that we conducted taking into consideration simulated soil parameters.
Fig. 3.6 presents the five-year trend of the field mean of monthly values of soil temperature and water content for the different layers of the model, obtained after decomposing the original time series into seasonal, trend and irregular components using the LOcal regrESSion method (LOESS) (Cleveland and Devlin, 1988). The results suggest that a five-year spin-up time is a good compromise between computational resources and quality of the results. In fact, in almost all the soil layers the model reaches an equilibrium state within five years, for both the considered variables. More time is required only in the deepest layers, for which the response-time is lower and the effects of the fixed lower boundary conditions are more pronounced.

3.5.2 Climate Forcings

For paleoclimate studies a particular implemention of the model code is required in order to set up the values of the climate forcings in accordance to the ones used in the GCM simulations. The CCLM has been already employed in other paleoclimate studies. Prömmel et al. (2013) used the CCLM in order to address the effect of changes in orography and insolation on african precipitation during the last interglacial. Fallah et al. (2015) investigated precipitation and dry periods during the little ice age and the middle age warm period over central Asia. Wagner et al. (2012) compared mid Holocene and pre-industrial climate over South America. In all of these cases, no specific indications were provided on the method used for the setup of GHGs concentration. For the computation of the effects of the atmospheric concentration of GHGs on the net radiative balance, the CCLM uses the definition of CO_2 equivalent concentration. This represents the mixing ratio of CO_2 required to produce the same radiative forcing that would be produced by the change in concentration of all GHGs for a fixed year in comparison to their concentration for the reference year 1750 (Ramaswamy et al., 2001). The formulas for computing the CO_2 equivalent concentration according to the values of CO_2, CH_4 and N_2O are:

$$\Delta F = \alpha ln(C/C_0) \tag{3.1}$$

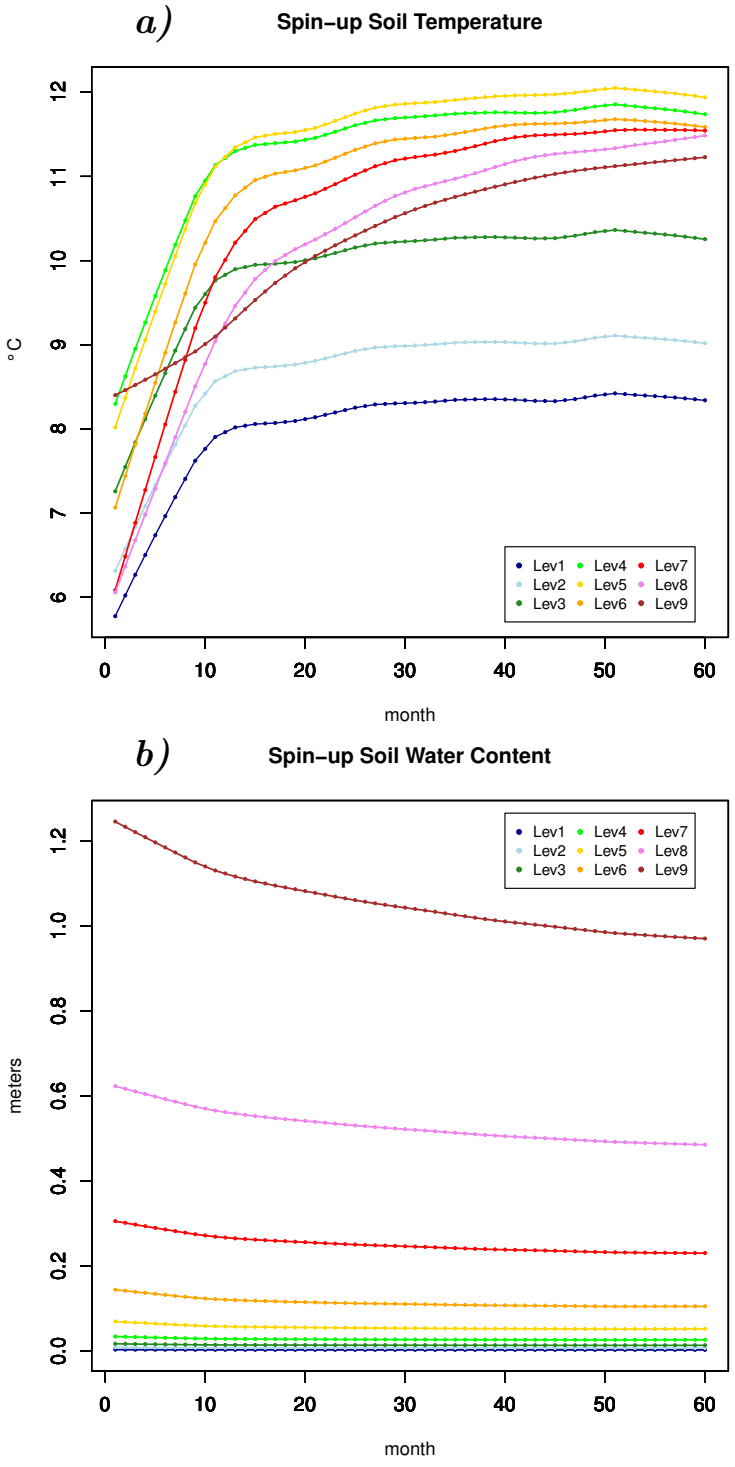

Figure 3.6: *Trend over the spin-up period of the field mean of soil temperature (a) and soil water content (b) monthly values for the 9 levels of the TERRA_ML.*

$$\Delta F = \alpha(\sqrt(2)(M) - \sqrt(2)(M_0)) - f(M, N_0) - f(M_0, N_0) \tag{3.2}$$

$$\Delta F = \alpha(\sqrt(2)(N) - \sqrt(2)(N_0)) - f(M_0, N) - f(M_0, N_0) \tag{3.3}$$

where $f(M, N) = 0.47ln[1+2.01\times10^{-5}(MN)^{0.75}+5.31\times10^{-15}M(MN)^{1.52}]$.

ΔF represents the radiative forcing, the measure of the perturbation of the radiation balance; it is the change in irradiance at the tropopause following the concentration change and is measured in watt per square metre (W/m^2) (Griggs and Noguer, 2002; Ramaswamy et al., 2001). C_0 represents the preindustrial concentrations of CO_2, assumed to be 278 ppmv (Griggs and Noguer, 2002). Equally, M is CH_4 and N represents N_2O, both in parts per billion by volume (ppbv). The constant α is equal to 5.35 W/m^2. Some model code modifications are necessary in order to implement the values of CO_2 equivalent concentration directly into the FORTRAN90 radiation routine.

The orbital parameters also have to be modified according to the values used for the GCMs simulations. For this purpose a modification of the model code is needed. Here the modifications employed by Prömmel et al. (2013) are used.

3.5.3 Performance of the Regional Simulations and Validation of the Results

In order to test the ability of the CCLM modified accordingly to our purposes, to properly reproduce present-day climate, in a first step a control simulation has been performed with present values of orbital parameters and GHGs.

The simulation covers a 10-year period, between 1991 and 2000. Even if the length of this simulation can be considered as "critical" for the model's validation, we want to acknowledge that due to computational reasons, it was not possible to cover a longer period. The model domain shown in Fig. 3.7, is the one used for the Euro-CORDEX experiments (Jacob et al., 2014), extending from southern Greenland to western Russia in the North and from the western Atlantic Coast of Morocco to the Red Sea in the South. As driving data the ECMWF (European Centre for Medium-Range Weather Forecasts) Interim Reanalysis (ERA-Interim) dataset (Dee et al., 2011) is used. ERA-Interim is a global atmospheric reanalysis dataset from the year 1979, continuously updated in real time. The spatial resolution

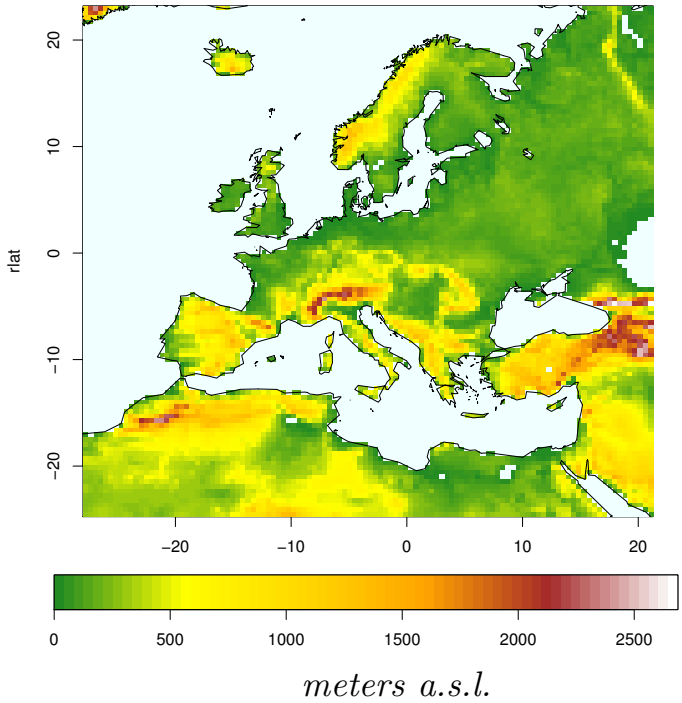

Figure 3.7: *Orography map of the CCLM simulation domain in rotated coordinates.*

of the dataset is approximately 80 km (T255 spectral) on 60 vertical levels from the surface up to 0.1 hPa. ERA-Interim data can be downloaded from the ECMWF public datasets web interface (http://apps.ecmwf.int/datasets/data/interim-full-daily/levtype=sfc/). For model validation, the European daily high-resolution gridded dataset (E-OBS) (Haylock et al., 2008) and the Climate Research Unit (CRU) (Harris et al., 2014) observational datasets covering the period 1991-2000, are used. The validation is conducted with respect to the total precipitation and the near surface temperature winter and summer seasonal means. Additionally, CCLM heat fluxes and evapotranspiration values from the same simulation are validated against the Global Land Data Assimilation System (GLDAS) dataset, available at http://disc.sci.gsfc.nasa.gov/gldas-version-2.0-data-sets.

In Fig. 3.8, 3.9, 3.10 and 3.11, winter and summer seasonal means of temperature and precipitation from the CCLM simulations are compared against the CRU and the E-OBS observational datasets. In the first column of each panel, the climatology of the different datasets is shown: the model is able to correctly reproduce, with an accuracy comparable with the one of other studies (Jacob et al., 2014; Kotlarski et al., 2014), the climatology of the observations for both temperature and precipitation in winter and in summer.

In the right column of every panel, the considered variables from the present-day control run are directly validated, through a Student's T-test, against the observations. The same test is conducted for evaporation and heat fluxes but against the GLDAS dataset in Fig. 3.12. The black dots represent the grid cells where the null hypothesis of the T-test, assuming that the data being sampled could be drawn from the same underlying distribution, is not rejected at a significance level of 5%. The biases between the CCLM results and the observations are represented with different colours. The results show that, for temperature, the model performs well over northern Europe in both winter and summer. Wintertime results are in particularly good agreement with observations over northeastern Europe and Scandinavia (Fig. 3.8II). However, larger deviations (up to 4^oC in some cases) are present over central Europe, Turkey and northern Africa. In particular the model tends to simulate generally colder conditions over these regions. Winter precipitation results are in good agreement over a major part of the domain, with some deviations from the observations over regions with particularly complex orography, in regions that are normally highly affected by westerlies and in the northern African coasts of the Mediterranean Sea (where the biases are particularly pronounced, and the model results diverge by almost 100% from the values of the observations) (Fig. 3.9II).

In summer, the main discrepancies are found over southern Europe both for temperature and precipitation (Fig. 3.10, 3.11). In particular, the temperature anomalies exceed 3^oC over most of the Mediterranean region. It has been shown in previous works (Christensen et al., 2008; Hagemann et al., 2004; Jerez et al., 2010, 2012; Kotlarski et al., 2014) that, in general, regional climate models poorly simulate southern European summer conditions. This seems to be related to deficiencies in soil-atmosphere coupling (Fischer et al., 2007; Seneviratne et al., 2006, 2010). In soil moisture-controlled evaporative regimes, such as the Mediterranean basin, low soil moisture contents (due to an underestimation of spring-time precipitation or not-properly represented soil properties in consequence of complex orography) limit the amount of energy transferred by the latent heat flux. This increases the sensible heat flux, ultimately leading to an increase of air temperature, on the one-hand, and to a decrease of local precipitation on the other (Zveryeav and Allan, 2010).

Based on these considerations, we assert that the model reproduces anomalously warm and dry conditions over a wide part of southern Europe and the Mediterranean basin, during summer, as a consequence of a wrong conversion of energy towards latent heat in these regions. This hypothesis is supported by the heat fluxes and evapotranspiration maps (Fig. 3.12) presenting a spatial distribution of the anomalies resembling the ones of temperatures and

precipitation. In particular, the model underestimates latent heat flux and evapotranspiration, while overestimating sensible heat over corresponding areas.

Nevertheless, the performances of the model with the applied changes are in good agreement with the results of other works focusing on the same region (Gómez-Navarro et al., 2011, 2013; Hollweg et al., 2008; Kotlarski et al., 2014; Schimanke et al., 2012), having in general the same features and spread of the anomalies. Indeed, the applied changes and configuration appear to be exploitable for paleoclimate applications.

3.6 Conclusions

In this section we introduced the different models employed in our study and their experimental setup. In addition, different tests have been performed. A first one, aiming to prove that the different GCMs simulations were consistent the ones with the others, provided good results. Another test was additionally performed for the evaluation of the performance of the RCM for present-day conditions, but using the same setup applied for the study of the mid-to-late Holocene time-slices. This time the analysis was more complex. The results were characterized by remarkable biases over some areas. The biases were particularly large over the Mediterranean region during the summer season, presenting the same spatial pattern for both temperature and precipitation. Analysis of surface variables allowed to determine that the cause of the evinced bias is related to a wrong representation by the RCM of soil-atmosphere interactions over the area. This seems to be a peculiar characteristic of climate models in general: the complex orography of the area most likely does not allow to correctly represent soil features, resulting in the poor skills of climate models. Nevertheless, the results of the RCM simulation proved to be in good agreement with the observations over a wide part of the domain. Additionally, the range of the bias and its spatial distribution, were comparable with the ones of other studies. Indeed, the modifications applied to the model for its application in paleoclimate studies are reliable and the study provides a robust reference for the performance of future paleoclimate simulations.

Additionally, knowing the biases characteristics of the RCM is useful for the interpretation of the mid-to-late Holocene simulations, giving indeed a substantial contribution to the goal of better understanding the possible causes of mismatches between proxy data and model results, and model sensitivity to changes in the external forcings.

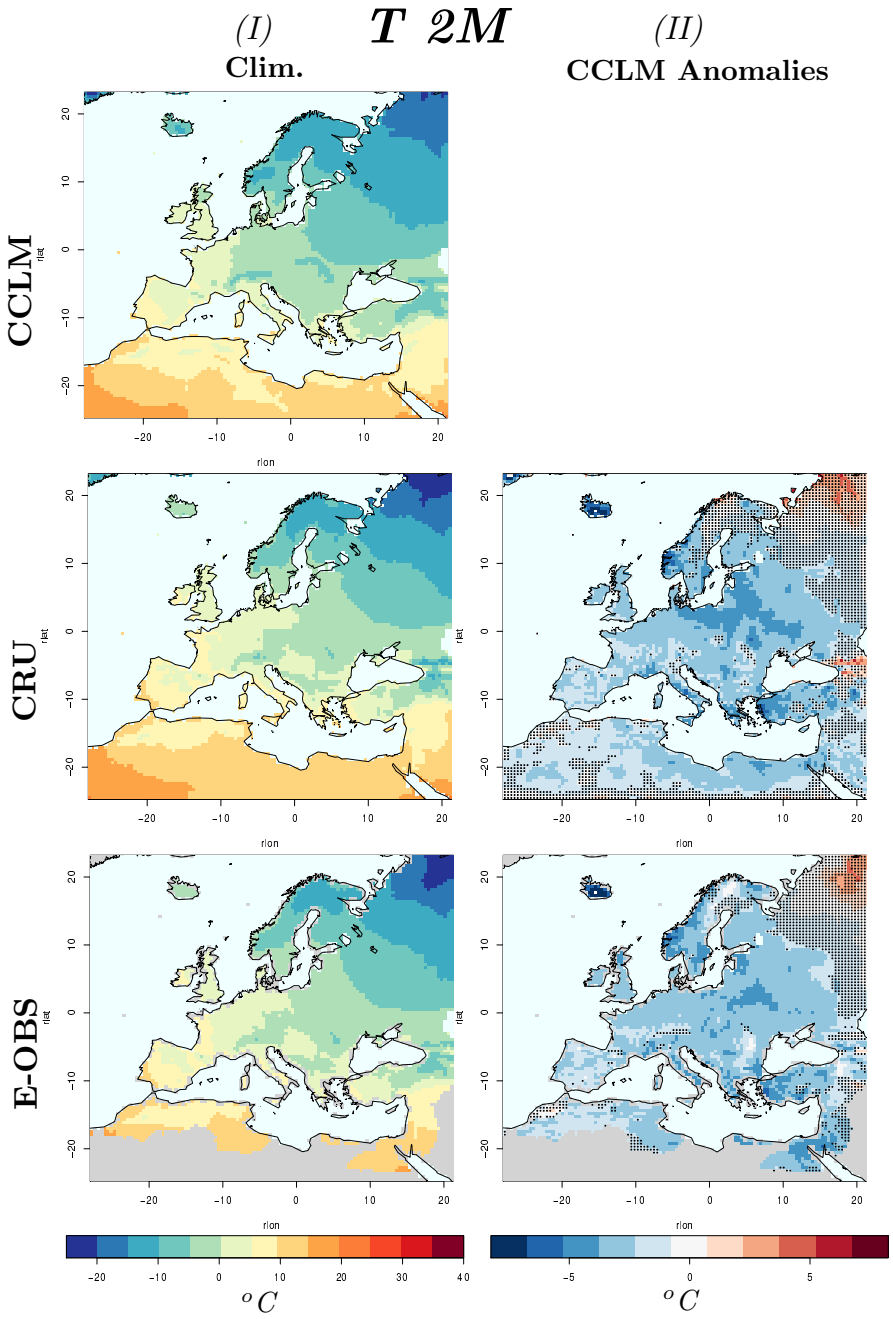

Figure 3.8: *Analysis of winter seasonal means of near surface temperature for the period 1991-2000. The first column (I) shows the mean climatology for the investigated period as represented in the three considered datasets: the CCLM in the first row, the CRU in the second and the E-OBS at the bottom. The second column (II) presents the biases between the CCLM results and the respective observational datasets. The areas with a dot represent the grid cells where the anomalies between the two datasets are not significant, according to a Student's T-test, at a significance level of 5%.*

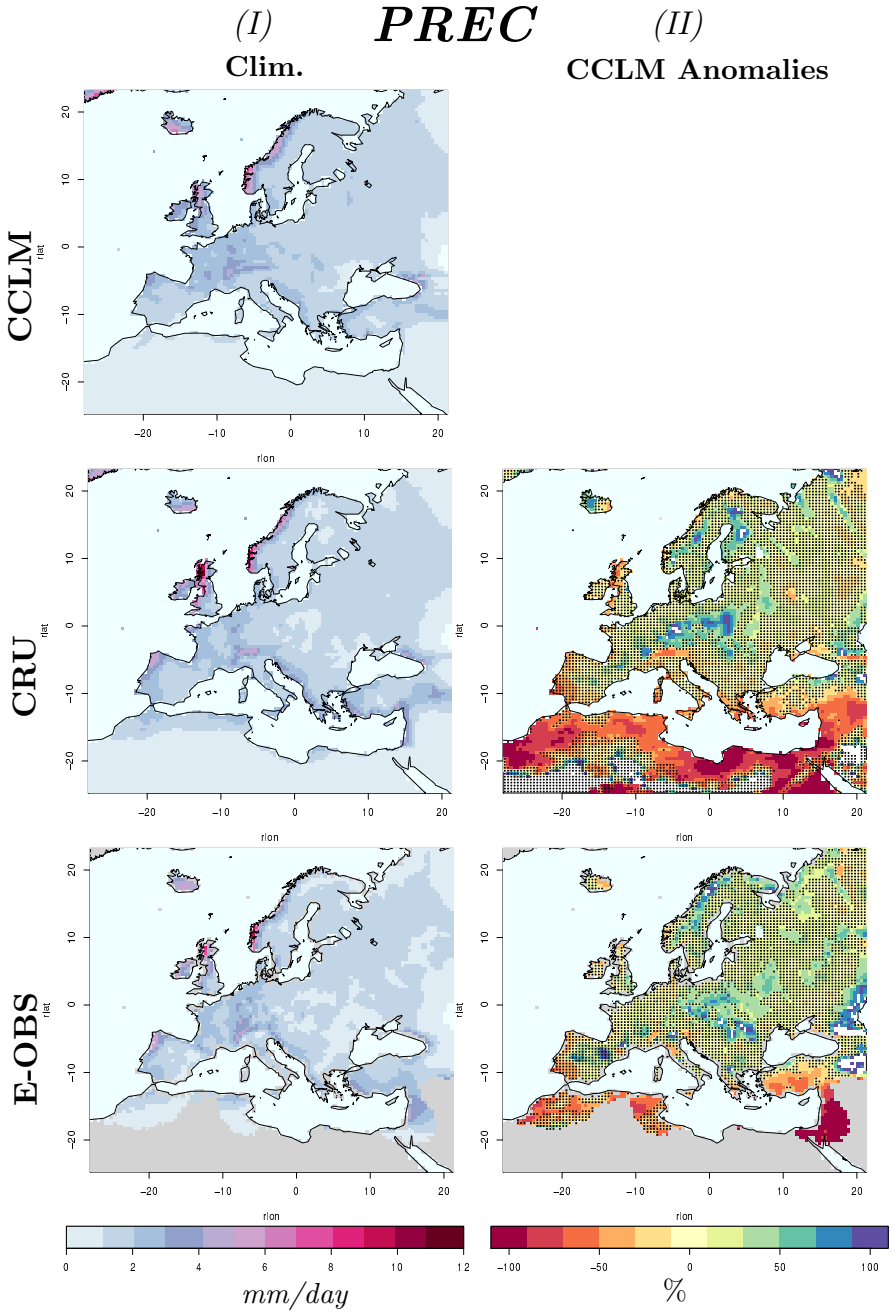

Figure 3.9: *Analysis of winter seasonal means of total precipitation for the period 1991-2000. The first column (I) shows the mean climatology for the investigated period as represented in the three considered datasets: the CCLM in the first row, the CRU in the second and the E-OBS at the bottom. The second column (II) presents the biases between the CCLM results and the respective observational datasets. The areas with a dot represent the grid cells where the anomalies between the two datasets are not significant, according to a Student's T-test, at a significance level of 5%.*

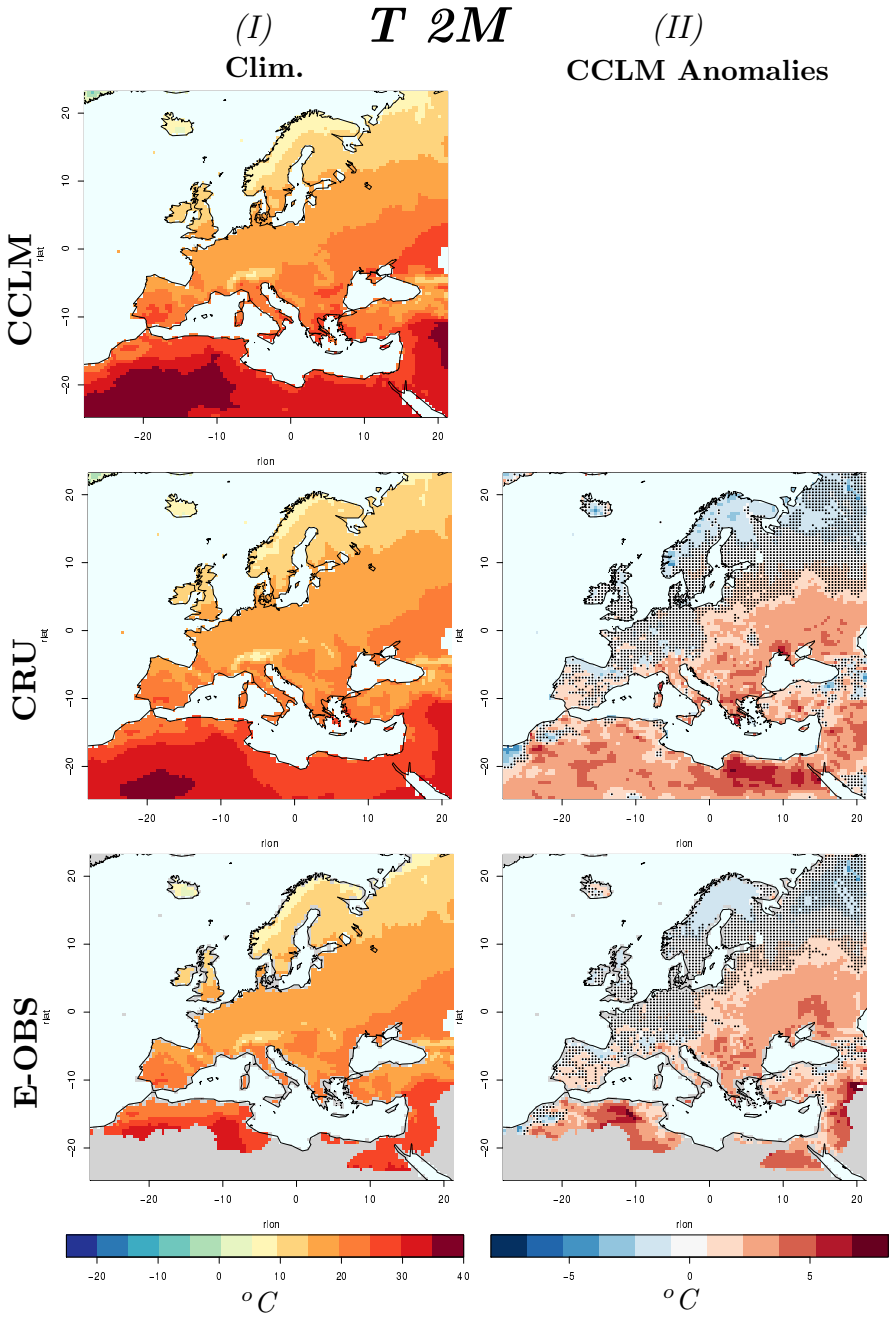

Figure 3.10: *Analysis of summer seasonal means of near surface temperature for the period 1991-2000. The first column (I) shows the mean climatology for the investigated period as represented in the three considered datasets: the CCLM in the first row, the CRU in the second and the E-OBS at the bottom. The second column (II) presents the biases between the CCLM results and the respective observational datasets. The areas with a dot represent the grid cells where the anomalies between the two datasets are not significant, according to a Student's T-test, at a significance level of 5%.*

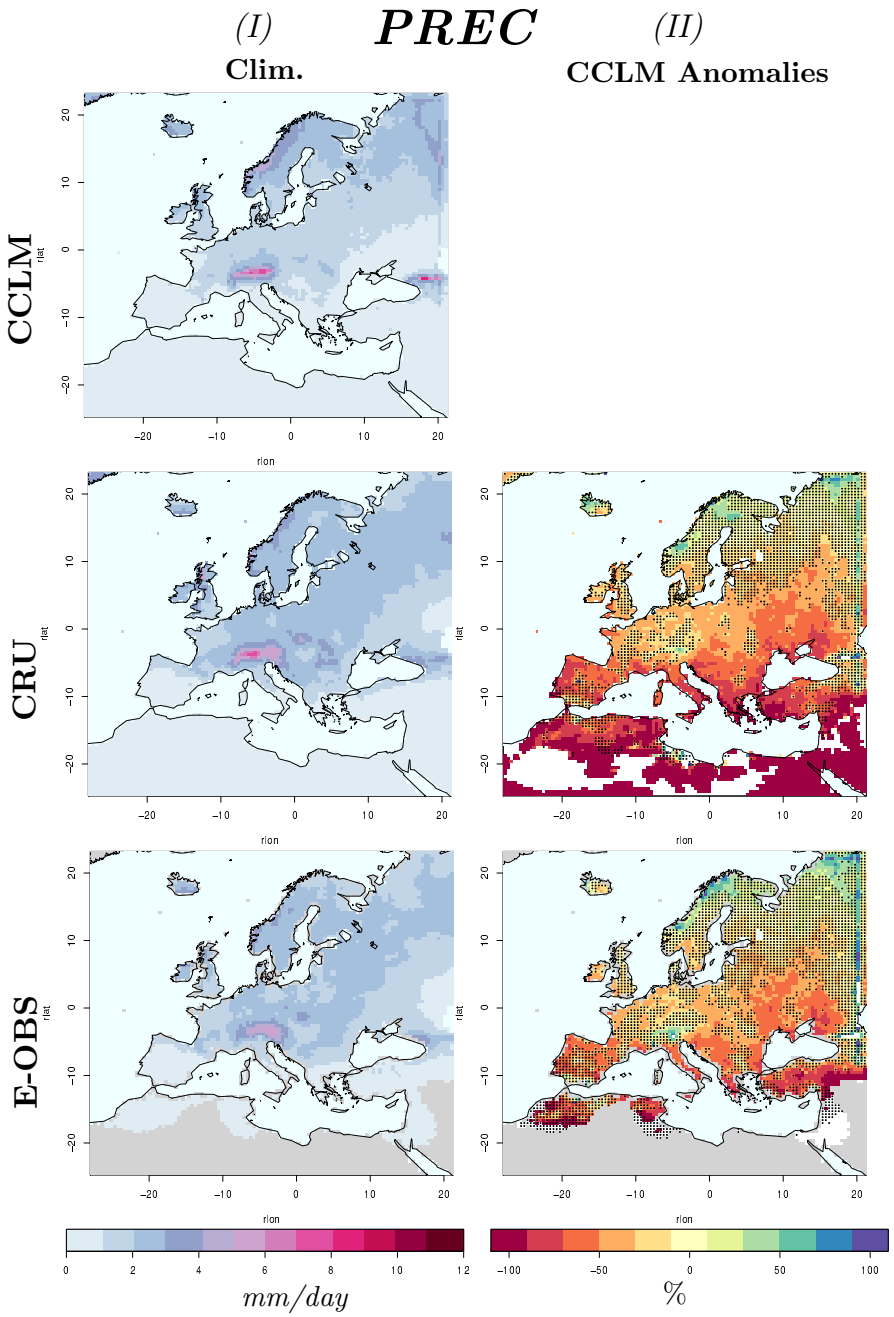

Figure 3.11: *Analysis of summer seasonal means of total precipitation for the period 1991-2000. The first column (I) shows the mean climatology for the investigated period as represented in the three considered datasets: the CCLM in the first row, the CRU in the second and the E-OBS at the bottom. The second column (II) presents the biases between the CCLM results and the respective observational datasets. The areas with a dot represent the grid cells where the anomalies between the two datasets are not significant, according to a Student's T-test, at a significance level of 5%.*

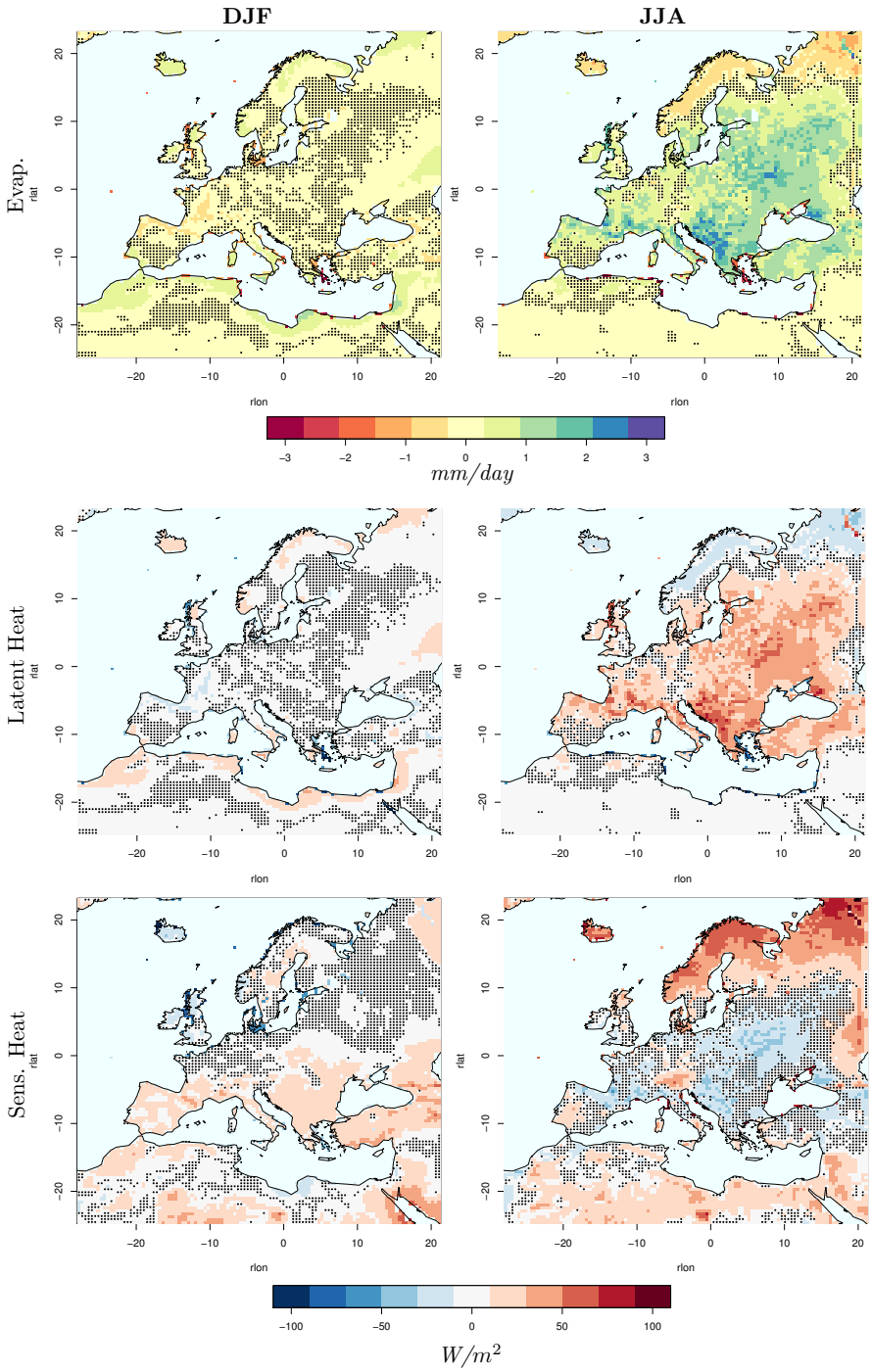

Figure 3.12: *Biases of seasonal means of evapotranspiration (left), latent (center) and sensible heat (right) fluxes, between the CCLM simulations and the GLDAS dataset, calculated for the reference period 1991-2000. As in the previous figures, the areas with a dot represent the grid cells where the anomalies between the two datasets are not significant, according to a Student's T-test, at a significance level of 5%. Winter (December January February (DJF)) results are presented in the first row, and summer (June July August (JJA)) results in the second.*

Chapter 4

The Added-Value of a Regional Climate Model for Paleoclimate Studies

"It is the mark of a truly intelligent person to be moved by statistics."
- George Bernard Shaw -

4.1 Introduction

According to Solomon (2007): "Paleoclimate data are key to evaluating the ability of climate models to simulate realistic climate change".

Since the 1970s, numerical models have been used to study past climates. To analyse model performance, the results of these studies have been compared with climate reconstructions based on palaeodata (Bonfils et al., 2004; Braconnot et al., 2007a,b, 2012; Coats et al., 2013; de Melo and Marengo, 2008; Kohfeld and Harrison, 2000; Lohmann et al., 2015; Texier et al., 1997; Wagner et al., 2007). Nevertheless, in many cases the resolution of the employed models was not high enough to allow for an assessment of the climate behaviour on a regional scale. As suggested by Renssen et al. (2001), if we want to evaluate the data of paleoclimate simulations against climatic reconstructions based on pollen data or any other record, an improvement in the resolution is highly required (Bonfils et al., 2004; Masson et al., 1999). Proxy data are often influenced by local-scale processes. Higher-resolution models, allowing the representation of processes taking place on smaller scales than the ones resolved in coarse-resolution models, and providing more detailed information on surface and soil features (Christensen et al., 2007; Feser et al.,

2011; Fischer and Jungclaus, 2011; Flato et al., 2013), are indeed expected to be a better suitable tool for paleoclimate studies (Russo and Cubasch, 2016).

Prompted by such consideration, in recent years the application of high-resolution regional climate models for paleoclimate studies has become more frequent (Fallah et al., 2015; Gómez-Navarro et al., 2011, 2012, 2013; Prömmel et al., 2013; Renssen et al., 2001; Schimanke et al., 2012; Strandberg et al., 2014; Wagner et al., 2012). Nonetheless, apart from the work of Renssen et al. (2001), the possible advantages of RCM simulations for the study of paleoclimate have never been addressed before.

Within this context, in our discussion we try to highlight the importance of RCMs for the simulation of past climate change. Aiming at investigating the value added by highly resolved simulations for the comparison against proxy-reconstructions, we follow a two steps approach:

1. Firstly, we conduct a qualitative analysis of the simulations performed with three models at different resolution in order to detect visible differences in the reproduced signals.

2. Secondly, we employ a quantitative approach in order to estimate the skills of the RCM, in comparison to the driving GCM, in reproducing the same mid-to-late Holocene changes in temperature as derived from proxy-reconstructions.

As a benchmark for such comparison we use the pollen-based reconstructions of Mauri et al. (2015).

In this way we aim at establishing whether the representation of smaller scale processes and improved orographic features of the region of study could lead to results that are in better agreement with the mentioned proxy-based reconstructions.

In the first paragraph, we better clarify the concept of added value of highly resolved climate simulations for their use in the investigation of climate change. Successively, we provide additional information on the pollen-based reconstructions that we aim to use for our analysis. Finally, the direct comparison between the reconstructions and the models's results is presented. Thus, we conduct a qualitative analysis, performing then a more detailed quantitative comparison between the different models, for each of the variables into consideration.

4.2 Added Value, RCMs and Climate Change

According to Di Luca et al. (2013) "the use of RCMs to dynamically downscale large-scale atmospheric fields in past, present and future climate condi-

tions has gained popularity as a way to circumvent the spatial scale gap that exists between the climate information provided by AOGCMs and the input needed in impact and adaptation studies. There is still a need, however, to objectively quantify the gains arising from the use of RCMs as climate downscaling tools".

In general, the ability of RCMs to lead to an improvement over some aspects of their driving GCMs when compared to observations is defined as *Added Value* (Di Luca et al., 2015). Quantitatively, the *Added Value* can be defined as the difference between the distance of the driving GCM results and the observations on the one hand, and between the RCM results and the observations on the other (Di Luca et al., 2015):

$$Added\,Value = d(X_{GCM}, X_{OBS}) - d(X_{RCM}, X_{OBS}) \tag{4.1}$$

An increase in the resolution of climate models is expected to lead to a more accurate and realistic representation of the climate system (Sakamoto et al., 2010; Watterson et al., 2014). The use of finer computational grids allows for an explicit reproduction of small-scale processes that are precluded in low-resolution models, such as mesoscale circulations, surface processes related to better reproduced surface fields (e.g. topography, coastal lines, etc.), and the development of specific hydrodynamics instabilities (Di Luca et al., 2013, 2015).

Nevertheless, a fundamental issue that needs to be addressed is whether RCMs add value to the investigation of climate change (Tselioudis et al., 2012). In fact, the arguments for the fine-scale features of the climate change signal are not the same as those asserted for the climate itself (Di Luca et al., 2013). One example could help in better comprehend this difference. *Added Value* in mountainous regions in present climate simulations could result from a more accurate representation of terrain elevation, as a consequence of higher resolution. Due to the relation between temperature and terrain elevation, simulated temperatures would also be improved in this case. Nevertheless, this mechanism may not generate *Added Value* in the climate change signal because its effects could be neutralized when the difference between two periods climate statistics are computed (Di Luca et al., 2013).

The evaluation of the *Added Value* of RCMs in simulating climate change is not an easy task. It often depends on the scale, region of interest, variable, considered statistics, specific application, and experiment configuration (Torma et al., 2015). In addition, its assessment often requires the use of high-quality observational data-sets, which are not available for many regions of the globe, in particular for paleoclimate studies. However, the term

Added Value should not be univocally considered in the way defined before. According to (Rummukainen, 2016), "*Added Value* in regional climate change does not need to be constrained by improved model skill. This does not mean that such information would be without utility; nor that demonstration of *Added Value* would not be valuable, but the issue at hand for the users has several dimensions in addition to the climate modeler's ones. For many applications, the additional spatial and temporal detail from RCMs constitutes added value" (Rummukainen, 2016).

In our analysis we try to estimate the possible added value of a regional climate model for the simulation of past climatic changes over Europe. Here we want to state that the analyses we propose are not exhaustive with respect to the estimation of the added value of regional climate models for the simulation of past climate change. Other proxy datasets and different GCM-RCM couples should be considered. The focus should be also put on different regions and periods of study. Nevertheless, we aim at introducing results that could be considered as the basis for further and future analyses.

4.3 Pollen-Based Reconstructions

The results of the mid-to-late Holocene simulations are compared against the dataset of Mauri et al. (2015). This is the latest updated pollen-based climate reconstruction dataset for Europe and constitutes an upgrade of the results of Davis et al. (2003). It is derived with the same methodology, but with a wider number of fossil and surface-samples, following a more rigorous quality control. The data cover a time slice every millennium for the entire Holocene and are derived through a 4-dimensional spline-interpolation in time and space. They are deduced with an analogue transform method and corrected with postglacial isostatic readjustment. Along with the data, a standard error estimate derived from the transform and the interpolation methods is also provided. Reconstructions contain information on seasonal (winter and summer) and annual values of precipitation and temperature, as well as a measure of moisture balance (i.e. precipitation minus evaporation) and of growing degree days above 5^oC (GDD5), and are provided on a regular grid with a resolution of 1×1 longitude degrees. The data represent the anomalies calculated, for each investigated period of time, with respect to the pre-industrial period. Uncertainties are provided only for seasonal values of temperature and precipitation anomalies.

The dataset of Mauri et al. (2015) constitutes a solid and valuable resource for the purposes of this study, due to a series of different reasons. First of all, it allows to perform a comparison against the model results

over most of the simulation domain, considering different variables. Then, it covers exactly the same time slices of our model simulations: no other dataset has this temporal and spatial coverage at such high spatial resolution. Additionally, the robustness of the data has been thoroughly tested, in Mauri et al. (2015), against other proxies (including chironomids, $\delta^{18}O$ from speleothems and lake ostracods, bog-oaks, glacio-lacustrine sediments, wood anatomy and other pollen reconstructions based on different reconstruction methods) leading to satisfactory results. Nonetheless, similar pollen-based climatic reconstructions have been extensively employed in other data-model comparisons, and, most recently, for the evaluation of the climate models of the Paleoclimate Modeling Intercomparison Project phase 3 (PMIP3) and the Coupled Model Intercomparison Project phase 5 (CMIP5) included in the last Intergovernmental Panel on Climate Change (IPCC) report (Harrison et al., 2015; Stocker et al., 2013). The map of the data from which the dataset of Mauri et al. (2015) is derived is presented in Fig. 4.1. Analysis are conducted on seasonal values of temperature and precipitation, GDD5 and moisture balance.

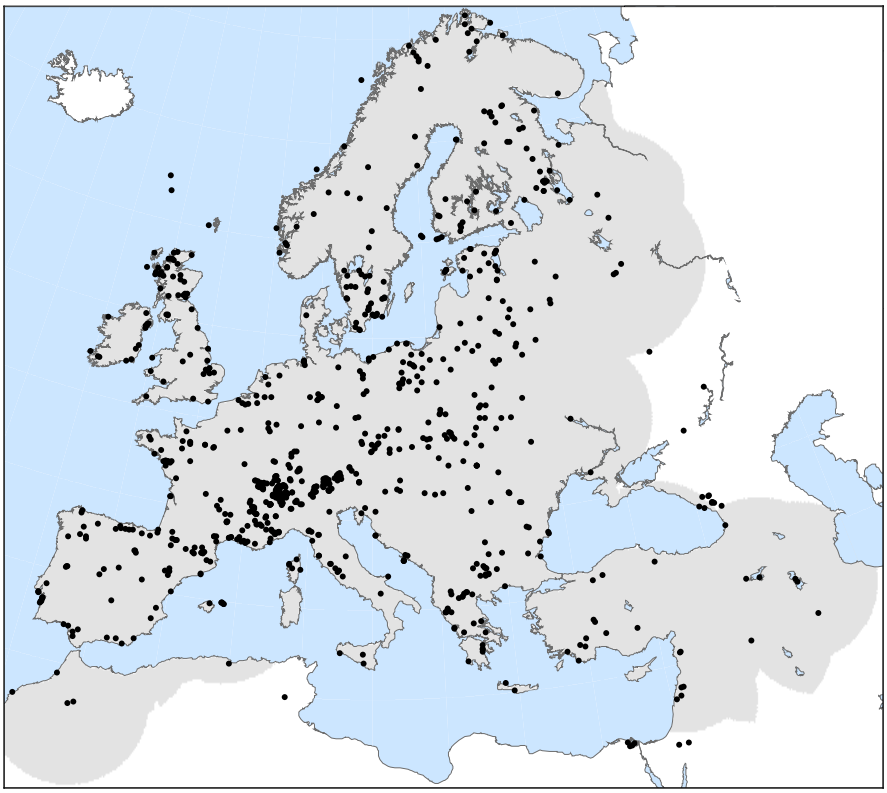

Figure 4.1: *Maps of the sites of the pollen-reconstructions employed by Mauri et al. (2015).*

4.4 Models-Proxies Comparison

4.4.1 Qualitative Analysis

In order to compare the signal of climate change as reproduced by the hierarchy of the three different climate models of our experimental setup and the mentioned proxy-reconstructions, we firstly employ a simple qualitative approach.

In Fig. 4.2 and 4.3, we present the anomalies of summer and winter seasonal mean between 6000BP and the pre-industrial period as reproduced by the different models, respectively for near surface temperature and precipitation. From these maps we first notice that for both the seasons a similar signal of climate change is present for all the simulations. This is expected, since, in every case, the data are constrained by the coarser resolution models. To a large extent, the climate variability of the driving GCM determines the variability of the climate produced by the RCM. Although regional climate models in general can improve on the details of GCM simulations through dynamical downscaling over complex terrain, they cannot, for example, improve upon or make substantial changes to features of the large-scale circulation or SSTs produced by a GCM. This means that, for example, if the jet stream is incorrectly placed in a GCM, it also will be incorrectly placed in the RCM (Di Luca et al., 2012, 2013, 2015).

Nevertheless, while the higher resolved simulations capture a warmer bias over northern Europe in winter, also present in the proxy data, the ECHO-G does not present such behaviour. Better defined patterns and more detailed information are also evident in the precipitation maps derived from the higher resolution models. Additionally, the land-sea area in the ECHO-G is considerably different than the ones of the other models. Regions such as southern Spain, the Black Sea area, southern Italy and Scandinavia are partly or completely masked-out in this case.

Consequently, we focus further analyses on the comparison between the ECHAM5 and the CCLM results. In both seasons additional details are easily detectable in the CCLM pattern. The coastline is also better reproduced in this case, resulting in a better detailed representation of the land-sea contrast and a more precise reproduction of surface processes, leading to more suitable information for possible comparison against proxy-data. Additionally, the CCLM shows better defined patterns as a consequence of higher resolution, being able to discriminate higher spatial variability.

On the base of such analysis, in the successive step, we try to quantify how better the CCLM reproduces the reconstructed climate parameters in comparison to the ECHAM5.

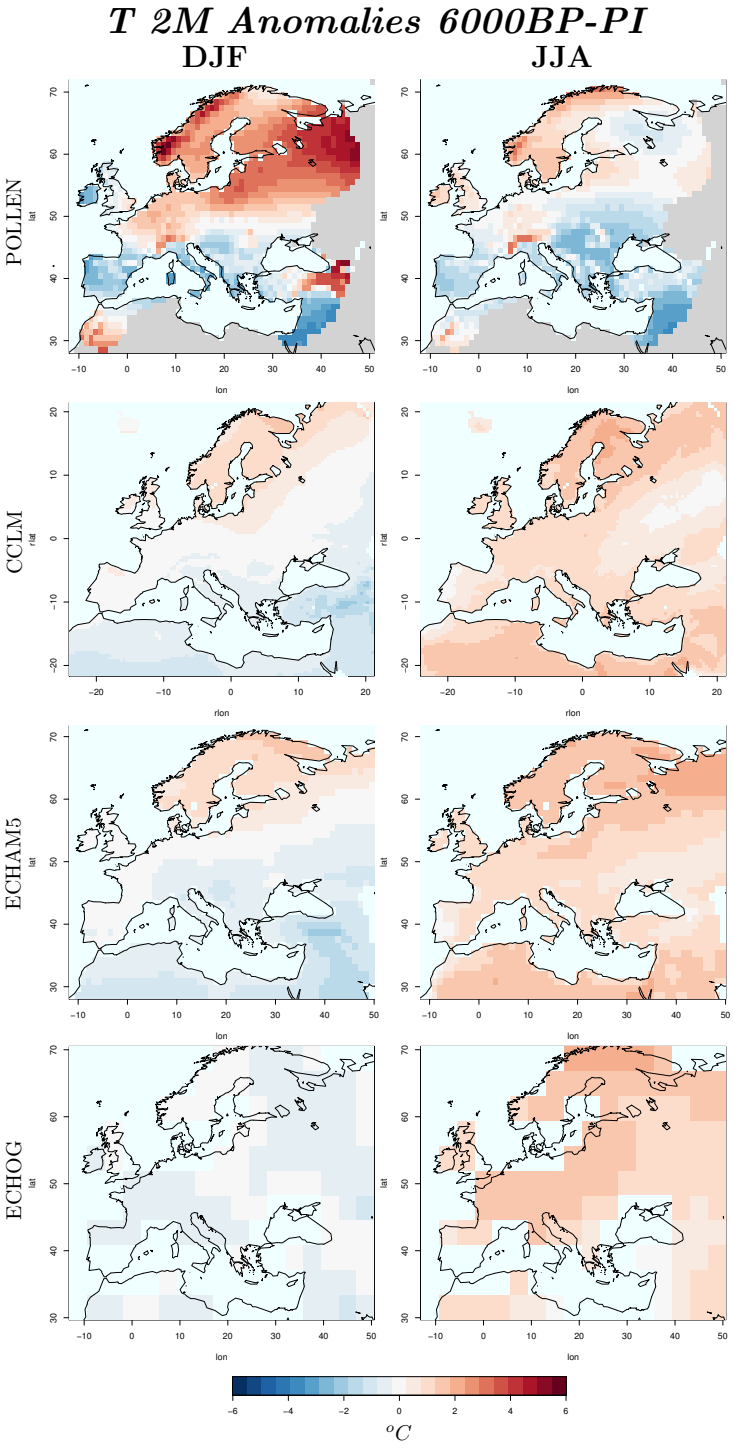

Figure 4.2: *Maps of Winter (left) and Summer (right) near surface temperature anomalies between 6000BP and the preindustrial period. The results of the pollen-based reconstructions of Mauri et al. (2015) (1^st row) and three different models are presented: CCLM (2^{nd} row), ECHAM5 (3^rd row), ECHO-G (4^{th} row).*

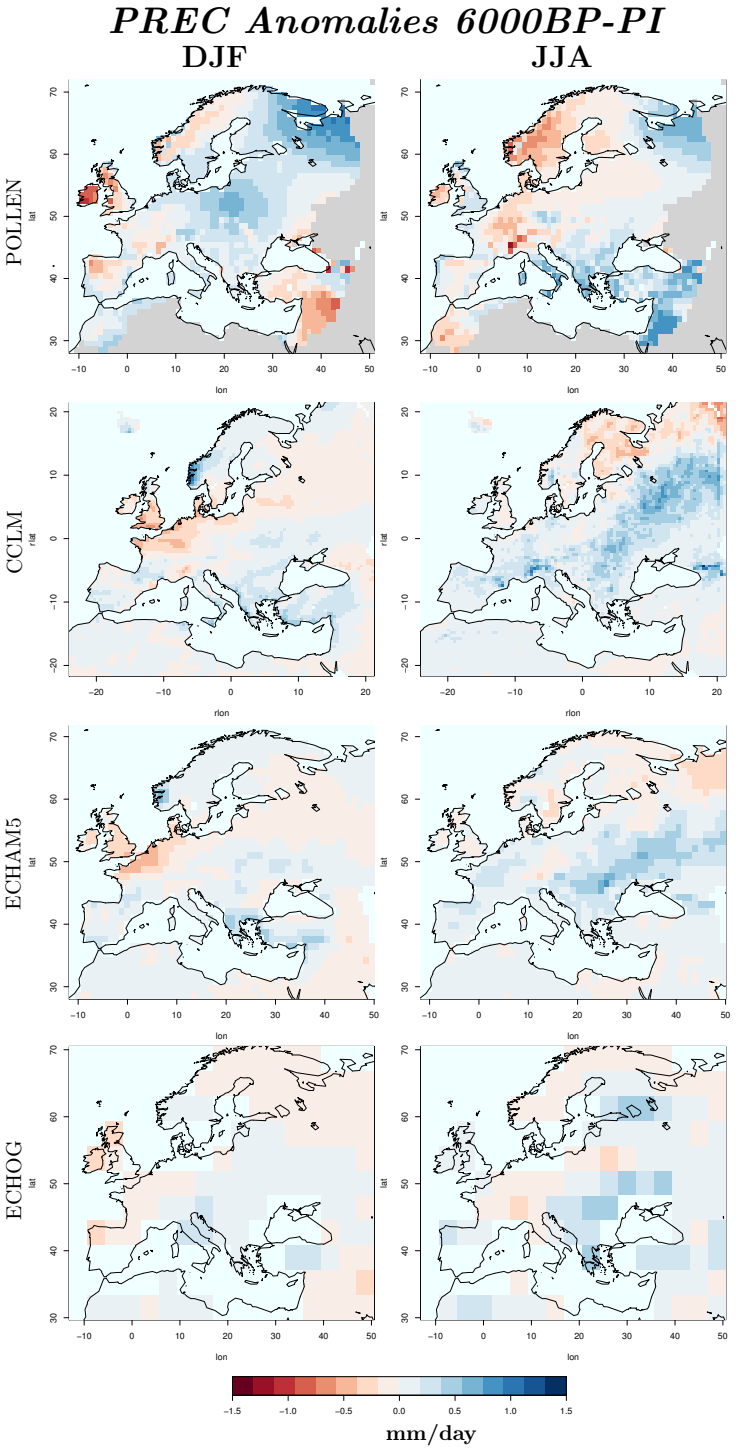

Figure 4.3: *Maps of Winter (left) and Summer (right) precipitation anomalies between 6000BP and the pre-industrial period. The results of the pollen-based reconstructions of Mauri et al. (2015) (1^st row) and three different models are presented: CCLM (2^{nd} row), ECHAM5 (3^rd row), ECHO-G (4^{th} row).*

4.4.2 Quantitative Analysis

Before providing further details on the applied method, we have to acknowledge the fact that proxy-reconstructions cannot be considered strictly as "observations". Nevertheless, we rely on them as plausible records of past climatic changes. Indeed, for the quantitative comparison of the CCLM and the ECHAM5 results against the reconstructions, we use an approach similar to the one employed by Zhang et al. (2010), and based on the work of Goosse et al. (2006). After regridding the CCLM and the ECHAM5 results on the reconstructions grid, we introduce a Cost Function defined as:

$$CF^k_{mod} = \sqrt{\frac{1}{n}\sum_{i=1}^{n} \omega_i{}^k (T^k_{rec,i} - T^k_{mod,i})^2} \tag{4.2}$$

where CF^k_{mod} is the value of the cost function for each considered time slice k of the mid-to-late Holocene and each model *mod*. The parameter n represents the number of the reconstructions grid boxes. $T^k_{rec,i}$ is the temperature of the proxy-data at every location i, while $T^k_{mod,i}$ is the corresponding temperature of the model simulation. Additionally, the parameter w^k_i takes into account the uncertainties of the reconstructions at every location and time period. Its value is given by:

$$\omega^k_i = \frac{1}{(SE^k_i)^2 + 1} \tag{4.3}$$

where SE_i represents the standard error of the reconstructions at every grid box i. The corresponding uncertainties of the model results are considerably small ($\sim 0.01^oC$ for T 2M) in comparison to the ones of the reconstructions, similarly to Goosse et al. (2006), and are indeed neglected. With the introduction of the parameter w^k_i, reconstructions with higher uncertainties will contribute less in the calculation of the Cost Function.

Before providing the calculation of the cost function relatively to each dataset and for every variable, in a first step we scale the values of the anomalies between the two different datasetes and the proxy-reconstructions, joint together, to the range [-1,1]. This is done in order to better compare the values of the cost function computed for the different variables.

The interpolation of the data is performed through bilinear interpolation in the case of temperature and GDD5, and using a distance-weighted average remapping method for precipitation and moisture content. In both cases the respective functions implemented in the Climate Data Operators software (CDO, https://code.zmaw.de/projects/cdo) are employed. We carefully compared several other available interpolation methods in the CDO soft-

ware, such as bicubic (REMAPBIC), and field conserving (REMAPCON), and found that, in the different cases, the selected ones produce the most consistent spatial patterns across resolutions. Additionally, we found that in these two cases the area averaged values of the variables are conserved with an error of $\sim 2\%$ between 0.44^o and 1^o and of $\sim 6\%$ between 1.125^o and 1^o. These errors are similar to those found, for example, with the REMAPCON method. We thus conclude that the choice of the interpolation procedure does not affect the main conclusions of our work, although we recognize that some uncertainty is present due to the specific interpolation method employed.

The values of the Cost Function for the two models and all the time slices are provided in Tab. 4.1, 4.2 and 4.3. Values closer to 0 indicate a better agreement with proxy reconstructions.

For temperatures, even if differences are not particularly remarkable, the Cost Function computed for the CCLM is in almost all the cases smaller than the ECHAM5 one. The CCLM results are, in some cases, closer by more than 10% to the values of the reconstructions.

For precipitation, on the other hand, the situation is inverted. The ECHAM5 results are in slightly better agreement with the pollen-based reconstructions in most of the cases, while the CCLM results are worse in some case up to 10%. This is expected, as the signal of climate change for precipitation is mainly constrained by the coarse-resolution driving simulation, in particular by patterns of atmospheric circulation. Another additional factor that influences the performance of the models at different resolution is the effect of the patchy nature of rainfall, which are more unevenly distributed at the higher resolution of the RCM (Cressie et al., 2012; Tapiador and Sánchez, 2008; Tapiador et al., 2011). Important to notice is that for precipitation, over a wide part of the domain, the biases between model results and reconstructions are higher than the uncertainties of the pollen (Fig. 4.4).

For the two other variables, moisture content and GDD5, no uncertainty is provided in the original datasets, and the computations of the CF are made just considering an equal weight of 1 for all the grid-boxes. Results show that, in both the cases, the CFs of the two models are particularly close, although the CCLM seems to perform better with respect to the ECHAM5, in particular for GDD5 (Tab. 4.3). For moisture content, the poorer performance of the CCLM for precipitation seems to be compensated by its better reproduction of surface processes and soil atmosphere flux exchanges, thus leading to a better representation of evaporation fluxes.

Table 4.1: *Winter (left) and summer (right) temperature Cost Function (CF) estimates for the CCLM and the ECHAM5 simulations, calculated for each time slice of the mid-to-late Holocene. Values closer to 0 indicate a better agreement between model results and proxy reconstructions.*

Time Slice	**DJF**		**JJA**	
	CCLM	ECHAM5	CCLM	ECHAM5
6000BP	0.34	0.35	0.59	0.61
5000BP	0.33	0.34	0.45	0.45
4000BP	0.27	0.29	0.39	0.40
3000BP	0.28	0.29	0.38	0.42
2000BP	0.24	0.24	0.26	0.28
1000BP	0.18	0.18	0.23	0.26

Table 4.2: *Winter (left) and summer (right) precipitation Cost Function (CF) estimates for the CCLM and the ECHAM5 simulations, calculated for each time slice of the mid-to-late Holocene. Values closer to 0 indicate a better agreement between model results and proxy reconstructions.*

Time Slice	**DJF**		**JJA**	
	CCLM	ECHAM5	CCLM	ECHAM5
6000BP	0.25	0.24	0.31	0.28
5000BP	0.22	0.21	0.25	0.23
4000BP	0.29	0.29	0.22	0.22
3000BP	0.31	0.30	0.28	0.27
2000BP	0.23	0.22	0.26	0.24
1000BP	0.25	0.24	0.22	0.20

Table 4.3: *Moisture Balance (left) and GDD5 (right) Cost Function (CF) estimates for the CCLM and the ECHAM5 simulations, calculated for each time slice of the mid-to-late Holocene. Values closer to 0 indicate a better agreement between model results and proxy reconstructions.*

Time Slice	**Moist. Balance**		**GDD5**	
	CCLM	ECHAM5	CCLM	ECHAM5
6000BP	0.20	0.21	0.21	0.22
5000BP	0.19	0.19	0.13	0.13
4000BP	0.26	0.26	0.12	0.12
3000BP	0.22	0.23	0.17	0.17
2000BP	0.20	0.20	0.12	0.13
1000BP	0.19	0.19	0.14	0.15

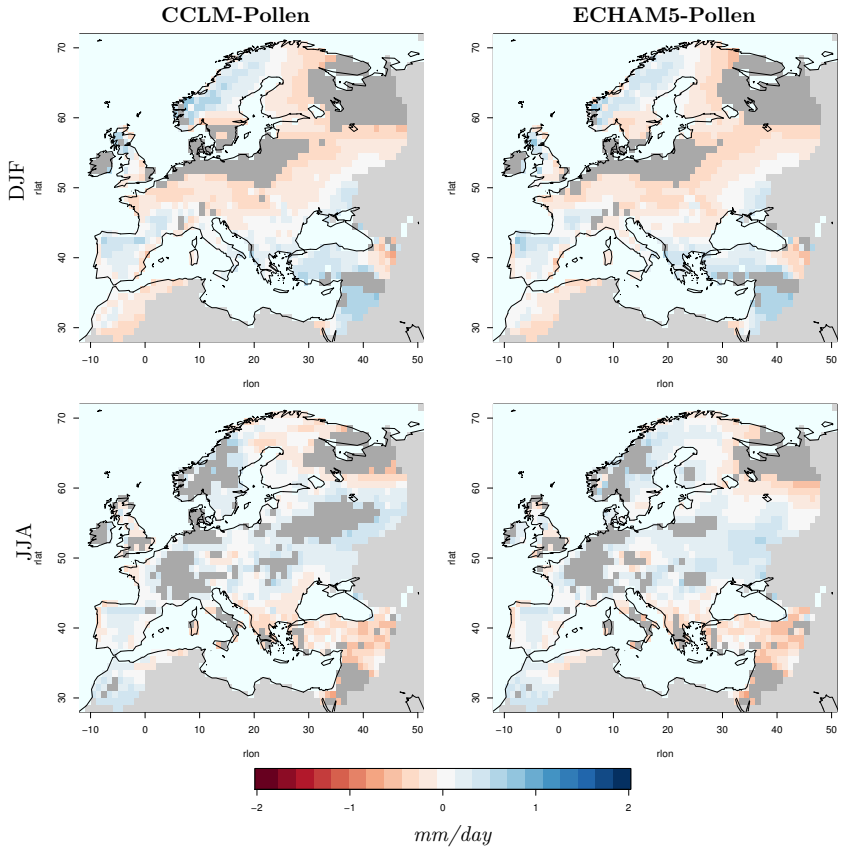

Figure 4.4: *Maps of precipitation anomalies between the two models and the pollen-based reconstructions for the 6000 BP time-slice. The dark-gray shaded areas represent areas where the differences between the pollen-data and models exceed the Standard Error (SE) of the reconstruction.*

4.5 Conclusions

In this chapter, a mid-to-late Holocene pollen-based European climate reconstruction dataset is used as a benchmark for the estimation of the added value of the CCLM with respect to its driving models, the ECHO-G and the ECHAM5. The main goal is to contribute to the estimation of whether RCMs are a better suitable tool for the simulation of past climate change than their driving GCMs.

Results show that the reproduction of the mid-to-late Holocene European climate change signal through dynamical downscaling does not always lead to an improvement of the results of the driving GCMs with respect to the considered reconstructions. While for some variables, such as temperature, an improvement is evident, for others the gain is either modest or negative,

as in the case of precipitation.

Different studies have demonstrated that RCMs do not generate *Added Value* in an unequivocal way and that it depends on several factors such as the variable, the season, the region of study and the specific climate statistics taken into consideration (Di Luca et al., 2013; Prömmel et al., 2010). With this respect, it is important to mention that the scale of the reconstructions considered in our analysis is closer to the resolution of the ECHAM5 than the one of the CCLM and of the ECHO-G. As suggested by Di Luca et al. (2015), given that the main difference between the GCM and the RCM is related to their horizontal resolution, it seems natural that the results may depend on the spatial scale of the analysis. Additionally, it is crucial to state that the evinced results are relative to this case study, and considering different couples of RCM-GCM and other proxy reconstructions datasets could lead to diferent results. Indeed, in order to better support the evinced results and having a more accurate estimation of the added value of RCMs for the study of past climate change, according to the presented discussion, further investigations are still required.

Nonetheless, the need for higher resolution climate simulations is not only related to the aforementioned scientific arguments. From a different perspective, such results, due to the greater level of detail, could be preferable for studies in which human adaptation or environmental response to past climatic changes would be investigated. The need for climate information at very fine scales, for their application in other fields of research such as archaeological studies or vegetation reconstructions, hence constitutes a strong incentive to perform higher-resolution climate simulations (Di Luca et al., 2015; Rummukainen, 2016).

Chapter 5

Mid-to-Late Holocene Temperature Evolution and Atmospheric Dynamics over Europe in Regional Simulations

"What we observe is not nature itself, but nature exposed to our method of questioning."
- Werner Karl Heisenberg -

5.1 Introduction

In Section 4 we have shown that the CCLM, when compared to climate reconstructions of the mid-to-late Holocene for Europe, does not always lead to an improvement of the results with respect to its driving global circulation model. The skills of the model are different according to the variable taken into consideration. The regional model proved to better reproduce changes in temperature, as reconstructed from the proxies, with respect to the driving global model. For this reason, in this chapter, we focus our attention on the pollen-based reconstructed, and the CCLM-simulated seasonal changes of temperature during the mid-to-late Holocene, in order to shed light into the possible phyisical drivers of such changes. Additionally, we aim at providing physically plausible explanations for eventual mismatches arising in the comparison between the two datasets. Giving an introduction on evidence from other studies, we successively compare the mid-to-late Holocene evolution of seasonal values of near-surface temperature, as represented in the two

datasets. By means of correlations with trends of insolation and changes in atmospherical circulation patterns, we then propose plausible physical interpretation for the evinced trends and mismatches.

5.2 Changes in Insolation and Temperature Evolution

During the mid-to-late Holocene, over northern latitudes in general, changes in the total amount of insolation during the year (with respect to present day conditions) were negligible ($\leq$4.5 W/m^2) when compared to the seasonal variations (up to more than 30 W/m^2 for summer insolation at high latitudes) (Fischer and Jungclaus, 2011) (Fig. 5.1). Therefore, relevant variations in the seasonal values of surface variables are expected. However, evidence shows that reconstructed climatic parameters, such as near surface temperature, over Europe, did not always follow directly the astronomical forcings (Bonfils et al., 2004; Braconnot et al., 2007a,b; Cheddadi et al., 1996; Davis et al., 2003; Mauri et al., 2014), but their signal seems to have also been influenced by other complex processes such as atmospheric circulation, geography, or land-surface interactions with the atmosphere.

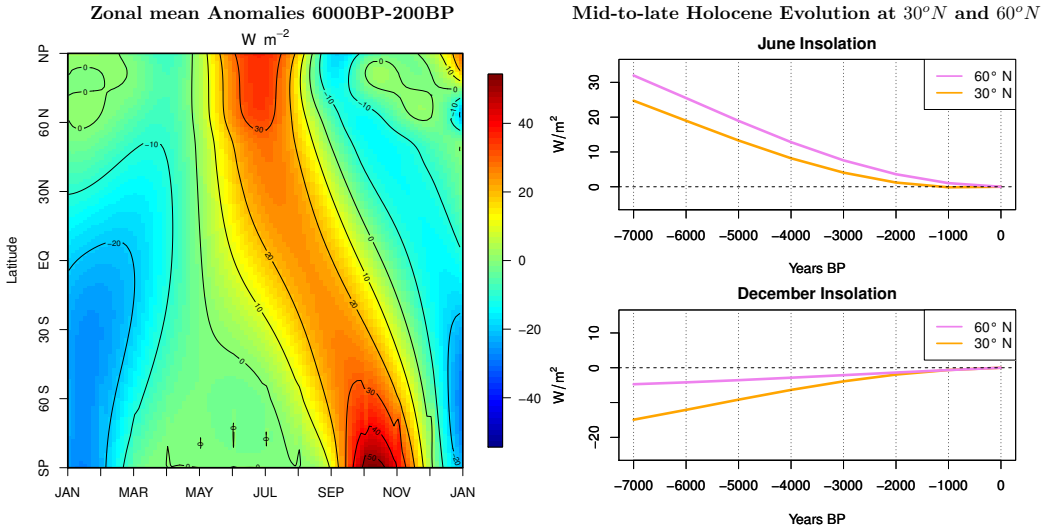

Figure 5.1: *(Left) Anomalies of the zonal mean of Top Of the Atmosphere (TOA) insolation between 6000 years BP and the pre-industrial period. (Right) Mid-to-late Holocene trends of the anomalies, with respect to present-day values, of December and June TOA incoming insolation, calculated for 30 and 60 degrees North (N). Units are W/m^2.*

Different studies have been conducted in order to understand the mechanisms driving the seasonal behaviour of European surface variables during the mid-to-late Holocene. Cheddadi et al. (1996), using the results of a pollen-based reconstruction dataset constrained by lake-level data, showed that summer and winter temperatures over northern and southern Europe were different at the mid-Holocene in comparison to present-day values. In particular, winters were warmer over northern Europe even though the insolation was reduced, while summers were colder over southern Europe, despite the higher insolation. Similar results were obtained by Davis et al. (2003) who provided an updated database of European pollen reconstructions for the entire Holocene. Bonfils et al. (2004), within the PMIP (Joussaume and Taylor, 1995)) collaboration, hypothesized that winter atmospheric patterns and summer soil conditions had an important influence on seasonal changes of temperature and precipitation. This has also been highlighted by a study from Starz et al. (2013) who performed a simulation for the mid-Holocene, with a coupled soil-ocean-atmosphere circulation model and dynamic vegetation, and improved representation of soil water storage and heat fluxes. They found that changes in the soil's physical properties of the model led to improved results and hampered biases, with respect to proxy-data, in surface variables. Fischer and Jungclaus (2011) studied the evolution of the European seasonal temperature cycle in a transient mid-to-late Holocene simulation with an AOGCM. They were unable to reproduce correctly the reconstructed data over the entire region of study. In particular, their results presented only a weak shift to a positive phase of the NAO at the mid-Holocene in winter, resulting in colder conditions over northern Europe and warmer over southern Europe, when compared to the values of reconstructions. In summer, again, the signal seemed to be mainly driven by changes in insolation, resulting in generally warmer conditions over the entire domain and period of study. Conversely, in their recent work, Mauri et al. (2014) suggested that the different response of surface variables at the mid-Holocene was most likely related to changes in atmospheric circulation, both in winter and in summer. Specifically, they proposed that in summer a major occurence of the "Scandinavian High" was most probably the reason for colder temperatures over southern Europe 6000 years ago. In winter, on the contrary, a more positive phase of the NAO would have been responsible for warmer and wetter conditions over northern Europe and an opposite behaviour in the South. Although these interpretations are all physically plausible, a general consensus is still missing on the correct explanation of the response of the climate system to changes in insolation for this period.

5.3 Methods

For the purposes of this study we adopt different statistical techniques. First of all, for the investigation of the trends of near-surface temperature in the two datasets, we use a weighted least squares linear regression method. Weighted least squares is an efficient method that makes good use of small data sets with different uncertainties. More specifically, the method of ordinary least squares assumes that there is constant variance in the errors (i.e. homoscedasticity). But this not always holds true: measurements may have different uncertanties. Weighted least squares is an estimation technique which weights the observation and so overcomes the issue of non-constant variance (Brunsdon et al., 1996; Cleveland and Devlin, 1988).

In weighted least squares parameter estimation, as in regular least squares, the unknown values of the parameters in the regression function are estimated by finding the numerical values that minimize the sum of the squared deviations between the observed responses and the functional portion of the model. Unlike least squares, however, each term in the weighted least squares criterion includes an additional weight, w_i, that determines how much each observation in the dataset influences the final parameter estimates. The weighted least squares criterion that is minimized to obtain the parameter estimates is

$$Q = \sum_{i=1}^{n} \omega_i [y_i - f(x_i; \beta)]^2 \tag{5.1}$$

Where β is the parameter to be estimated. x_i and y_i are the coordinates of the data point i and w_i its relative weight.

If the standard deviation in the data is not constant across all the explanatory variables, using weighted least squares with weights inversely proportional to the variance of the explanatory variable, yields the most precise parameter estimates possible.

In a second step, in order to investigate possible correlation between changes in near-surface temperature and atmospheric dynamics during the mid-to-late Holocene, we make use of a particular technique: Canonical Correlation Analysis (CCA). CCA is a statistical technique that helps to identify spatial patterns of maximum correlation between climate variables, indicating potential underlying physical mechanisms (Gómez-Navarro et al., 2015; Russo and Cubasch, 2016; von Storch and Zwiers, 1995; Wilks, 1995). If we have two vectors X = (X1, ..., Xn) and Y = (Y1, ..., Ym) of random variables, and there are correlations among the variables, then canonical-correlation analysis will find linear combinations of the Xi and Yj which have

maximum correlation with each other (Härdle and Simar, 2007).

Just as Empirical Orthogonal Function (EOF) analysis is used to study the variability of a random vector X, CCA is used to study the correlation structure of a pair of random vectors X and Y. As specified in von Storch and Zwiers (1995), the main goal of CCA is to find a pair of patterns $\vec{f}_X^1$ and $\vec{f}_Y^1$ (subject to $\|\vec{f}_X^1\| = \|\vec{f}_Y^1\|$) so that the correlation between linear combinations $\vec{X}^T\vec{f}_X^1$ and $\vec{Y}^T\vec{f}_Y^1$ is maximized. Afterwards, a second pair of patterns $\vec{f}_X^2$ and $\vec{f}_Y^2$ is found so that $\vec{X}^T\vec{f}_X^2$ and $\vec{Y}^T\vec{f}_Y^2$ are the most strongly correlated linear combinations of X and Y that are not correlated with $\vec{X}^T\vec{f}_X^1$ and $\vec{X}^T\vec{f}_X^1$, and so on (von Storch and Zwiers, 1995). Canonical Correlation Analysis was first described by Hotelling (1935).

In CCA, according to Gómez-Navarro et al. (2015), "from a physical point of view, the leading patterns should show similar characteristics when the mechanisms leading to the relationships between the climate fields are controlled by the same processes". Indeed, CCA is particularly suitable for our purposes.

In our analysis we adopt the method of Barnett and Preisendorfer (1987) in which an EOF analysis is conducted prior to the CCA, retaining only a few leading EOFs, in order to remove part of the random noise from the data. More specifically, after conducting the EOF analysis on the anomalies, with respect to the pre-industrial period, of Mean Sea Level Pressure (MSLP) and T 2M, we select the first eight Principal Components (PCs) of both the variables in winter, and the first eight and twelve principal components of, respectively, MSLP and T 2M in summer. In this way, in both the cases, the selected PCs will explain approximately 80% of the total variance in the original datasets. We then apply the CCA analysis on the retrieved PCs.

5.4 Model and Proxies Behaviour

In a first instance, we directly investigate the anomalies between the model results and the pollen-based reconstructions.

Fig. 5.2 and 5.3 present, respectively, the winter and summer seasonal temperature anomalies between the two datasets. These are calculated after upscaling the CCLM results on the grid of the pollen-based reconstructions for every time slice of the mid-to-late Holocene, by bilinear interpolation. Additionally, they are accompanied by the maps of the corresponding pollen uncertainties.

In winter generally colder conditions are reproduced by the model over northern continental Europe, with slightly warm biases over most of the South (Fig. 5.2). In Scandinavia a negative bias is present at 6000 and 5000

BP, after which the situation then reverses. In this case, the bias is indicative of a different temporal evolution of the two datasets over the area. The largest anomalies (in some cases up to $\sim 4^oC$) are present over northeastern Europe (likely related to high pollen-data uncertainty partly due to the fact that seasonal values derived from pollen in this area are biased towards the winter season) and Turkey.

In Summer CCLM results present positive anomalies over most of the domain, with particularly pronounced values (in some cases larger than 3^oC) over different parts of southern Europe and the Mediterranean Basin (Fig. 5.3). It is evident that the anomalies decrease from 6000 to 1000 BP, following the insolation trend. We have to acknowledge the fact that even if summer uncertainties are smaller than winter ones, in some cases, in particular over southern Europe, they are still remarkable ($\sim 2.5^o$). Additionally,

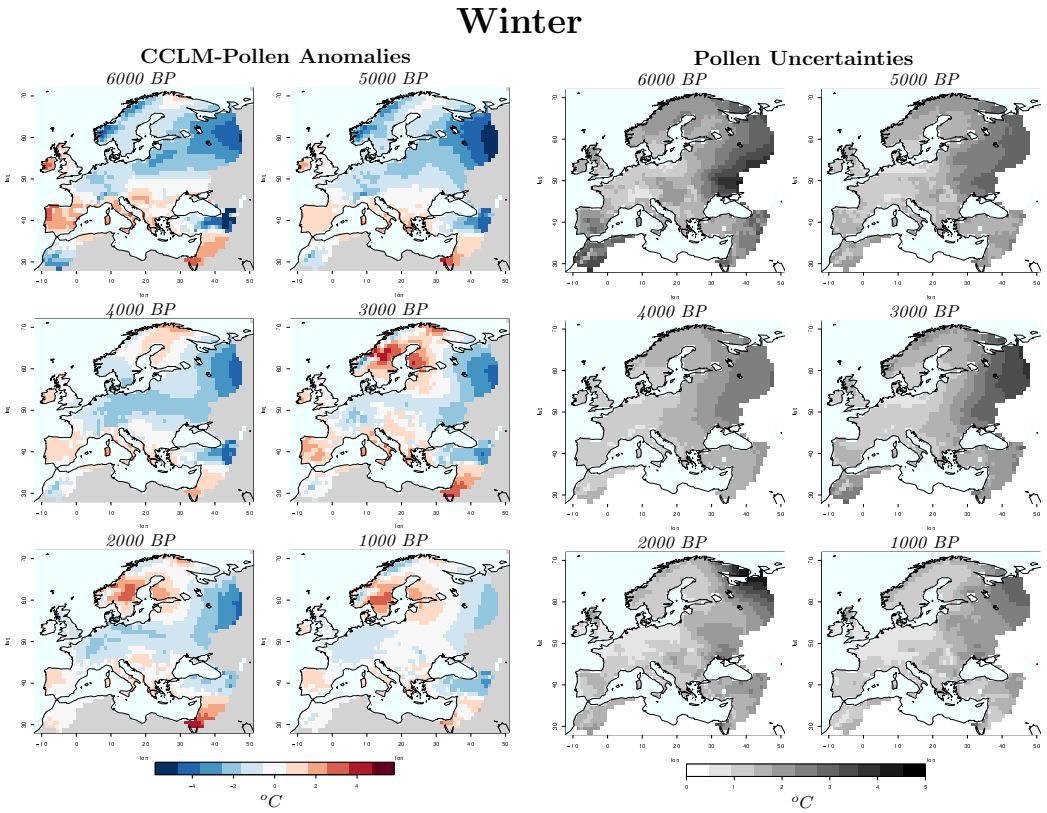

Figure 5.2: *(Left) Maps of winter 2 meters temperature anomalies between CCLM results and the Pollen-based reconstructions of Mauri et al. (2015) for the different time slices of the mid-to-late Holocene. (Right) Standard error of winter temperature seasonal mean derived from the pollen-based reconstructions of Mauri et al. (2015) for each time slice of the mid-to-late Holocene.*

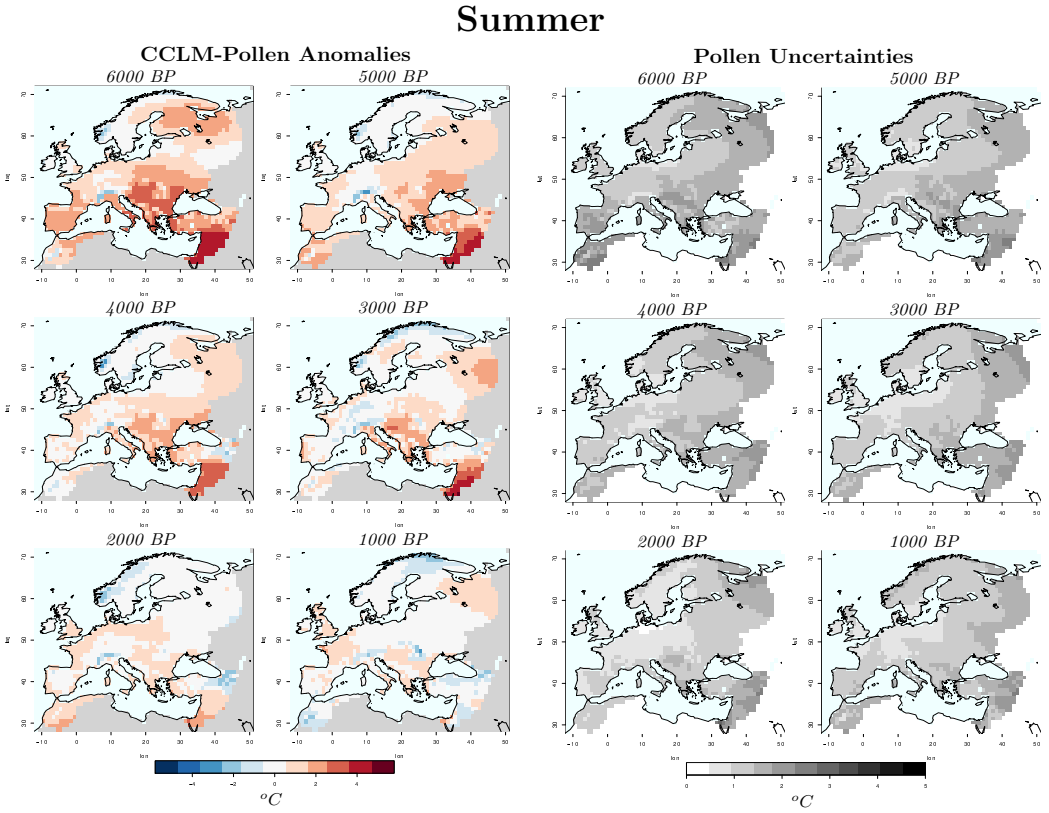

Figure 5.3: *(Left) Maps of summer 2 meters temperature anomalies between CCLM results and the Pollen-based reconstructions of Mauri et al. (2015) for the different time slices of the mid-to-late Holocene. (Right) Standard error of summer temperature seasonal mean derived from the pollen-based reconstructions of Mauri et al. (2015) for each time slice of the mid-to-late Holocene.*

for both the seasons there is a progressive reduction of the uncertainties from 6000 to 1000 BP, reflecting an improvement in the accuracy of the datation of the samples closer to present day.

In addition to the previous analyses, the maps of the trends in temperature anomalies are presented in Fig. 5.4. They show the slope of the mid-to-late Holocene linear trends of temperature anomalies with respect to the pre-industrial period, calculated at every grid box by means of a weighted least squares method, taking into account the contribution of the different uncertainties. The points for which the trends are not significant, according to an F-test at a significance level of 10%, are masked out in grey. From these maps we see that, in winter, even if over part of southern Europe the two datasets present similar trends, their behaviour is different in the North: CCLM results show no significant trend (Fig. 5.4a), while the pollen-based

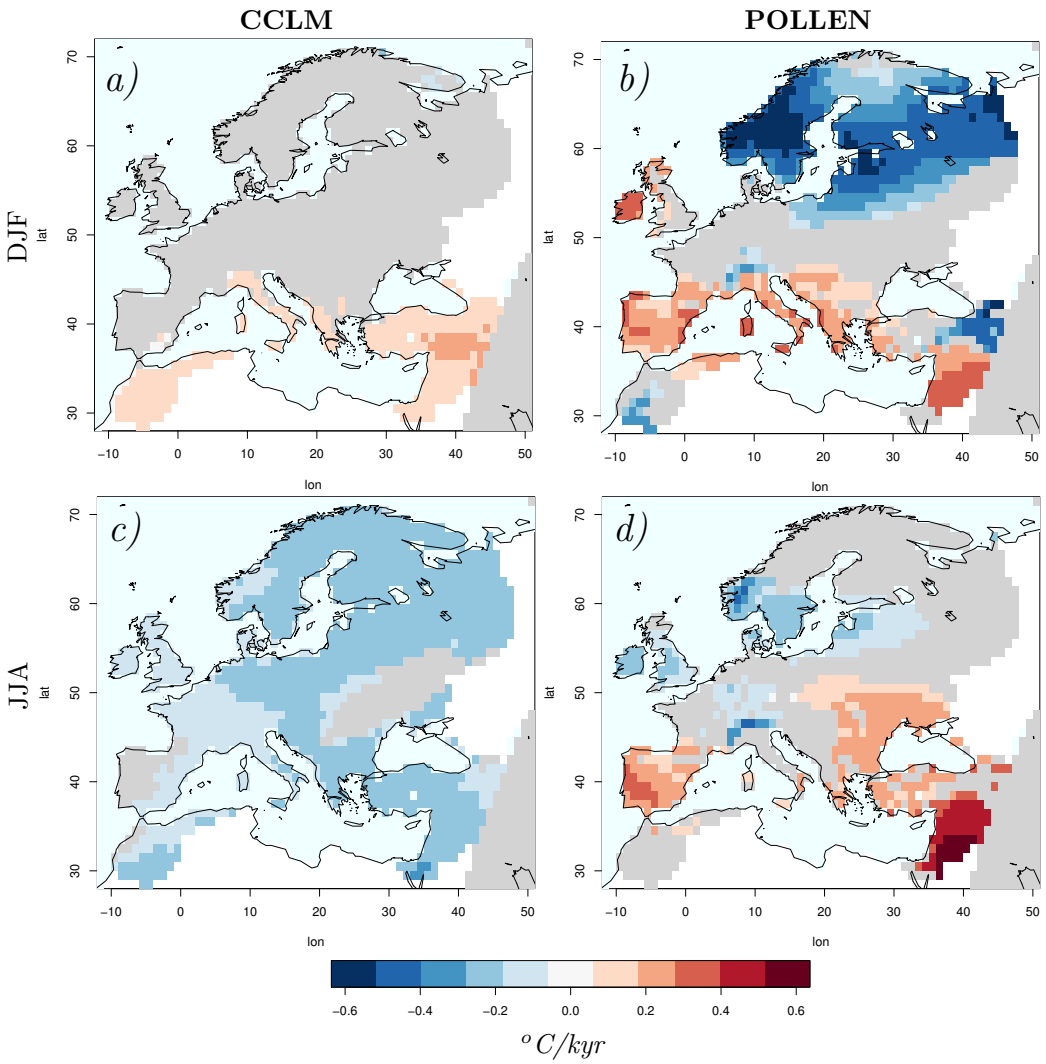

Figure 5.4: *Mid-to-late Holocene temporal evolution of the anomalies, with respect to the pre-industrial period, of near-surface temperature of winter (first row) and summer (second row) seasonal means. Values from the CCLM simulations are presented on the left and the ones from the pollen-based reconstructions of Mauri et al. (2015) on the right. The maps show the slopes of the linear trends calculated, for every grid box, taking into consideration the uncertainties associated to the two datasets by means of a weighted least squares method. The area masked out in grey indicates the area where the trends are not significant, according to an F-test at a significance level of 10%.*

reconstructions present significantly decreasing temperatures over a considerable part of the domain (Fig. 5.4b). In particular, over Scandinavia, while the pollen-based reconstructions show a strong, significant cooling trend, no significant trend is evident for the model results.

Conversely, in summer, the model results are characterized by a negative trend over most of the domain (Fig. 5.4c), highly correlated to changes in insolation. The pollen data, instead, show a significant negative trend similar to the CCLM results over part of northern Europe only, and an opposite positive trend over most of southern Europe (Fig. 5.4d).

5.5 Changes in Atmospheric Circulation

Changes in atmospheric circulation have often been suggested as possible drivers of temperature evolution during the mid-to-late Holocene winters and summers (Bonfils et al., 2004; Braconnot et al., 2007b; Fischer and Jungclaus, 2011; Mauri et al., 2014). In order to obtain further insights into the causes of the evinced model bias, in a second step we investigate simulated changes in atmospheric circulation and their effects on the evolution of near-surface temperature, by means of CCA. The analysis is conducted on the anomalies, with respect to the pre-industrial period, of seasonal values of MSLP and T 2M. Fig. 5.5 and 5.6 show the first two canonical pairs of patterns with the largest canonical correlation for both winter and summer.

The MSLP pattern explaining most of the variance, in winter, resembles the NAO (Fig. 5.5c). The model seems to reproduce well the spatial pattern of the NAO when compared to other studies (Gómez-Navarro et al., 2015). Nevertheless, the trend of the temporal evolution of its expansion coefficients (Fig. 5.7c), seems not to be pronounced enough in order to reproduce a response in temperatures comparable with the respective results of pollen data. Additionally, the value of the canonical correlation, even if high, is slightly smaller than the one of a secondary mode of atmospheric variability, in this case represented by a blocking system centered over the Baltic Sea. The trend of the expansion coefficients of this pattern is again not particularly pronounced (Fig. 5.7a). As a result of the combined effects of the evinced patterns of atmospheric variability, the CCLM temperature trends will be significant only over part of Southern Europe.

In summer, the first CCA pair (Fig. 5.6a, 5.6b) is highly related to changes in insolation (Fig. 5.1, 5.7b). It is key to note that the first canonical pattern of summer MSLP anomalies seems to be a proper product of this particular case study and is most likely due to the different response of land and sea masses to the changes in insolation. Even if it implies changes in circula-

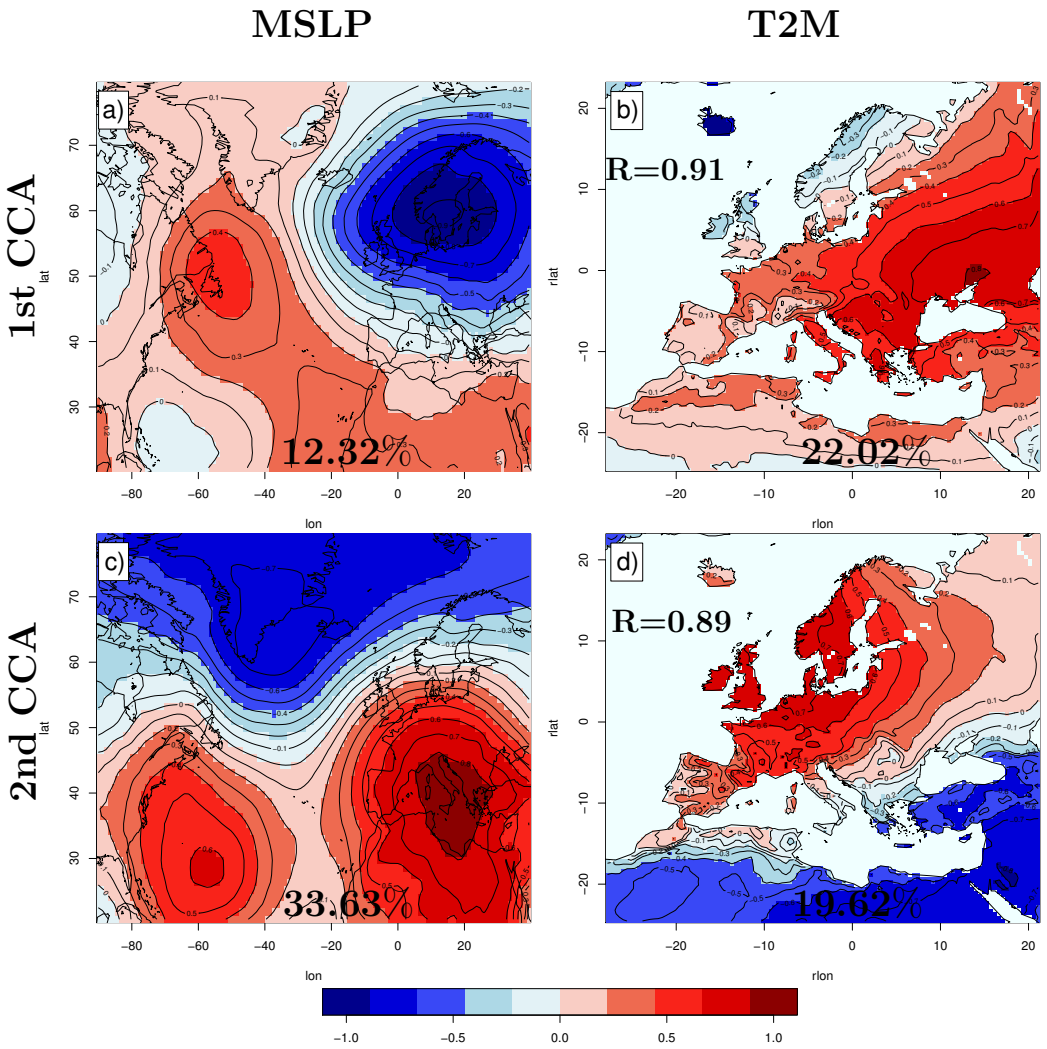

Figure 5.5: *First (a, b) and second (c, d) canonical correlation pattern pairs of MSLP (left) and T 2M (right) in winter, calculated accordingly to the Barnett and Preisendorfer (1987) method. Each panel illustrates the percentage of variance explained by the patterns and the canonical correlation associated with the pair. The results are calculated for the mid-to-late Holocene, from 6000BP to pre-industrial times. Note that the MSLP has been obtained directly from the driving GCM, since the window of interest lies outside the RCM domain. For both the variables the analysis has been conducted on the standardized anomalies with respect to the pre-industrial period. Red (blue) areas indicate positive (negative) correlations, for each grid point, between the data and the corresponding canonical score series.*

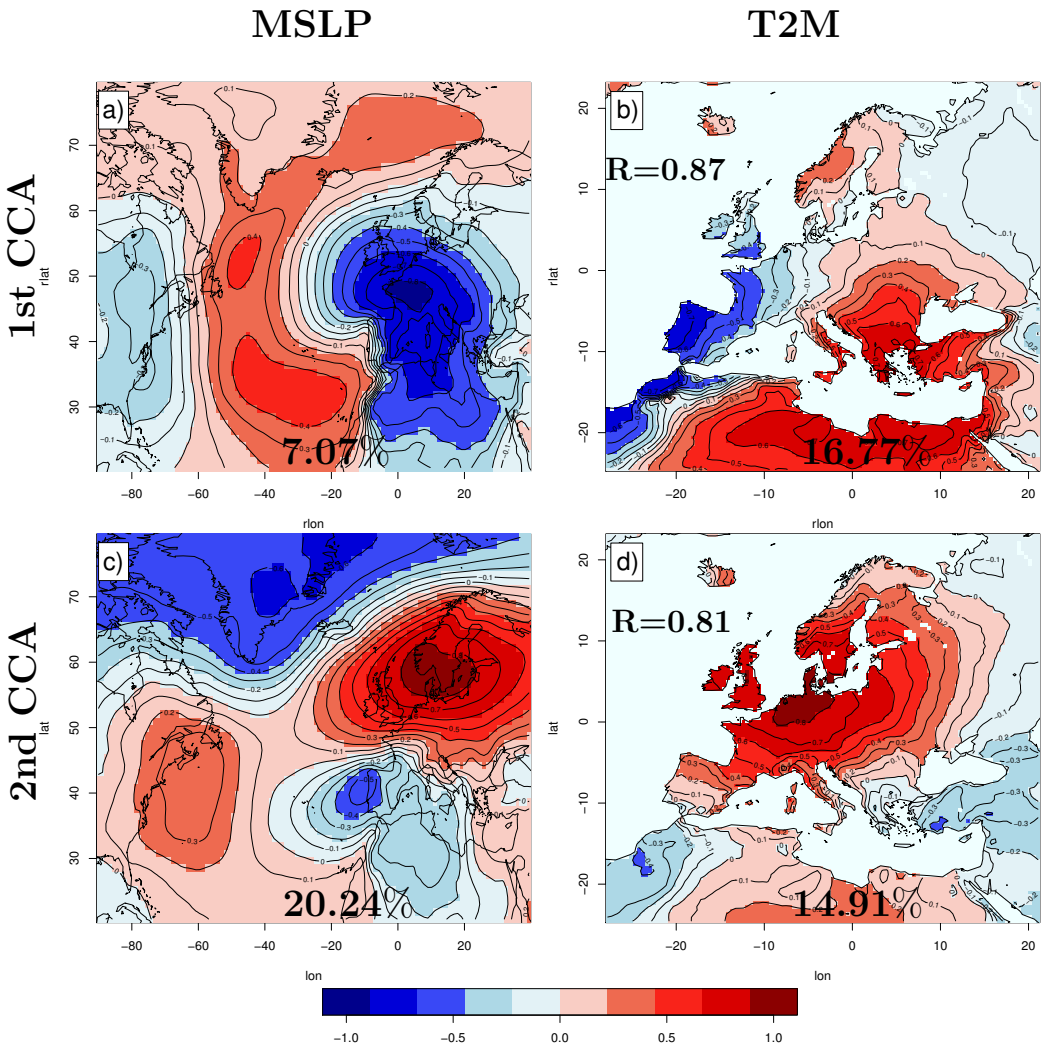

Figure 5.6: *First (a, b) and second (c, d) canonical correlation pattern pairs of MSLP (left) and T 2M (right) in summer, calculated accordingly to the Barnett and Preisendorfer (1987) method. Each panel illustrates the percentage of variance explained by the patterns and the canonical correlation associated with the pair. The results are calculated for the mid-to-late Holocene, from 6000BP to pre-industrial times. Note that the MSLP has been obtained directly from the driving GCM, since the window of interest lies outside the RCM domain. For both the variables the analysis has been conducted on the standardized anomalies with respect to the pre-industrial period. Red (blue) areas indicate positive (negative) correlations, for each grid point, between the data and the corresponding canonical score series.*

tion, we do not see any particularly prominent dipole structure characteristic of other well-known circulation patterns for the region. Its effects on temperature are particularly high on the Atlantic Coast of continental Europe, resulting in a smoothing of the trend of summer temperature over this region.

In the second CCA pair, the pattern of the MSLP (Fig. 5.6c) resembles the positive phase of the summer NAO (Folland et al., 2009). The trend (Fig. 5.7d) of its expansion coefficients is again not particularly pronounced. As a consequence, the changes in the corresponding temperature pattern (Fig. 5.7d) are also not paticularly strong. Even if, according to the pattern of changes in temperature arising from the pollen-based reconstructions, the hypothesis of Mauri et al. (2015) of a major influence of secondary modes of atmospheric variability, such as the Scandinavian high, seems to be plausible, based on the model results and on the evidence of other studies (Bonfils et al., 2004; Starz et al., 2013) we suggest that in summer, during the mid-to-late Holocene, the changes in circulation alone would not have been enough to explain the variations in near surface temperature, as reconstructed from the proxies.

While over northern Europe the relatively good agreement between the temperature of the two datasets over part of the domain suggests that for this region the insolation is probably the main driver of changes, for southern Europe, however, the role of land-atmosphere coupling needs to be considered, as also suggested in other studies (Seneviratne et al., 2006).

According to Bonfils et al. (2004) and Starz et al. (2013), over southern Europe, the presence of more moisture in the soil during mid-Holocene summer, due probably to more early spring precipitation, is responsible, as a direct effect of higher insolation, for cooler conditions due to stronger latent heat transfer. According to the mentioned studies and to the previously presented analyses of model's heat-fluxes, we support this interpretation and suggest that the reason why the model does not manage to capture this trend could be most probably related to a wrong simulation of soil-atmosphere heat exchanges. As previously discussed in Sec. 3.1, model deficiencies in the representation of soil-atmosphere fluxes for this area leads to an underestimation of evaporation and, consequently, to drier and warmer conditions. Further experiments, with improved soil properties, are indeed necessary in order to better reproduce soil moisture content, and to obtain more robust results for the comparison against reconstructions.

It is important to mention that the behaviour of the mid-to-late Holocene summer temperature over Europe has been highly debated during recent years. While a dipole behaviour between southern and northern Europe has been suggested by several studies based on pollen analyses (Cheddadi et al., 1996; Davis et al., 2003; Huntley and Prentice, 1988; Mauri et al., 2015;

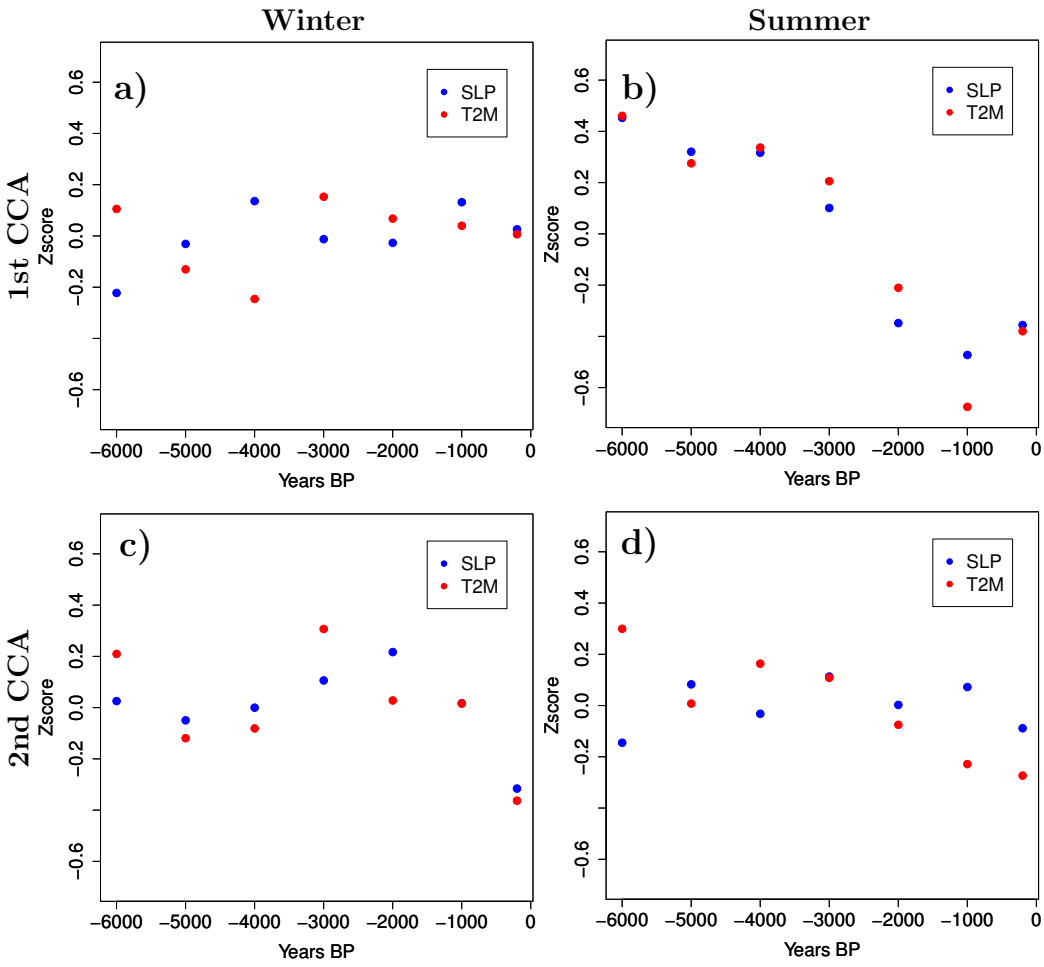

Figure 5.7: *Mean values of the Canonical score series of the first two pairs of Canonical Correlation patterns of MSLP and T 2M for winter (a, c) and summer (b, d) seasonal mean anomalies with respect to the pre-industrial period.*

Prentice et al., 1998) and others relying on a combination of different proxies, such as the one of Magny et al. (2013), which suggested a North-South paleoclimatic contrast in the central Mediterranean during the Holocene, other studies argued against such hypothesis. In particular, Osborne et al. (2000) proposed that reconstructions of summer temperature based on pollen could be erroneous for the Mediterranean region, since here the vegetation distribution is mainly limited by effective precipitation, rather than by summer temperature. The latter hypothesis should be taken into account for the comparison between pollen-based reconstructions and model simulations. Nevertheless, additional investigations have shown that when directly compared to the pollen record, the mid-Holocene vegetation simulated from the output of climate models is way too dry over southern Europe, with an expansion of Mediterranean and steppe/desert vegetation and contraction in forest cover, a direct consequence of simulated warmer conditions (Benito-Garzon et al., 2007; Gallimore et al., 2005; Kleinen et al., 2010; Prentice et al., 1998; Wohlfahrt et al., 2004).

Based on these considerations, recognizing the dataset of Mauri et al. (2015) as a valuable source for the investigation of European temperature evolution during mid-to-late Holocene, we acknowledge the fact that joint efforts from specialists of different disciplines are still required in order to further clarify possible uncertainties.

5.6 Other Modelling Studies

An important benchmark for the comparison of our results against other modelling studies is represented by the outcomes of the PMIP3 experiment (Braconnot et al., 2011), for which several simulations have been performed for the mid-Holocene and the pre-industrial time, with different coupled circulation models. Here, we focus our attention on the results of twelve of the PMIP3 simulations. Specifically, we perform a direct comparison of the regional mean of winter and summer near-surface temperature calculated over northern and southern Europe for the PMIP3 simulations as well as each of ours. The results are presented in Tab. 5.1. The corresponding values derived from the pollen-based reconstructions are also included in the table. Two main features arise from such analysis: first of all common positive anomalies ($\sim +1^oC$) over southern Europe in summer for all the models are evident, while the reconstructions present a negative value ($\sim -1.2^oC$). This indicates that the temperature differences are positive in the model simulations as a result of the higher summer insolation at the mid-Holocene than at the pre-industrial period. Additionally, another feature that seems to be

Table 5.1: *Comparison of regional means of winter (left side) and summer (right side) temperature anomalies, between 6000BP and the pre-industrial period, from different simulations of the PMIP3 experiment and as represented in the ECHO-G, the ECHAM-5 and the CCLM simulations. The corresponding values calculated from the pollen-based reconstructions are also provided. The region considered covers the area in between 55°:72°N and -10°:40°E (northern Europe), and 35°:50°N and -10°:40°E(southern Europe). Units are °C.*

Model	**Winter**		**Summer**	
	North	**South**	**North**	**South**
BCC-CSM1-1	1.09	-0.20	1.62	1.15
CCSM4	-0.68	-0.49	0.97	1.25
CCSM4	-0.63	-0.30	1.24	1.48
CNRM-CM5	1.43	0.29	1.30	1.22
CSIRO-Mk3-6-0	0.70	0.20	1.27	1.75
FGOALS-g2	0.22	-0.99	0.42	0.47
FGOALS-g2	-1.16	-0.21	0.94	1.31
GISS-E2-R	0.43	-0.07	1.25	0.47
IPSL-CM5A-LR	0.58	0.05	1.27	1.32
MIROC-ESM	0.17	-0.48	0.88	1.35
MPI-ESM	-0.47	-0.35	1.28	1.13
MRI-CGCM3	0.25	-0.16	1.04	1.25
CCLM	0.87	-0.23	1.33	0.75
ECHAM5	0.80	-0.37	1.33	0.71
ECHO-G	-0.15	-0.21	1.39	0.73
Pollen	2.40	-0.66	0.58	-1.19

common to all the models is represented by the failure in representing winter anomalies over both northern and southern Europe. This is attributable to a wrong reproduction of changes in the amplitude of the NAO (Fischer and Jungclaus, 2011; Strandberg et al., 2014). While some models present a value similar to the one of reconstructions for southern Europe ($\sim +0.5^oC$), in the North the differences are significant, with the pollen-based reconstructions presenting a warm temperature anomaly ($\sim +2.5^oC$), and the models having slightly positive values (between 0 and $+1^oC$) in some cases, and negative (down to $\sim -1^oC$) in all the others.

5.7 Conclusions

In this chapter, the results of the mid-to-late Holocene CCLM simulations are used in order to investigate the response of the climate system to changes in the seasonal cycle of insolation, with the aim of proposing plausible phyisical interpretation of the mismatches arising in the comparison against the reconstructions.

The results show that over southern Europe, winter temporal evolution and spatial distribution of temperature in the two datasets are comparable. Conversely, the model tends to reproduce generally colder conditions over central and northern continental Europe. The analysis of atmospheric circulation patterns suggests that this bias is due to a different representation by the model of the changes in circulation, as a result of reduced influence of westerly winds and an increased importance of secondary modes of atmospheric variability, such as a blocking system centered over the Baltic Sea in winter. Additionally, in some areas, such as northeastern Europe, the differences are most likely related to high uncertainties of the pollen data.

In summer, the simulated northern conditions agree well with the proxy data over part of the domain. Their behaviour seems to be a direct response to insolation changes. Conversely, while the model produces warmer summer conditions over southern Europe at the mid-Holocene, in comparison to the pre-industrial times, again mainly due to insolation changes, the pollen data exhibit an opposite trend. According to the results of previous works and to the analysis of atmospheric dynamics, we suggest that this behaviour is mainly due to a higher partition of radiation towards latent heat. This results in a cooling effect of the surface that the model is not able to reproduce due to deficiencies in the representation of soil-atmosphere heat fluxes over the area. The comparison against previous studies shows that the evinced bias is not only inherent to this research, but it is also a common feature of other climate models. Nonetheless, it is important to mention that the validity of reconstructions of European summer temperature over the Mediterranean region based on pollen data has been highly questioned in recent years. Even though several evidences confirmed the reconstructed trend of temperature over the area from 6000BP to present day, further investigations are still necessary in order to further clarify possible uncertainties.

This work sets the basis for further investigations: in particular a set of new simulations with improved radiation schemes, soil properties and land use could lead to important contributions to climate modelling and, consequently, to the improvement of future climate change projections.

Chapter 6

Mid-to-Late Holocene European Vegetation Changes

"Memories are the key not to the past, but to the future. "
- Corrie Ten Boom -

6.1 Introduction

In this chapter, using the results of the CCLM simulations, we investigate the evolution of vegetation distribution in Europe during the mid-to-late Holocene. For the achievement of this goal we use a bio-equilibrium vegetation model.

Using different climatic factors as input, bio-equilibrium vegetation models determine the dominant plants of a given geographical area. Their simple design makes them a particularly useful tool for the study of time-slices, requiring 10 to 100 times less resources in terms of storage space and computing power than more complex vegetation models, such as Dynamical Vegetation Models (DVM) (Bond-Lamberty et al., 2005; Kaplan et al., 2003; Pearson and Dawson, 2003). While a DVM is particularly suitable for the study of periods in which the climate changes rapidly and where the ecosystem "memory" is crucial, equilibrium models are more appropriate for the analyses of "time slices" where an equilibrium approximation is satisfactory (Kaplan et al., 2003).

In our study we employ the off-line version of the BIOME4 model of Kaplan et al. (2003), in order to translate climate model outputs from the mid-to-late Holocene CCLM experiment (specifically the seasonal cycle of temperature, precipitation, and solar radiation) into biome distributions. Such

an approach has two specific advantages: the first is that it groupes climate data into a small number of biomes producing a practical and informative overview of the mid-to-late Holocene CCLM simulations (Haywood et al., 2002). Secondly, it constitutes an alternative method for the comparison of model-simulated climate with estimates of palaeoclimate derived from fossil pollen.

After providing a brief description of biomes and plant functional types, in this section we present a review of previous studies on the mid-to-late Holocene vegetation changes over Europe. Successively, we introduce the BIOME4 model structure and its development history. Finally, after a description of the experimental setup, we discuss, first, the results of a test of model performance for present-day and, successively, the ones of the mid-to-late Holocene potential natural vegetation simulations. The reconstructions of the BIOME6000 project (Prentice and Jolly, 2000) are used as a benchmarck for the comparison of model's results.

6.2 Biomes and Plant Functional Types

A biome is defined as a major ecosystem spreading over a wide geographic area, characterized by different plants and animals adapting to its environment (Cain et al., 2014). Biomes are defined by abiotic factors such as climate regimes, soil and orgraphic features. Temperature, soil characteristics, and the amount of light and water availability help to determine what life exists in a biome. Biomes may migrate as the climate changes. One of the most important case in Earth's history is represented by the green Sahara. Ten thousand years ago, parts of north Africa was covered with abundant vegetation and crossed by flowing rivers. Hippopotamuses, giraffes, and crocodiles populated the area. Gradually, the area became more arid. Today this region is part of the Sahara Desert, the world's largest desert.

The concept of biome is the basis on which different bio-equilibrium models have been developed during recent decades. One of the first of these models is the BIOME model of Prentice et al. (1992). Biome models allow the results of climate simulations to be translated into maps of potential natural vegetation. They have been employed in several studies of past, present and future vegetation distribution, with noteworthy results (Harrison and Prentice, 2003; Huebener and Körper, 2013; Kaplan et al., 2003; Salzmann et al., 2008). Underpinning all biome models is the concept of Plant Functional Type (PFT). PFTs are broad classes of plant defined by stature (e.g. tree/shrub), leaf form (e.g. broad-leaved/needle-leaved), phenology (e.g. evergreen deciduous), and climatic adaptations. Biome models assign to each

PFT specific characteristics. Successively, according to the environmental conditions given as input, the models select, first, those PFTs that could survive and grow under the given conditions and, then, among these PFTs, the one that could dominate (Prentice et al., 1996). Biomes are then defined according to which PFT(s) are dominant.

The PFT concept can also be applied directly to paleoecological data, such as pollen and plant macrofossil records, in order to derive maps of palaeobiome distributions. One of the most important study in this sense is the one of Prentice et al. (1996). More specifically, they developed a method for "biomization" using modern pollen data from surface samples in Europe as a test and applied it to 6 ka[1] pollen data. The use of this method allowed palaeobiome maps derived from data, and palaeobiome maps simulated from AGCM experiments, to be compared systematically. Such comparisons provided a powerful test of climate change prediction methodology.

6.3 Reconstructions of the Mid-to-Late Holocene European Vegetation

Climate is the major determinant of present broad-scale patterns of distribution and abundance of vegetation (Huntley et al., 1989). The changes in vegetation distribution during the Holocene are therefore likely to reflect broadscale paleoclimate change (Prentice, 1986; Webb III, 1986) providing an indication of the large-scale dynamics of European vegetation in response to large-scale changes in climate.

Many studies have tried to reconstruct Holocene European vegetation both at the regional (Andrič and Willis, 2003; Collins et al., 2012; Huntley, 1990; Jalut et al., 2009; Odgaard and Rasmussen, 2000) and at the local scale (Berglund et al., 1996; Fyfe et al., 2003; Lotter, 1999; Magny et al., 2003; Mercuri et al., 2012; Noti et al., 2009; Pérez-Obiol et al., 2011; Roberts et al., 2011; Tanţău et al., 2011). European biome distributions for the mid-Holocene (Gallimore et al., 2005) or the pre-industrial period (Prentice et al., 2011) have also been modelled based on climate model output, and have been used for data-model comparisons against pollen-based vegetation reconstructions (Prentice et al., 1996, 1998).

One of the first attempts of reconstructing the mid-to-late Holocene European vegetation was made by Huntley (1990). Through multivariate analysis of an extensive palynological database they produced maps for selected timeslices. Their goal was to outline the major features of the vegetation history

[1] 1 ka=1000 ^{14}C-years before present

of Europe during this time, particularly considering the extent to which compositional changes have occured within broad-scale vegetation units. Huntley et al. (1993), using empirical pollen-based classification rules, also produced simple paleovegetation maps and semi-quantitative inferences about paleoclimate from pollen data. Using an objective biome reconstruction (biomization) based on the work of Prentice et al. (1996), Prentice and Webb III (1998) obtained a 6000 yr BP biome map directly from pollen data. This was successively used for the comparison against BIOME model results derived from climate simulations. Gachet et al. (2003) proposed a new probabilistic approach for the use of pollen indicators for plant attributes and applied it to reproduce the mid-Holocene European biomes distribution from pollen proxies. They confirmed the results of previous studies showing an extension of deciduous forest to the north, east and south of Europe, explained by milder winters in western and northern Europe, and cooler and wetter climate in the Mediterranean region for 6000 BP. Cheddadi and Bar-Hen (2009) used functional principal component analysis on 216 European pollen records in order to evaluate the patterns of vegetation change over the last 14000 years. One of the most important case study in which vegetation dynamics across the whole of Europe for the entire Holocene have been investigated, is represented by Davis et al. (2015). They assessed overall changes in potential natural vegetation using a revised biomisation method based on the previous work of Prentice et al. (1996) and Prentice and Webb III (1998). To reconstruct continental-scale vegetation patterns, they grouped pollen taxa into PFTs. In this way they managed to employ a very large number of pollen data (1,869 out of 2,390 pollen taxa present in their database), by combining ecologically similar taxa across diverse geographic regions, additionally reducing issues related to the use of pollen data processed and made available by a wide range of individuals and projects. The method showed several improvements over that of its predecessors Prentice et al. (1996) and Prentice and Webb III (1998).

Different attempts have been conducted in order to reproduce changes in the mid-to-late Holocene European vegetation based on the results of climate models. In addition to the already mentioned studies (Gallimore et al., 2005; Prentice and Webb III, 1998; Prentice et al., 2011), Huntley and Prentice (1988) showed that the early Cooperative Holocene Mapping Project (COHMAP, Anderson et al. (1988)) simulations of July and January conditions at 9000, 6000 and 3000 BP, showed only certain qualitative points of similarity with well-established features of the European paleoecological records (Prentice and Webb III, 1998).
More recently, Brewer et al. (2009) investigated the mid-to-late Holocene conditions under a set of different past climate scenarios and sensitivity studies

with a global vegetation model. They used as a testbed for comparison with model results, the data of the BIOME6000 project (Prentice and Jolly, 2000). In the next paragraph we try to give an overview of changes in European vegetation during the mid-to-late Holocene as reconstructed from some of the mentioned studies.

6.3.1 Reconstructed Patterns

In general, reconstructions of the distribution of vegetation at the mid-Holocene suggest less pronounced climatic differences than present-day, between northern and southern Europe (Brewer et al., 2009; Davis et al., 2015).

During the mid-to-late Holocene in northern Europe there was first a large northward advance of temperate deciduous forest replacing what is today tundra and boreal forest, and then a southward retreat: this followed a general poleward shift in forests seen across high latitudes (Prentice et al., 1998). In central Europe evidence has shown that there was a generally spatial stability of forest biome distribution (Cheddadi and Bar-Hen, 2009; Davis et al., 2015), while a subtle advance and retreat of the southern limit of temperate deciduous forest relative to the non-forest biomes characterized southern Europe during the same period (Cheddadi and Bar-Hen, 2009; Davis et al., 2015; Huntley, 1990; Prentice et al., 1996; Prentice and Jolly, 2000).

In the North, changes during the mid-to-late Holocene consisted in a reorganization of biomes, with temperate deciduous forest dominating in the middle Holocene, and cool mixed forest and taiga replacing them in the late Holocene (Prentice and Webb III, 1998). Temperate deciduous forests extended up to central Sweden in the mid-Holocene, displacing cool mixed and cool conifer forests. Taiga was present only in northern Russia, and its place was largely replaced by cold mixed forests and cold deciduous forests (Gachet et al., 2003). The tundra biome (boreal grassland) was restricted to a few sites in north-east Finland and western Siberia. Such dynamics reflect a trend in climate to a mid-Holocene optimum, followed by late Holocene cooling over the area, as described by Prentice and Webb III (1998) and Davis et al. (2003).

In central Europe, throughout the Holocene, after the cold mixed forest and taiga disappeared in an early period, the main biomes were temperate deciduous and cool mixed forests, present in roughly consistent proportions (Davis et al., 2015). The lack of significant changes in biome types, distribution and abundance over central Europe during the Holocene, suggests that the climate of the area most likely remained stable in the considered period (Davis et al., 2003).

In southern Europe, changes consisted of an expansion of temperate de-

ciduous forest in the middle Holocene, replaced then by warm mixed forest, xerophytic wood/scrub, and warm and cool steppe in the late Holocene (Collins et al., 2012; Gachet et al., 2003). The non-forest steppe biomes decreased in relative abundance from the early to the mid-Holocene, and then increased, while the xerophytic non-forest biome maintained a relatively constant abundance throughout the Holocene (Davis et al., 2015; Gachet et al., 2003).

In the Mediterranean region, especially in Spain, Greece and Turkey, there was an expansion of woodland from the early to the mid-Holocene (Davis and Stevenson, 2007; Huntley, 1990; Huntley and Prentice, 1988), with greater presence of temperate deciduous forest and a general reduction in the extent of grass and shrubland. Successively, cool forest was replaced by xerophytic vegetation (Cheddadi et al., 1996; Prentice et al., 1996). The replacement of today's xerophytic vegetation in the Mediterranean region by temperate forests at 6 ka implies a combination of colder than present winters, and wetter than present conditions during the growing season over the area (Cheddadi et al., 1996; Davis et al., 2003; Prentice et al., 1996).

6.3.2 Human Impact

Huntley (1990), Huntley and Prentice (1988), Bartlein and Prentice (1989), Mauri et al. (2014), Strandberg et al. (2014), Trondman et al. (2015) and Gaillard-Lemdahl and Berglund (1998) have discussed the extent to which broad-scale vegetation changes in Europe during the Holocene may have been a consequence of human impact, rather than primarily determined by climate change. They have concluded that the magnitude, geographical extent, and nature of the observed changes are consistent with the hypothesis that climate change is their ultimate determinant. Human disturbance has likely facilitated these changes at a local scale in some cases, but has not in general determined their direction or rate. In support of such hypothesis, the main reconstructed vegetation transitions over Europe are synchronous with those identified in North America during the Holocene which suggests that they were primarily driven by large-scale atmospheric circulation (Gajewski et al., 2006) and that human impact became more detectable only in more recent times. According to Davis et al. (2015), Collins et al. (2012) and Gaillard et al. (2010), at the mid-Holocene, humans had not yet begun to significantly alter the natural environment at the continental scale. They suggest that influence of human activities became more relevant after 5000 and 4000 years BP, and significantly important only after 1500 years BP, when human activity increased as the result of human population growth (Fig. 6.1).

Important to mention is the fact that the biomisation method of Prentice

et al. (1996), upon which most of the data and the methods employed in this study are built, was developed in order to recostruct maps of vegetation in equilibrium with climate and is expected to be relatively unbiased by human activity (Davis et al., 2015). The biomisation method is based on the concept of potential natural vegetation, representing the vegetation that would be expected given environmental constrains such as climate, geomorphology or geology, without human interference.

6.4 The BIOME4 Model

6.4.1 Model Structure and Development

The BIOME4 model (Kaplan et al., 2003) is the most recent version of a set of bio-equilibrium vegetation models based on physiological processes regulating the growth and regeneration of different plant functional types. Physiological tresholds are calculated via the use of limiting factors for plant growth, such as monthly averages of temperature, precipitation, relative sunshine and absolute minimum temperature. In addition, the model uses information on soil texture and soil depth and a global survey of rooting depth (Canadell et al., 1996; Haxeltine and Prentice, 1996; Jackson et al., 1996).

The BIOME4 model has been developed based on previous versions of biome models (Prentice and Webb III, 1998; Prentice et al., 1992, 1993). With respect to its predecessors, the BIOME4 has additional PFTs for tundra climates and is able to better reproduce the impact of differing atmospheric CO_2 concentrations on plant growth (Kaplan et al., 2003). To minimise any model bias, the BIOME4 model has been thoroughly validated against vegetation distribution, productivity and other biogeochemical data for present-day and the recent past, with satisfactory results (Kaplan et al., 2003). Known biases in the BIOME4 model relate to the precise location of the forest-grassland boundary in temperate and subtropical latitudes (Kaplan et al., 2003).

The BIOME4 model simulates the vegetation of the Earth in 28 biomes which are representative of a broad admixture of plant types based on physiological factors such as composition, phenology and climate regime (Kaplan, 2001). Fig. 6.2 presents the European biomes distribution for the period 1961-1990 as simulated by the BIOME4 model driven by the CRU climatology (Harris et al., 2014). The model is run globally at a 0.5^o resolution and is based on 12 PFTs representing physiologically distinct classes, from arctic/alpine cushion forbs to tropical evergreen trees (Kaplan, 2001). For each PFT bioclimatic limits are fixed (Tab. A1), determining whether or

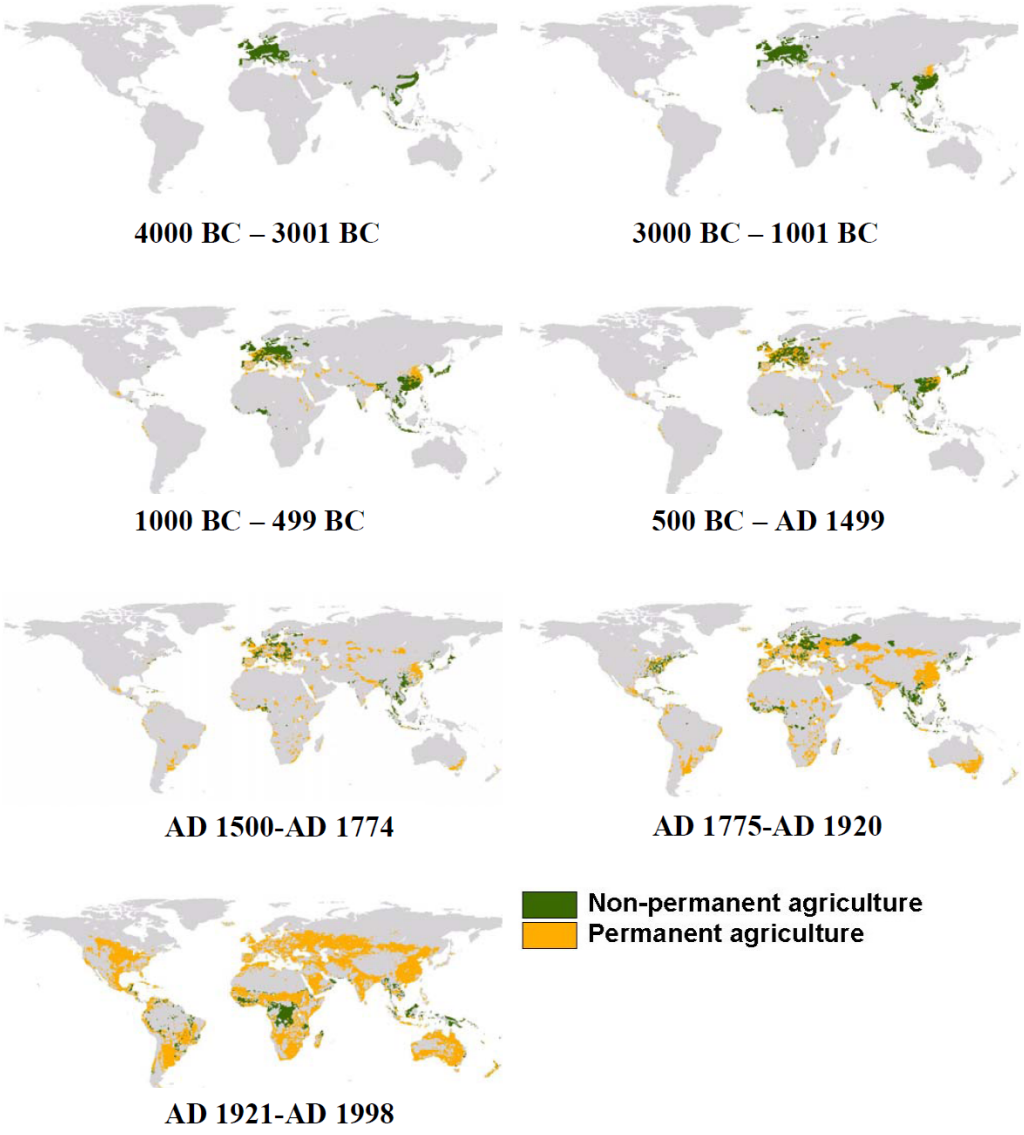

Figure 6.1: *Reconstructions of the spatial extent of permanent and non-permanent agriculture for seven time slices of the Holocene . The reconstructions are based on archaeological maps of the spread of different societal forms, History Database of the Global Environment version 2.0 (Hyde 2.0 (Goldewijk, 2001)) for the last 300 years, global changes in population, and an estimate of land suitability. The figure is adapted from Gaillard et al. (2010).*

not the specific PFT Net Primary Productivity[2] (NPP) should be calculated (Kaplan, 2001). The main computational part of the model consists in a

[2]representing how much carbon dioxide vegetation takes in during photosynthesis minus how much carbon dioxide the plants release during respiration

coupled carbon and water flux scheme based on the simulation of soil water balance, canopy conductance, photosynthesis, and respiration. This scheme determines, for any given PFT, the Leaf Area Index (LAI) maximizing NPP (Kaplan, 2001), according to a series of environmental factors such as variable soil texture with depth and seasonal patterns in precipitation, as well as the concentration of atmospheric CO_2 (Kaplan, 2001). For every grid box, the woody PFT with the maximum annual NPP is generally considered the dominant PFT. An exception is represented by those cases for which, due to soil moisture constraints, grass or mixtures of grass and trees are expected to dominate. Successively, the boundaries between forests, savannas, and grasslands are assigned according to semi-empirical rules based on inferred fire risk and the balance of NPP between trees and grasses. Finally, for each grid cell, the model orders the tree and non-tree PFTs in terms of NPP, LAI and mean annual soil moisture and uses the semi-empirical rule-base to assign one of the 28 biomes (Kaplan, 2001).

6.4.2 Experimental Setup

The model setup consists in providing the decadal monthly means of near surface temperature, total cloud cover and precipitation, together with the absolute minimum temperature, for the period under investigation. Addi-

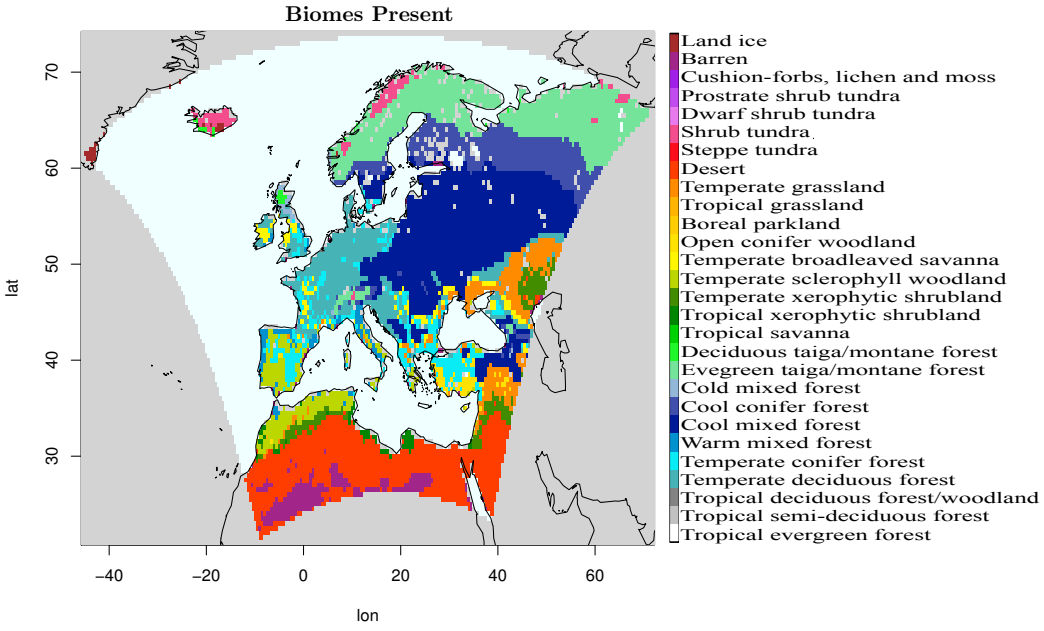

Figure 6.2: *European biomes distribution for the reference period 1961-1990, as simulated by the BIOME4 model driven by the CRU climatology (Harris et al., 2014).*

tionally, the CO_2 concentration values have to be set accordingly to the values characteristic of each period of study.

The experimental framework consists of two experiments: the first one for present-day conditions and the second for the mid-to-late Holocene. In the first case, the main goal is to test the performance of the off-line vegetation model. For this purpose, the BIOME4 model is driven by a 30-year climatology for the period 1961-1990, derived from the CRU dataset (Harris et al., 2014). This step is of fundamental importance in order to properly interpret CCLM driven results, allowing to discriminate between the vegetation and the climate model bias. Additionally, since no up-to-date guide on the use of the model exists, in this way we can test whether the model configuration we adopt leads to results that are consistent with the ones of other studies.

Once that the performance of the stand-alone version of the vegetation model is tested, in a second step we use the output of the CCLM simulations in order to investigate the effect of the simulated climate changes on the mid-to-late Holocene European vegetation distribution. For this purpose we apply the Delta-change method, which has previously been employed in other studies (De Castro et al., 2007; François et al., 1999; Huebener and Körper, 2013). First, we select a climatology derived from an observational dataset and covering a 30-year period, as close as possible to the pre-industrial times. Then, we calculate the anomalies between the simulated climatic conditions for the different mid-to-late Holocene time-slices and the pre-industrial period. Finally, we add such anomalies to the reference climatology and use the results in order to derive the biome maps for the different time-slices of the mid-to-late Holocene. In this way we are able to estimate how the climate changes simulated by the CCLM reflect into vegetation changes.

As a first step, all the data are upscaled by means of bilinear interpolation to the original 0.5^o regular grid of the BIOME model. Successively, monthly anomalies are calculated for each parameter required as the simulated mid-to-late Holocene time-slice climate less the pre-industrial climate. The anomalies are then added to a climatology for the period 1901-1930 derived from the CRU dataset (Harris et al., 2014), in order to obtain corrected fields, as described in François et al. (1998), François et al. (1999), Kaplan et al. (2003), Huebener and Körper (2013) and De Castro et al. (2007). This procedure may produce negative values of precipitation and total cloud cover. In order to avoid non-physical situations, the points for which negative precipitaton and total cloud cover values are obtained, are given a value of zero. Additionally, atmospheric CO_2 concentration values for every time-slice are set according to the values of Flückiger et al. (2002) reported in Section 3.

The BIOME6000 database (Prentice and Jolly, 2000) is used as a benchmark for the comparison of the results. The database contains global maps

describing the vegetation pattern at 6000+/-500 yr BP, the last glacial maximum and a reference for present day. Huntley and Birks (1983), Huntley (1990), Gliemeroth (1997) and Davis et al. (2015) already attempted to map and quantify vegetation dynamics across the whole of Europe for the entire Holocene. Unfortunately, such studies either used a complete different approach or a different biomes classification with respect to the ones employed in this study, making a direct comparison difficult. The names of the BIOME6000 dataset are instead standardised using names mostly consistent with the BIOME4 model. For this reason, even though it only contains information for a single time slice of the mid-to-late Holocene, the BIOME6000 dataset is particularly suitable for our purposes. Although the BIOME6000 database is built to be consistent with the BIOME4 model, it includes some additional biomes defined for a total amount of 40 (against the 28 of the BIOME4 model). These are successively classified into 9 broader units (mega-biomes). The model simulates far fewer PFTs, and hence discriminates far fewer biomes, than the palaeodata allow. In order to facilitate direct comparison with model output, we group the biomes of the BIOME4 model into the same mega-biomes on the basis of their structure and functioning, following the classification of Harrison and Prentice (2003). More details on such classification are reported in Tab. 6.1.

Table 6.1: *BIOME4 biomes re-classification into the corresponding mega-biomes broader units of the BIOME6000 database (Prentice and Jolly, 2000). In bracket the short name of each mega-biome that is employed in our analysis.*

Biomes	**Mega-biomes**
Tropical Evergreen Forest	TROPICAL FOREST (TRF)
Tropical Semi-Deciduous Forest	
Tropical Deciduous Forest	
Warm Mixed Forest	WARM-TEMPERATE FOREST (WTF)
Temperate Deciduous Forest	TEMPERATE FOREST (TEF)
Temperate Conifer Forest	
Cool Mixed Forest	
Cool Conifer Forest	
Cold Mixed Forest	
Evergreen Taiga/Montane Forest	BOREAL FOREST (BOF)
Deciduous Taiga/ Montane Forest	
Tropical Savanna	SAVANNA (SVN)
Temperate Sclerophyll Woodland	
Temperate Broadleaved Savanna	
Open Conifer Woodland	
Tropical Xerophytic Shrubland	GRASS (GRS)
Temperate Xerophytic Shrubland	
Tropical Grassland	
Temperate Grassland	
Boreal Parkland	
Desert	DESERT (DES)
Barren	
Steppe Tundra	TUNDRA (TUN)
Shrub Tundra	
Dwarf Shrub Tundra	
Prostrate Shrub Tundra	
Cushion-forbs, lichen and moss	

6.5 Results

6.5.1 Present Day

Fig. 6.3a presents the vegetation patterns (mega-biomes) simulated by the BIOME4 model driven by the CRU climatology for the period 1961-1990. This is compared against the reconstructions of the BIOME6000 dataset for the same period (Fig. 6.3b). Qualitatively, there is a general good agreement between the two datasets, and the simulated large-scale pattern of vegetation seems to be consistent with the one of the observations. The largest differences are evident over the Iberian peninsula, where the model simulates a large area as savanna-like and dry shrubland biome, while the observations are characterized by grassland and warm-temperate forests. Additionally, poor agreement is evident over Ireland and central England, where the BIOME4 seems to reproduce drier vegetation types. Temperate forest extends over most of the domains in both the datasets. Also the transition zone between the temperate forest and the Boreal forest in Scandinavia coincides in both the cases. In southeastern Europe and the Black Sea area, both the model and the observations reproduce a prevalent grassland-like biome. A point-by-point comparison of the two datasets shows that model results coincide with the reconstructions for approximately 80 % of the total number of observations, in good agreement with the results of previous studies (Kaplan et al., 2003). The area where the model produces better results, with respect to the observations, is central Europe, with an $\sim$ 85% agreement between the two datasets.

6.5.2 Mid-to-Late Holocene

After testing the BIOME4 model performance for present-day conditions, we analyse the results of the mid-to-late Holocene CCLM-driven simulations. In this case, the results are in good agreement with the BIOME6000 proxy-reconstructions only over part of the domain. Model results match the values of reconstructions in approximately 60 % of the cases (Fig. 6.4). Good agreement between model results and the BIOME6000 reconstructions is evident over central Europe, most likely due to the relatively high number of proxies available for this area, and to the fact that both the vegetation model and the climate model proved to have the best performance over the area. The analysis of southern Europe is more complicated, since the total number of proxies for the area is considerably low ($\sim$30). Nevertheless, even though the BIOME6000 reconstructions are outnumbered over this region, the widespread of temperate forests and the displacement of arid and warm

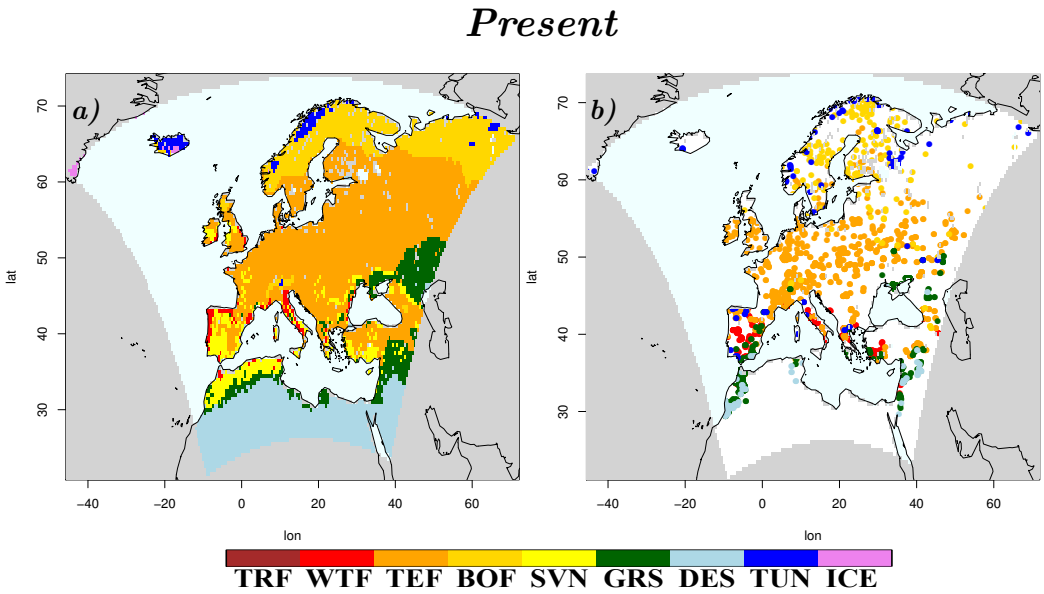

Figure 6.3: *Maps of present day (1961-1990) mega-biomes distribution as simulated by the BIOME4 model using the CRU climatology (Harris et al., 2014) (a) and as reconstructed from the BIOME6000 database (Prentice and Jolly, 2000) (b). For the extended name and description of the mega-biomes units see Tab. 6.1.*

biomes at the mid-Holocene evinced from such data are in accordance with the results of more recent and statistically consistent studies (Brewer et al., 2009; Cheddadi and Bar-Hen, 2009; Collins et al., 2012; Davis et al., 2015).

Conversely, the BIOME4 results present a different situation over southern Europe. In particular, the model simulates an excess of grassland and savanna-like biomes with respect to the observations over Southeastern Europe and the Black Sea region (Fig. 6.4a). This behaviour is likely due to general warmer conditions simulated by the climate model over the area, in accordance with the results of previous Sections 3 and 5. Different behaviours are also evident over Italy and the Iberic Peninsula, with the model simulating drier vegetation. A better agreement is evident over part of northern Europe. The main differences consist in a minor northward extension of temperate forests over Scandinavia and the presence of warm mixed forests over southern British Islands in the model results. In this case, differences in the simulated climatic conditions are likely amplified by the bias proper of the vegetation model.

Considering the simulations of the different time-slices of the mid-to-late Holocene, changes in the broad scale pattern of vegetation are particularly evident over Southern Europe (Fig. 6.5). A progressive remarkable spread of savanna- and grass-like vegetation from 1000BP to the mid-Holocene is

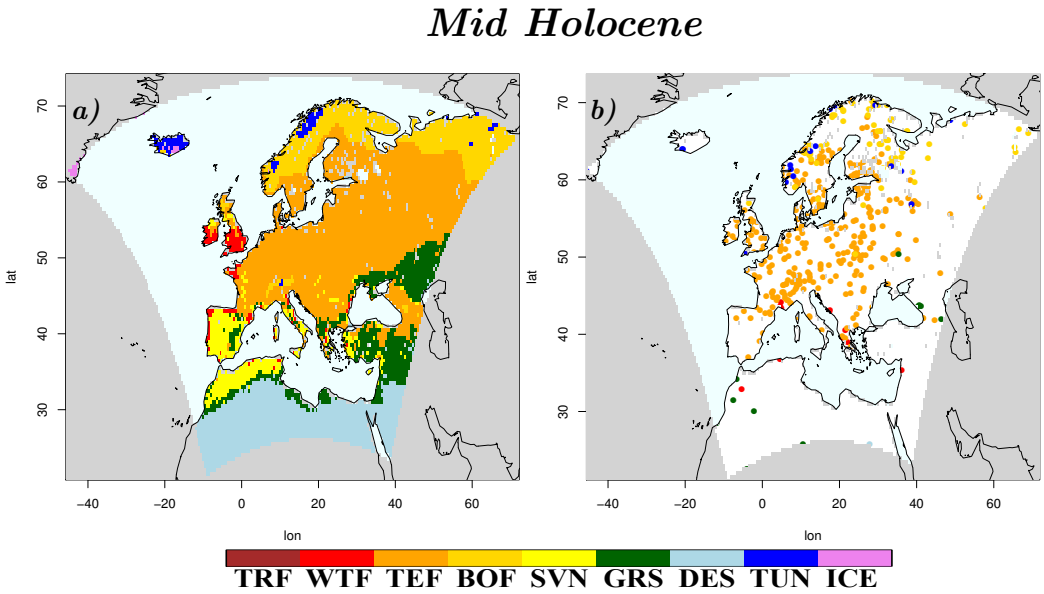

Figure 6.4: *Maps of the mid-Holocene (6000 BP) vegetation distribution as simulated by the BIOME4 model driven by the outputs of the CCLM simulations (left) and as reconstructed from the BIOME6000 database (Prentice and Jolly, 2000) (right). For the extended name and description of the mega-biomes units see Tab. 6.1.*

evident, reflecting the warm bias characteristic of the climate model over the region. In the North, the changes consist in a northward extension of temperate forest at the expenses of boreal forest. There is also a reduction of tundra biomes. These changes are also amenable to increasingly warmer conditions simulated by the climate model over the region from the late to the mid Holocene.

Finally, in order to give a more quantitative estimate of the simulated changes in vegetation distribution between different time-slices of the mid-to-late Holocene, we calculate the differences in relative abundance of the simulated biome at every latitude between 6000BP and 1000BP. Fig 6.6 shows the differences of the relative biome abundance for every latitude between the two considered time-slices. Particularly pronounced differences are present over northern and southern Europe, where the changes in the simulated climatic conditions were more remarkable. The most significant evidence is a gradual shift from boreal to temperate forest from late-to-mid Holocene at higher latitudes, and an increase of more than $\sim 30\%$ of grass-like biomes over the Mediterranean area for the same period, consistently with an increase of the simulated temperatures over the area during the mid-to-late Holocene.

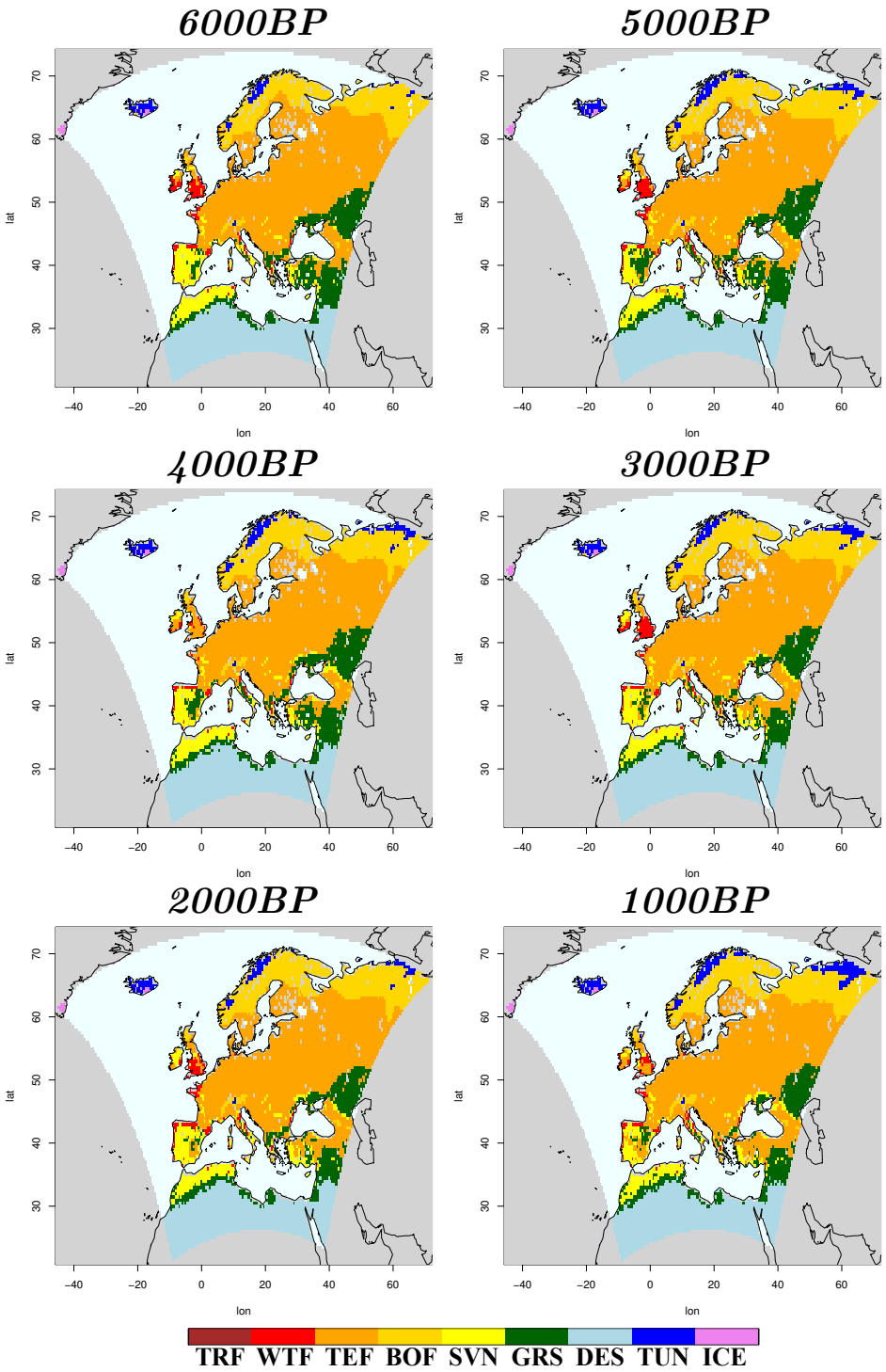

Figure 6.5: *Maps of simulated mega-biomes of the mid-to-late Holocene time slices, reconstructed utilizing the Deltha-method. For the extended name and description of the mega-biomes units see Tab. 6.1.*

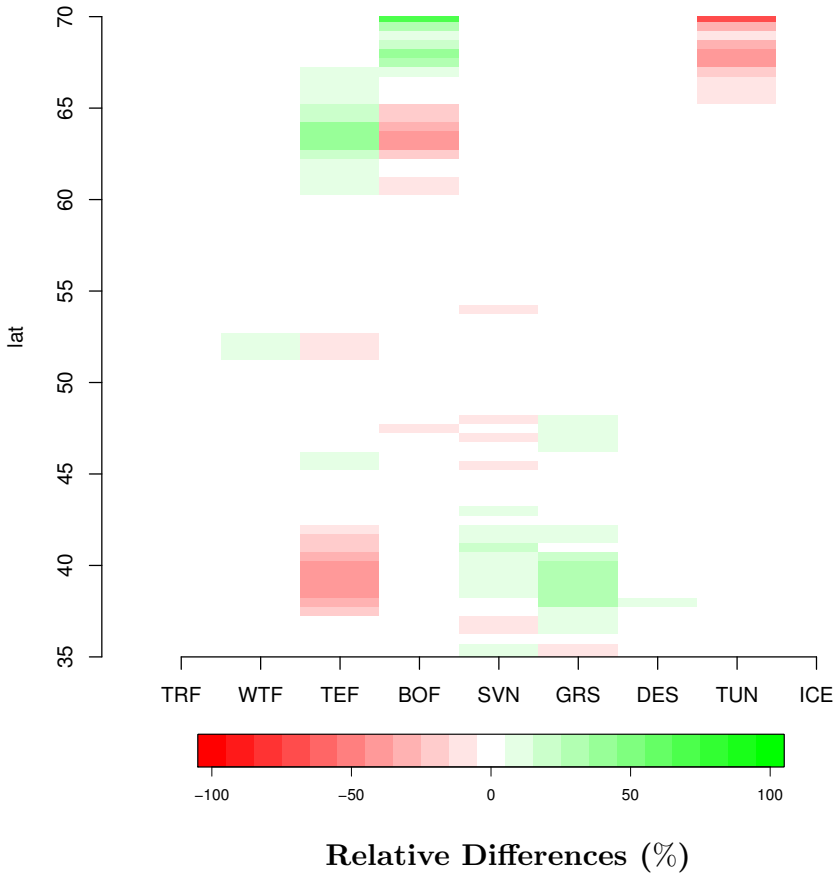

Figure 6.6: *Zonal relative differences between the 6000BP and the 1000 BP simulated mega-biomes. For the extended name and description of the mega-biomes units see 6.1. The green (red) boxes indicate that at 6000BP, for that specific latitude, there was a higher (lower) distribution of that corresponding biome with respect to 1000BP .*

6.6 Conclusions

In this chapter we used the output of the CCLM simulations in order to reconstruct changes in the potential vegetation of Europe during different time slices of the mid-to-late Holocene, by means of the BIOME4 bioequilibrium-vegetation model of Kaplan et al. (2003). According to previous studies, during the mid-to-late Holocene, spread of temperate forests characterized Southern and Northern Europe, probably due to a reduction of the temperature gradient between the two area, with a climate milder over the North and colder over the South with respect to present days. In our results the spread of temperate forests at the mid-to-late Holocene seems to be mainly constrained to Northern Europe. For the South, instead, a more grass/savanna-like vegetation is simulated at 6000 yr BP, contrasting with the evidence from proxy

reconstructions of the BIOME6000 project (Prentice and Jolly, 2000). This is related to significantly warmer conditions simulated by the climate model over the area, as a direct response to changes in insolation. Most studies (Braconnot et al., 2007b; Brewer et al., 2009; Prentice et al., 1996) did not reconstruct the temporal evolution of European vegetation distribution during the entirety of the mid-to-late Holocene. Our study represents the first approach in which such reconstructions are carried out by using the outputs of climate models. The obtained results represent a valuable benchmark for future investigations.

Chapter 7

A Case Study: Climate Trends Changing Threads in the Prehistoric Pannonian Plain*

"A people without the knowledge of their past history, origin and culture is like a tree without roots."
- Marcus Garvey -

7.1 Introduction

In the recent decades, major interest has risen in the media concerning future climate change and its possible impact on society. Adaptation and mitigation policies became main discussion topics within scientific research.
Analysis of the past events are often referred to for predictions of the future developments. Thus, archaeological and historical data can substantially contribute to our understanding of climate change consequences and influence on culture and society. Most importantly, the way civilization reacted or adapted to different environmental conditions in the past, could give us vital information on how to respond to the effects of recurred climate stress (Riede, 2014).

One of the main goals of our research was to develop an innovative framework consisting of climate and vegetation models, together with a collection

*The results presented in this chapter have been produced in collaboration with the colleague Ana Grabundzija, from the Prehistoric Archaeology department of the Freie Universität Berlin. The outcomes of the study have been published in the peer-reviewed journal "Documenta Prehistorica" (Grabundzija and Russo, 2016).

of numerous proxy data, suitable for the investigation of archaeological case studies. The advantage of this chain of different components is that it allows to choose the most appropriate method in order to answer the specific research questions addressed in every case. In this context, several multidisciplinary studies have been conducted. Outcomes of the ECHAM5 simulations have been used for the investigation of changes in precipitation patterns over Iran for different time slices of the mid-to-late Holocene. The results, presented in Fallah et al. (2015), suggested that when early Persians settled in the Iranian Plateu at ca. 3700 BP, rainfall was probably enhanced over the region. A collection of proxy data has been used in order to reconstruct Holocene environmental conditions of Göbekli Tepe, an area of Anatolia for which recent archaeological findings have revolutionized previous hypothesis on the birth of religion (Curry, 2008). Results of the CCLM and the BIOME4 model simulations have been used in order to investigate changes in subsistence strategies of non-sedentary communities of the Black Sea area between the 6th and the 5th millennium BP, even though, in this case, the interpretation of the results was more challenging and further investigations are still required.

In this chapter, we present the study of Grabundzija and Russo (2016), in which the results of the ECHO-G transient run have been used to investigate the textile revolution in the Pannonian Plain between the 7th and the 5th millennium BP. This represents an interdisciplinary case study, incorporating archaeological analysis and climate modelling results for the evaluation of the effects of past climate change on cultural development, and in particular on innovation and technology.

Giving first a general overview on the goal of the study, we provide further details on prehistoric textile production, particularly focusing on the description of the main materials considered in our analysis. Finally, after describing the methodology employed, we present our results and conclude with a general outlook of the study.

7.2 Scope of the Study

The Pannonian Plain is a region of central Europe enclosed within the Alps on the West and the Carpathian Mountains on the East, and extending from the southern borders of Serbia in the South to northern Hungary in the North (Fig. 7.1). Previous studies have suggested that climate was one of the main driver of social changes over the area during the 7th and the 6th millennium BP (Berglund, 2003; Magny and Haas, 2004; Schibler et al., 1997; Weninger et al., 2009).

Motivated by such consideration, the main objective of this work is to investigate the possible influence of climate changes on the development of the prehistoric textile production in the Pannonian Plain. Period of interest, beginning with the middle Eneolithic (Lasinja spindle-whorl sample representing the earliest tools) and ending with the early Bronze Age (Somogyvár-Vinkovci spindle-whorl sample representing the latest tools) falls roughly between the late 7th and the end of the 5th millennium BP.

Figure 7.1: *Geographical map of the area of study, enclosed in the inner-black rectangle.*

Study of technological trends and changes that occurred in the manufacturing traditions focused on fibre processing and production, through the distinction of fibres and their reliance on cultural and environmental contexts. In particular, two main fibres were considered: flax and early-wool, known to be the two most exploited resources in textile production for the period and the area of study (Barber, 1991; Cybulska and Maik, 2007; McCorriston,

1997; Nosch and Michel, 2010).

Research of the prehistoric textile production was conducted based on indirect evidence dated to the period between the 7th and the 5th millennium BP. Functionality analysis of spindle-whorls was used in order to gain information on the exploited raw materials and on the final manufacturing products. Subsequently, the results of the archaeological investigations were used together with the outcomes of a climate simulation, in order to propose plausible interpretation of altering technologies in the prehistoric textile production of the Pannonian Plain. The analysis was additionally supported by multi-proxy climate reconstructions. Both climate information and the recorded archaeological evidence were considered, analysed, compared and finally discussed for possible correlations.

The objectives of our study were:

1. Explore and detect trends of change in the Pannonian Plain prehistoric textile production.

2. Reconstruct and interpret main climate changes within the geographical and chronological section of the research.

3. Explore cultural-historical and climate conditioning on the textile production for the investigated area and the considered period.

Results revealed that climate changes might have influenced the observed dynamics of the production traditions on a significant level. The contents of the next sections are adapted from Grabundzija and Russo (2016).

7.3 Flax Fibres and Early Wool: Prehistorical Evidences for Their Use and Development in the Context of Textile Production

Textile fibres can be roughly divided into two main categories: vegetal fibres and animal fibres.

Within vegetal fibres, flax or linum usitatissimum and tree basts were, at least according to the preserved textile evidence, both in Europe (Barber, 1991; Gleba and Mannering, 2012; Médard, 2006; Rast-Eicher, 2005) and in the Near East (Alfaro, 2002; Helbaek, 1963; Schick, 1988) the most frequently used textile fibre resources during the Neolithic period (∼10000-4000 BP). The earliest preserved linen cords from the circum-Alpine area of Europe

account for its use for textiles in the 6th millennium BP (Barber, 1991; Gleba and Mannering, 2012; Rast-Eicher, 2005), although the earliest flax seeds in the same area predate the textile findings for almost 2 millennia. The importance of flax in Eneolithic contexts, within the investigated area of the south east Europe, has also been well documented in more recent reports such as the one of Reed (2016). Interestingly, in central Europe flax seems to have split into two varieties at an early stage, one with large seeds used for both linseed oil and fibre production similarly to the Near East (Maier and Schlichtherle, 2011), and another with smaller seeds mainly specialized for the textile fibre generation (Herbig and Maier, 2011). The latter allows the production of longer fibre (Herbig and Maier, 2011). An extensive study on the 6th and the 5th millennium BP flax seeds from a series of wetland settlements in the Alpine region revealed that the early phase (6000–5700 BP) seeds were significantly larger in comparison to samples from the following periods (Herbig and Maier, 2011). At the same time, already in the middle of the 6th millennium BP, around 5400–5300 BP, the smaller seed fibre type was introduced and cultivated in the area to fit the needs of textile production (Herbig and Maier, 2011). Its preference for colder and wetter conditions could offer an explanation as to why this new fibre variety of improved length and quality, became the primary resource in Europe at the end of the 6th millennium BP (Herbig and Maier, 2011; Maier and Schlichtherle, 2011).

Although already Helbaek (1959) suggested that flax was initially used for its seeds and consequently for its fibre, linen evidence is direct proof of its early use for textiles. Preserved textiles confirm that flax was used for its fibre already in the early Neolithic in the southern Levant (Schick, 1988).

Concerning animal fibres, wool is one of the oldest material employed in textile production. Already developed and established wool economies were present in Mesopotamia in the 5th millennium BP. Although, numerous sources (Charvát, 2011) raise an argument that wool's first appearance should be dated much earlier. Analysis of the textile tools from Arslantepe (Laurito et al., 2014) proposed household wool spinning already in the 6th millennium BP and ethnological research in Greece showed that unspecialised herding can and did account for ample amount of spun thread (Rokou, 2004).

Sherratt (1981) assembled different strands of evidence from archaeology and zooarchaeology into a consolidated model of the secondary products revolution. With suggesting that the main products of domestication (traction, riding, milk and wool) occurred simultaneously, first in a narrow time span in the 6th millennium BP, he conceptualized them as economic achievements that developed several millennia after primary, meat-focused consumption. In this model, the main commodity, namely meat, was the objective of Neolithic herders, against the full range of exploitation, an achievement of the

Eneolithic ones (the age between the Neolithic and the Bronze Age). Consequently, the model addressed the secondary products potential for cultural evolution and social complexity at the transition from the 6th to the 5th millennium BP. The economic importance of secondary products, even if known for a long time, as proved in the case of milk (Bartosiewicz, 2007; Craig et al., 2005; Evershed et al., 2008; Vigne and Helmer, 2007), increases during the 6th millennium BP, which further shaped our research objectives.

Due to the gradual specialization and to the secondary products character ascribed to both flax and wool, it is extremely difficult to investigate the origin of their use and the dynamics of their development in the area of study. On the other hand, following the importance and representation of the different fibres in the textile production, it is to some degree possible to determine when, where and why they became a primary resource, as their intensified exploitation was more culturally and environmentally dependent.

7.4 Methodology

7.4.1 Spindle-Whorls

As textile tools for the fabrication of yarn, spindle-whorls are the most commonly preserved evidence of fibre processing and production practice found in the prehistoric contexts. It has been widely accepted, within the respective field of textile archaeology, that the morphological traits of the spindle-whorl impart to its functionality (Bichler et al., 2005; Mårtensson et al., 2006; Verhecken, 2010). Information on the tools morphological and structural traits constitute an indirect evidence for the processed materials and final products, reflecting difference in tensile strength between contradistinct fibres. In this study, spindle-whorls, spindles, loom weights and finished fragments of netting and fabric allowed for the reconstruction of the textile techniques throughout the Pannonian Plain between the middle Eneolithic and the early Bronze Age.

Focus on the 6th and 5th millennium BP textile productions in the Pannonian Plain placed the research within the context of three periods: middle Eneolithic, late Eneolithic and early Bronze Age.

1152 spindle-whorls recorded by Grabundzija and Russo (2016) in a textile tools database were used. Initially, the study included tools from 34 archaeological sites but the final analysis was conducted on a restrained sample of 836 spindle-whorls from only 20 sites. The chronological division we used placed spindle-whorl samples from the first half of the 6th millennium BP into the middle Eneolithic and the samples from the second half of the

Figure 7.2: *Late Eneolithic spindle-whorl (left) beside a late Neolithic loom-weight from the Sopot context found at Slavča-Nova Gradiška (right). The large size of the very heavy spindle-whorl type is evident from this picture.*

Table 7.1: *Table showing ranges and mean values for all the recorded variables.*

	Min	**Max**	**Mean**
Diameter (mm)	26.00	96.00	56.40
Height (mm)	5.00	76.60	25.58
Perforation Diameter (mm)	3.50	17.00	7.93
Weight (g)	6.39	317.70	68.34
Height-Diameter Ratio	0.10	1.32	0.46
Weight-Diameter Ratio	0.14	4.25	1.14

6th, and the very beginning of the 5th millennium, into the late Eneolithic assemblage. Samples from the advanced 5th millennium contexts thus entered the early Bronze Age assemblage. Middle Eneolithic tools account for 34.6 % (289), late Eneolithic for 42.0 % (351) and early Bronze Age for 23.4 % (196) of the entire spindle-whorl sample. Ranges and mean values of the recorded spindle-whorls are presented in Tab. 7.1.

The entire sample of spindle-whorls was divided into three main weight (light, medium, heavy) and height (flat, high, and steep) categories, according to the distribution of the spindle-whorl's weight and height-diameter ratio

Table 7.2: *Table of height-diameter ratio and weight classes, with the corresponding classification limits.*

Cum. Abundance	***Height/Diam.***	***Weight (g)***	
10	0.20	22.00	
20	0.23 **FLAT**	27.40	**LIGHT**
30	0.30	33.00	
40	0.35	41.30	
50	0.43 **HIGH**	56.00	**MEDIUM**
60	0.52	68.00	
70	0.60	82.00	
80	0.68 **STEEP**	104.40	**HEAVY**
90	0.80	140.00	**VERY HEAVY**

values (Tab. 7.2). Additionally, a fourth weight class was defined, due to extremely high values measured in some cases. Samples exceeding a treshold of 140g were included into this category, representing the ten percent of the entire dataset. Both whorl's size and weight account for the rotational properties of the spindle-whorl, determining the tool's moment of inertia. This plays the central role for the determination of the tool functionality, being connected with both the raw material (Verhecken, 2010) and the spun thread properties (Bohnsack, 1981; Crewe, 1998). Changes in both of the qualities affect the functional characteristics of a given spindle-whorl. Accordingly, when one wants to increase the moment of inertia of a particular spindle (i.e., to slow down its rotational speed), this could be accomplished by the manipulation of its diameter, that will be consequently characterized by a higher variability (Keith, 1998; Kimbrough, 2006; Loughran-Delahunt, 1996). Conversely, when an increase of the moment of inertia is not required but it is necessary to enlarge the mass of the spindle itself (to gain a better tension on the yarn while spinning), the height of the spindle whorl will increase rapidly, whereas the diameter variability will be reduced (Chmielewski and Gardyński, 2010).

Various fibres require a different degree of twist. For example, wool is characterized by much shorter fibres than flax and has to be twisted much more tightly (Barber, 1991; Vallinheimo, 1956). Therefore the spindle with which a woollen yarn is spun should rotate much faster in order to give a higher number of twists for a given length of the drafted fibre: small and moderately light tools would be required in this case. On the other hand

more weight would be required for spinning longer fibers, in order to increase the tension on the yarn while spinning.

Indeed, knowing the height/diameter ratio and weight of the tool we can make inferences on the final product and on the raw material processed in the spinning process. The substantial difference in tensile strength between the two investigated fibres (fibre flax and early wool) should be distinguishable in the distribution of the extremely different tool categories.

It is generally accepted that lighter weights would be preferred for thinner and lighter threads and heavier for thicker and heavier ones (Andersson, 2015). Very-heavy spindle-whorls are generally connected with long fibres and plying (Barber, 1991; Hochberg, 1979) heavier thick yarns or ropes (Vakirtzi et al., 2014). The fact that the fibre flax plant would have provided fairly long fibres, especially in comparison to the much shorter length of wool expected for the early woolly types, accounts for the main reason why this distinction of raw materials resonated soundly in the dichotomy between spindle-whorl types, with an emphasised contrast between big and heavy and small and light categories.

The adopted metrical standards allow, indeed, to determine the prevalent raw material employed in every period, according to the relative abundance of spindle-whorls in each of the height-weight categories. Nonetheless, the outlined metrical standards have to be considered cautiously, because the spinning process is influenced by many combined factors.

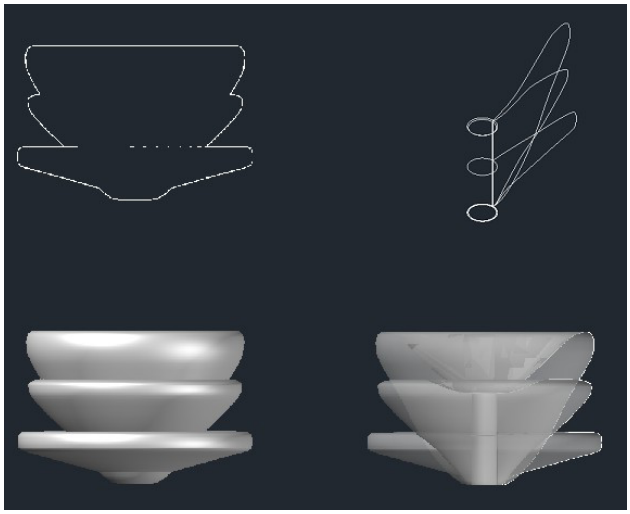

Figure 7.3: *Reconstructed three-dimensional models of a flat, high and steep spindle-whorl type, based on published conical spindle-whorls found at Balatonoszod-reti dulo site (Horváth et al., 2013).*

7.4.2 Climate Simulations

In order to interpret altering technologies through the distinction of fibres and their reliance on cultural and environmental contexts, our research analysed the Eneolithic and early Bronze Age textile tools in the light of the results of the continuous transient ECHO-G simulation described in Section 3. The decision to adopt this particular approach to support our analysis was made due to several reasons. First of all, the model allows a full coverage of the investigated area for the entire period in question. Further, the temporal resolution of such analysis permits focus on different temporal scales, leading to the representation of inter-annual to millennial climate variability. But, most importantly, besides allowing the simulation of possible changes of different climatic parameters, the model also enables finding plausible physical interpretations for them. Nonetheless, as a support to the conclusions based on the model results, we additionally address several studies which rely on proxy-reconstructions.

The region considered in the analysis of the climate model results extends from 14^oW to 21^oW in longitudes and from 42^oN to 48^oN in latitudes, covering most of the Pannonian Plain region. The analysis covered the period between 7000 BP and 3000 BP, taking into consideration seasonal values of different variables that are particularly relevant for plant growth, such as near surface temperature, moisture balance (i.e. precipitation minus evaporation) and growing degree days above 5 degrees (Masson et al., 1999). Additionally, Sea Level Pressure (SLP) anomalies were considered.

7.5 Results

7.5.1 Adapting Technologies

On the level of robust period to period comparison, the observed differences in spindle-whorls weight and diameter distributions pointed to a significant increase in values for both variables through time.

Fig. 7.4 shows the diameter and weight variability for the samples of the three different periods. The middle Eneolithic samples are characterized by a low weight variability, suggesting a rather small specialization of the textile production. Conversely, the late Eneolitic and the early Bronze age samples show a wider weight distribution. While the late Eneolithic values are to a certain degree constrained to the frequency of the large diameter sizes, early Bronze Age assemblage is more evenly distributed, indicating a major specialization of techniques and final products demand in the latter period.

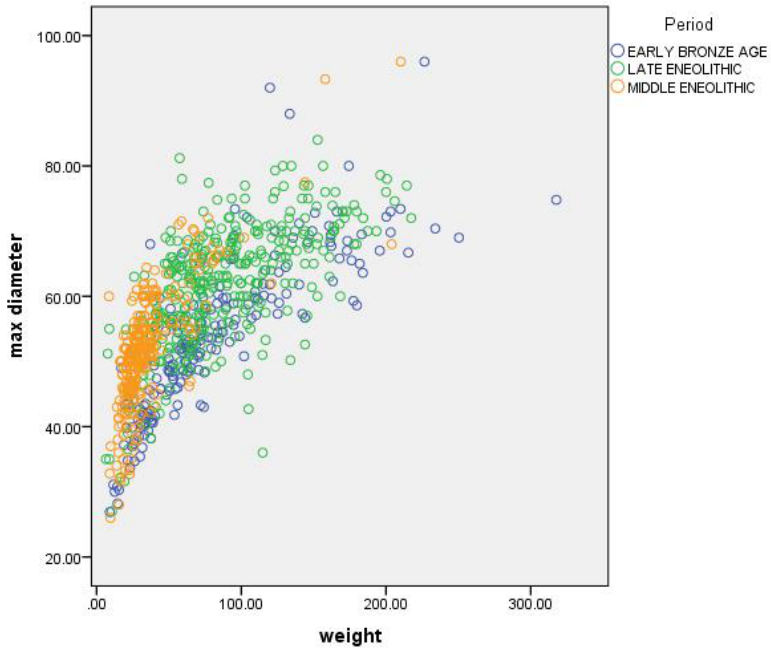

Figure 7.4: *The weight-diameter distribution for each investigated period, shown together.*

Similar trends can be observed for the height-diameter and height-weight categories (Fig. 7.5). For all the considered plots, the distribution of the samples corresponding to each period is easily distinguishable, suggesting high differentiation in textile production between them. Additionally, we notice that the early Bronze Age samples are characterized by higher values of height and weight for fixed diameters, suggesting the use of taller and heavier tools with respect to the other periods.

Considering the classification of the spindle-whorls into the 4 weight and the 3 height classes described in Tab. 7.2, in the earliest, middle Eneolithic assemblage, light and medium weight types are convincingly dominant and they appear to be clustered in only one height group: the lowest category or the flat spindle-whorl type (Fig. 7.6a). Almost the opposite distribution is evident in the latest, early Bronze Age assemblage (Fig. 7.6c). Here, again, the majority of the tools is clustered into one height group: the steep spindle-whorl type. In this category, this time, all four weight groups appear to be more evenly distributed, even though heavy and medium spindle-whorls are the most represented. The late Eneolithic assemblage seems to fit the transitional period between these two extremes. First, because it shows an increase in the relative amount of heavy weight types with respect to the former middle Eneolithic period. Second, because the distribution across all

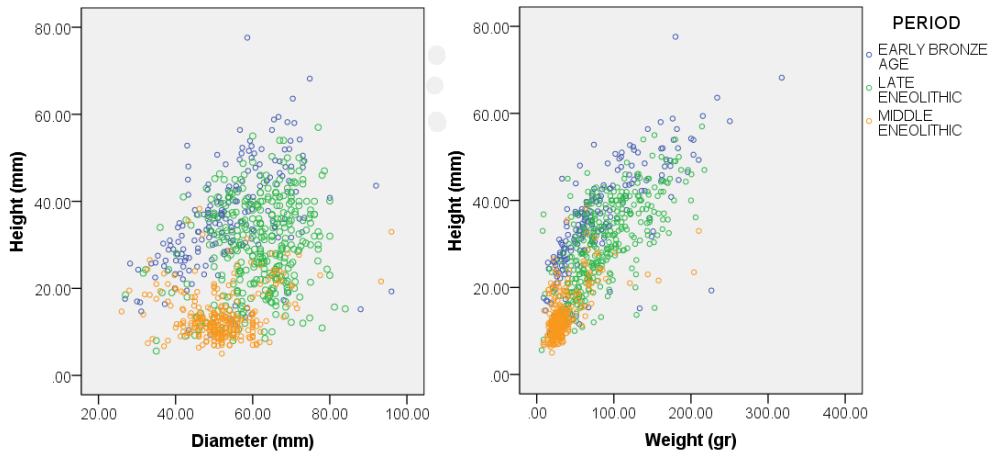

Figure 7.5: *The distribution of correlated: (left) maximum diameter and maximum height values; (right) weight and maximum height values, for the three period assemblages together.*

the different weight groups in each height category is more evenly balanced (Fig. 7.6b).

In the middle Eneolithic, the most prominent category is represented by the light flat type spindle-whorls (Fig. 7.6a), suggesting a major use of the old flax fibre, characterized by moderate length. Relatively high values of the light high category would also suggest spinning wool. Recently reported results of a technological analysis of the 6th and early 5th millennium BP textile tools from Arslantepe, Turkey (Laurito et al., 2014) support this conclusion.

Largest height and weight type variability characterizes the late Eneolithic assemblage (Fig. 7.6b). This could be interpreted as a pronounced differentiation in the textile production during this period. The high relative abundance of heavy and very heavy types in this case, could be connected to the long plant fibre processing. Even though they have large height-diameter ratio values and show tendency to cluster generally in the high and steep height groups, their weight imparts to a significantly larger moment of inertia values (too big for the processing of short, or even moderately long fibres that call for more twist). Additionally, their weights alone are too big for the smaller tensile strengths of animal fibres. They can be thus considered appropriate for spinning long plant fibres, for example full-length flax. These spindle-whorl types become dominant in the late 6th millennium and continued to be highly represented during the early Bronze Age (Fig. 7.6).

Additionally, light-steep categories of tools acquire significantly more rel-

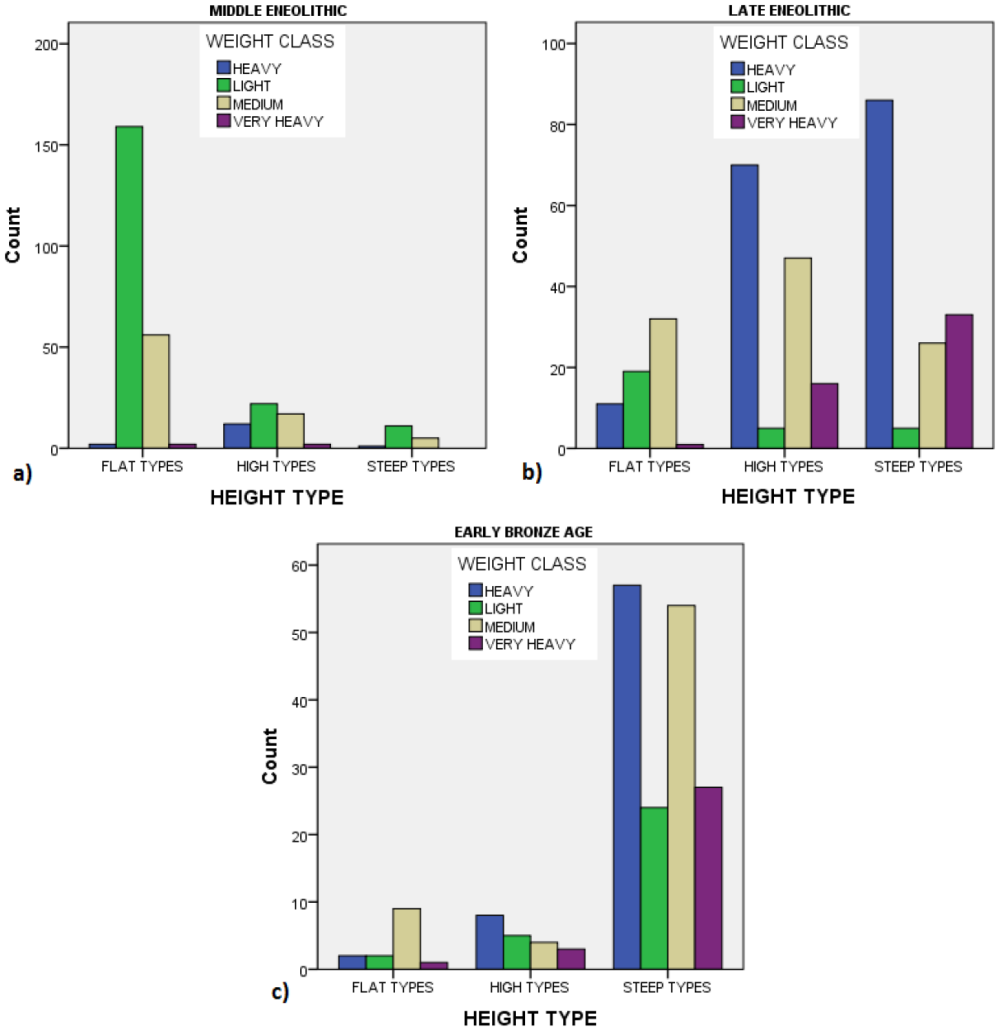

Figure 7.6: *The distribution of weight classes according to the height type, shown for each respective period, separately.*

evance during the early Bronze Age (Fig. 7.6c). These types, together with the medium steep ones already moderately represented in the late Eneolithic sample, could be appropriate for spinning shorter fibres, presumably wool. In fact, they present a significantly low moment of inertia, due to their high height-diameter ratio.

Finally, three main trends are evident in the spindle-whorl sample.

1. Middle Eneolithic assemblages suggest a principle use of the old short vegetal fibres. Additionally, the use of wool, even if moderate, is distinguishable, indicating more intense animal husbandry that consequently

led to the first exploitation of animal fibres.

2. On the basis of the late Eneolithic tools a continued wool use may be argued, which was substantially accompanied by the intensified long plant fibre production, characteristic of colder environments. More variability in the employed raw materials is evident.

3. The results of the analysis of the early Bronze Age spindle-whorls reveal a specialisation of fibres, most probably due to the refinement of both, textile fibre resources and final product demands.

The investigation of climate changes during the investigated periods could help in the understanding of the possible drivers of the evinced changes in the prehistoric textile production of the Pannonian Plain.

7.5.2 Climate Conditioning

Holocene climate has been highly variable, and there are multiple controls that must have been responsible for this variability (Mayewski et al., 2004). According to Wanner et al. (2011), the Holocene climate was dominated by the influence of summer season orbital forcing. Our results are in accordance with such interpretation. In particular, our model simulations revealed that from the 7th millennium BP summer climatic conditions started to deteriorate in the middle latitudes of the NH, mainly due to a decrease in summer insolation, which had its maximum at around 9000 BP (not shown). For all the simulated climatic parameters a pronounced trend is evident for the summer season, which resembles the one of the total decrease in insolation (Fig. 7.7). Although, the moisture balance reveals an opposite increasing trend, mainly due to the effect of evapotranspiration, as a consequence of the more enhanced insolation at the mid-Holocene.

Such conclusions are also supported by other studies for the investigated area and its surroundings, based on proxy-reconstructions. In particular, by analysing Holocene conditions through pollen-reconstructions from several lakes from southern to northern Italy and the Alpine Region, Magny et al. (2012) concluded that the mid-Holocene summer precipitation regimes appear to be opposite between the south- and north-central Mediterranean. Later, Magny et al. (2013) analysed a time series of wetness for the Lake Ledro basin in northern Italy spanning the last 10000 years: while the early and mid-Holocene periods show relatively low flood frequency, the late Holocene, from ca. 4500 cal. BP on-wards, is characterized by an increase in water availability, which is in full agreement with the reconstructions from

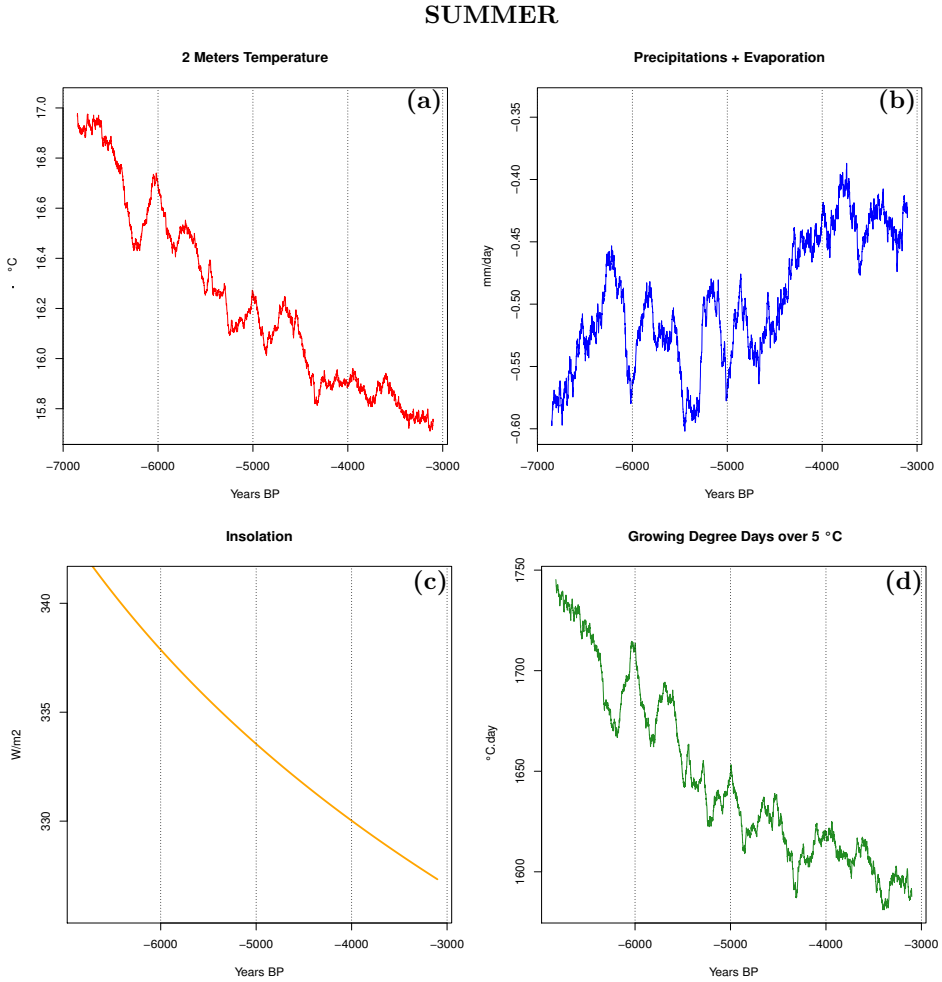

Figure 7.7: *a) Summer temporal evolution of near-surface temperature regional mean computed over the area of study; b) time series of summer precipitation+evapotranspiration calculated in mm/day; c) insolation changes over the period of study in W/m^2; d) time series of growing degree days above 5 degrees. All the time series are smoothed using 200-year running-mean.*

the neighbouring Lake Iseo. The pattern of contrasting mid-Holocene summer precipitation regimes was confirmed by Peyron et al. (2013), on the basis of pollen-inferred quantitative estimates and a multi-method approach that revealed minima (maxima) of summer precipitation and lake levels to the north (south) of ca. 40°N. Summer temperature showed a similar partition for the mid-Holocene in the central Mediterranean, with warmer (cooler) conditions to the north (south). Tóth et al. (2012) presented an Holocene summer air temperature reconstruction based on fossil chironomids from the Lake Brazi, a shallow mountain lake in the southern Carpathians. Their

results suggested that from ca. 8500 cal. BP, chironomid-based summer temperatures decreased in the area. In particular, the period between 6000 and 3000 cal. BP was characterized by cooler temperatures in comparison to the earlier period.

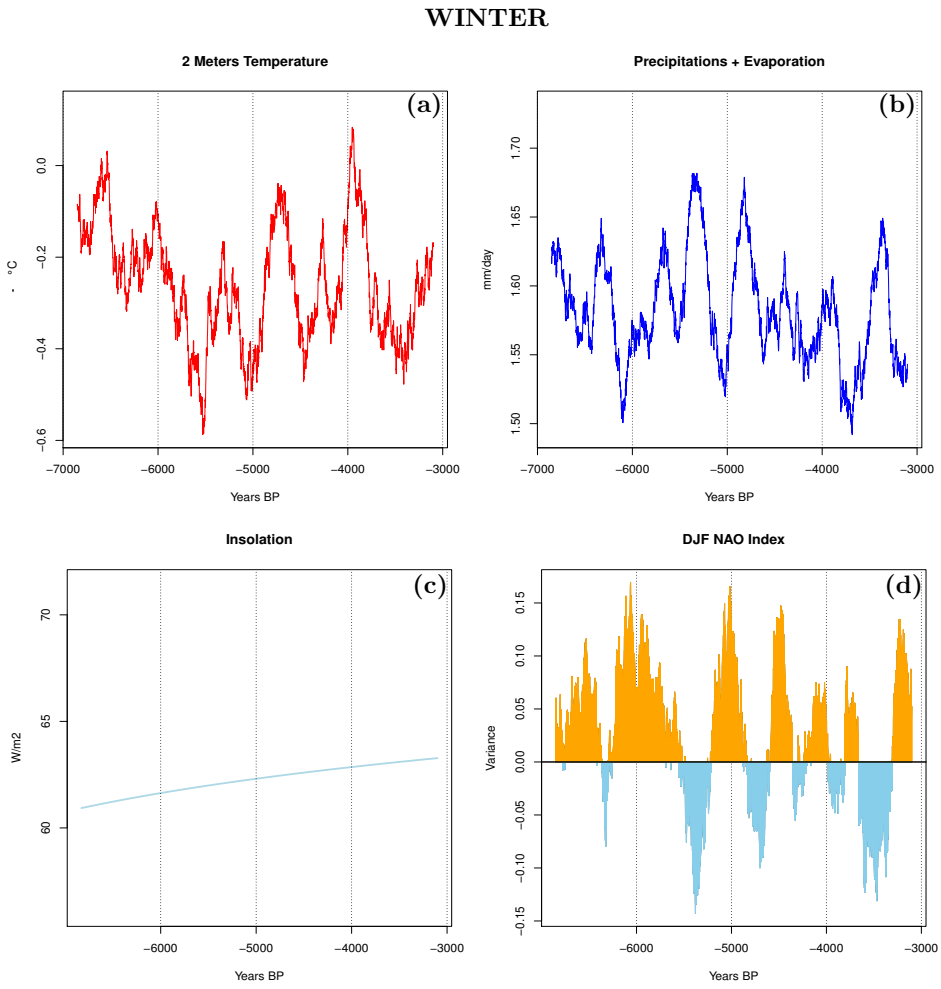

Figure 7.8: *a) Winter temporal evolution of near-surface temperature regional mean computed over the area of study; b) time series of winter precipitation+evapotranspiration calculated in mm/day; c) insolation changes over the period of study in W/m^2; d) DJF NAO index for the corresponding period. All the time series are smoothed using 200-year running-mean.*

Conversely, wintertime model results do not show a clear trend and the data are characterized by significant multi-decadal to inter-centennial fluctuations (Fig. 7.8). For winter, the trend of insolation during the mid-to-late Holocene, at the mid-latitudes of the NH, is not particularly pronounced (Fig. 7.8c). The behaviour of the simulated data is most likely a result of the

system internal variability. In winter, climatic conditions over Europe are mainly driven by changes in atmospheric circulation (Hurrell, 1995; Hurrell et al., 2003). In particular, the first mode of the winter atmospheric variability over the North Atlantic is represented by the NAO, which explains the one-third of the total variance of the SLP field over the area (Hurrell et al., 2003). A positive phase of the winter NAO is associated with an increase in strength and a northward shift of the westerly winds. This results in moist and warm air advection from the Atlantic to northern Europe (55^o-70^o N) and, consequently, in drier and colder conditions over southern Europe. Conversely, the negative phase of the NAO is accompanied by weaker and southward shifted (35^o-50^o N) westerlies, responsible for wetter and warmer winter conditions over southern Europe. The use of the NAO index (Fig. 7.8d) allows us to speculate that the oscillations of the simulated winter temperature and precipitation are caused by the variability between positive and negative phases of this atmospheric pattern. Different studies hypothesize that around 6000 BP the NAO was in a more pronounced positive phase with respect to the present-day conditions (Bonfils et al., 2004; Braconnot et al., 2007a,b; Davis et al., 2003; Mauri et al., 2014). This is not directly evident in our results. Nevertheless, the changes in the simulated winter conditions can be considered physically consistent: the model simulates a reasonable, internally consistent climate (Goosse et al., 2012; Von Storch et al., 2004). Although in the case of winter no distinct trend is evident in our simulations and the model results do not display the same level of correspondence with other studies (as they do in the case of summer, in particular for temperatures and moisture balance), the evinced oscillations in climatic parameters can be considered physically plausible.

7.6 Discussion and Conclusions

The period between the mid-7th and the end of the 5th millennium BP, in which the spread of both fleece bearing sheep husbandry and new fibre flax most likely occurred in south-east and central Europe, was characterized by profound social changes and has been studied so far in terms of intensified contacts and mobility (Anthony, 2007; Leary, 2014), environmental change (Barker, 1985; Binford and Binford, 1968) and economic transformation (Greenfield, 2005; Greenfield et al., 1988; Sherratt, 1981, 1997, 2006). Apart from the extensive research on the textile production in Romania (Mazăre, 2014) and Bulgaria (Petrova, 2011), which took into consideration indirect archaeological evidences from larger and confined geographical sections, textile tools and production of the period have not yet been system-

atically approached in the Pannonian Plain contexts. Narrowing the focus on the particular region enabled us to raise specific questions regarding textile fibre raw materials and final product demands, and their plausible dependence on the changing climate.

The impact of climate may not have been the only explanation for the evinced trends in the prehistoric textile production of the Pannonian Plain. Other factors such as social, economical or technological developent could have been the main drivers of changes. Nevertheless, evidences of other studies (Budja, 2015; Gronenborn et al., 2014; Weninger et al., 2009) suggest that climate changes had a significant role to play in the societal changes that characterized the populations inhabiting the area and its surroundings between the 7th and the 5th millennium BP. Weninger et al. (2009) found that at different times of the 6th Millennium BP there were abrupt abandonments of different settlements in Romania, Bulgaria and northern Greece, most likely due to the deterioration of climatic conditions. In the Alpine Region, during the same period, abrupt climatic oscillations on the scale of decades or century seem to have caused changes in hunting and farming patterns (Schibler et al., 1997). Similar causal connection was proposed by Kotova and Makhortykh (2010) in order to interpret migration fluxes and proxy reconstructions in the northern Pontic Steppe, a part of southeastern Europe, during the mid-Holocene.

Encouraged by such evidences, with the aim of finding possible correlations, we investigated the changes in textile production in the light of the reconstructed climate.

Analysis of climate simulations derived from the ECHO-G continuous run showed that significant changes in the climatic conditions of the region took place over the considered period of study. The declining summer trend of temperatures and the corresponding rising trend in moisture content might have caused the cultural-historically defined groups of the Post-Neolithic inhabiting the area, to be more sensitive to possible climatic fluctuations, such as the ones simulated during winter seasons. Such events could have acted as a trigger for shifts in the fibre procurement practices, resulting in the broadening of their resources and, especially, in the intensified selection in favour of their fitness. Through a complex causal network, this could have led to substantial perturbations within human societies (Berglund, 2003; Budja, 2015; Magny and Haas, 2004; Weninger et al., 2009).

According to our results, during the middle Eneolithic period, which marked the turn and the first centuries of the 6th millennium BP, the long-seed flax variety was likely the most exploited material for textile production in the area. Simultaneously, along with the deteriorating climate conditions, the use of animal products, presumably including fibres, started to be more

important.

In the following centuries of the 6th millennium BP, a continuous worsening of climatic conditions led to a broadening of the textile production of the Pannonian Plain, with populations inhabiting areas with less favourable conditions likely prompted to the employment of alternative resources. Increased variability of the late Eneolithic spindle-whorl assemblages, in favour of balanced distribution of moderate weight types between three main height categories, is something that might reflect this kind of broadened fibre assortment, both in regard to the raw material resources and end-product demands. Although, the obvious dominance of heavy and very heavy weight types of tools, particularly in high and steep height categories, greatly accounts for longer plant fibre preferences. Our evidences suggest that, between the late Eneolitic and the beginning of the Bronze Age, foraged plant material and possibly the long-seed variety of flax might have been partially substituted with a new fibre flax, more adaptable to colder climatic conditions characterizing this period (Chemikosova et al., 2006; Faruk and Sain, 2014). Analysis of the results of the BIOME4 model give support to such interpretation. In fact, comparison between the simulated changes for the 6000BP and the 5000BP time slices (Sec. 6), indicate that from the first to the second time slice, temperate deciduous forests were reduced by 20% in favour of cool mixed forests. Additionally, at 5000BP, montane forest and cool conifer forest appeared, supporting the suggested hypothesis.

More organized fibre material resources had to have been acquired and established by the end of the 6th millennium BP, during the early Bronze age. Both altered environmental and cultural conditions resonated further in the new demands for the specific types of textile products, which quite possibly corresponded to the intensified use of transport and traction. The dominance of very large tools, used probably for splicing and plying plant fibres, or their filaments, in order to make thick and strong threads and ropes which could have been used for harnessing animals, would support this scenario.

Despite the large textile tool sample that this research is based on and regardless of the climate conditions that support the outlined timeline for the introduction of both the sheep wool and the new fibre flax already during the Eneolithic in the Pannonian Plain, further zooarchaeological and archaeobotanical evidence is required to understand and explain the dynamics of these processes in finer details. Most likely, the exploration of the new fibre resources occurred simultaneously in remote contexts and could have been provoked by both cultural and environmental conditions. Numerous intertwining factors were likely responsible for the intensification of their exploitation and, to some degree, their further development.

Results of the analysis propose that in the studied region of southeastern

and central Europe, wool was exploited most probably already during the 6th and certainly during the 5th millennium BP, although on a smaller scale, first in comparison to flax, and second in comparison to the established wool economies of the contemporary urban centres in the Near East. Continuous deterioration of summer climatic conditions in the Pannonian Plain region during these two millennia would have still provided supportive conditions for the fibre flax. Areas with less favourable conditions for its cultivation might have focused their developing textile productions on other resources, causing them to specialise in alternatives. This is a question of difference in fibre specialisations, which have, so far, been interpreted as indications of use, creating an unacceptable dichotomy in the period of intensified mobility and contacts. Although wool's appearance and origin were for a long time considered within the striving textile economies of the urban revolution package in the Bronze Age Mesopotamia (McCorriston 1997; Kimbrough 2006), oldest preserved findings, genetic reasoning, and the analysis of the prehistoric textile tools forced its earlier appearance on the fibre scene. At the same time, archaeobotanical research on the flax plant places its fibre evolution into the same period of striving copper trade of the 6th millennium BP, proposing both resources were exploited in the production of Eneolithic threads. Even though both scenarios were connected to many cultural and environmental trends, climate change was certainly accountable, if not for their evolution, then for influencing the dynamics of their exploitation.

Chapter 8

Conclusions and Outlook

"An expert is a person who has made all the mistakes that can be made in a very narrow field."
- Niels Bohr -

The main goal of this study was to develop an experimental framework composed of global and regional climate models together with vegetation models that, while giving an important contribution to the better understanding of past climate and ecological changes, would allow to gain useful information suitable for its application in archaeological case studies. The selected period of study is the mid-to-late Holocene between 6000 years before present and the pre-industrial period (∼200 years ago), while the geographical area of research is Europe.

We summarize the main results of the study by revisiting the research questions posed in the introduction. Afterwards, we give an outlook by proposing possible directions of future research.

8.1 Conclusions

After providing a brief introduction on paleoclimate and climate forcings, and a description of the climate simulations experimental setup, we conducted an evaluation of the performance of the different models. Consistency between simulations performed with two GCMs at different resolution was tested with satisfactory results. Successively, the RCM model performance for present day conditions was evaluated. The model tuned with a specific configuration, which was deemed for implementing changes in the climate forcings, performed successfully and the results were comparable with the ones of other studies focusing on the same period and area of study.

Afterwards, by analysing the results of the different climate simulations, we firstly attempted to address the following research question:

1. How do climate models perform in comparison with proxy reconstructions, according to their spatial resolution? Based on this comparison, what are the possible advantages of the use of a regional climate model for paleoclimate studies?

Results have shown that, in general, an increase in the resolution of climate models leads to an improvement of the results. Nevertheless, significant improvements in the simulation of climate changes were not found between a high resolution GCM and an RCM. Main differences involved variables such as near surface temperature and growing degree days above 5 degrees, for which surface processes play a major role and are better reproduced at the higher resolution of the RCM.

Analysing temperature reconstructions based on pollen proxies and comparing them with the results of the RCM simulation, we successively answered the following research questions:

2. What is the development of the mid-to-late Holocene European seasonal temperature cycle towards present day conditions? Which processes is it related to?

3. What is the main behaviour of the simulated mid-to-late Holocene temperature over Europe? What are the reasons for possible mismatches with reconstructions?

Changes in the seasonal cycle of insolation, particularly over the high latitudes of the Northern Hemisphere, were the most influential forcings of the mid-to-late Holocene climate. Their impact on the evolution of surface temperature would have been expected to be significant. Nevertheless, reconstructions have shown that the mid-to-late Holocene temperature behaviour over Europe did not always directly follow the astronomical forcings. In particular, a different behaviour was evident between northern and southern Europe. Northern European temperature was characterized by a decreasing trend for both winter and summer. Conversely, the temperature evolution over southern Europe presented an opposite increasing trend in both seasons. Through the analysis of climate simulations results and by means of correlation with insolation and changes in atmospheric circulation, and additionally supported by the results of previous studies, we propose two main explanations for such behaviour. Northern European warmer winter temperature at

the mid-Holocene, with respect to the pre-industrial period, was mainly due to a major positive phase of the NAO at that time, having simultaneously an opposite cooling effect over southern Europe. Conversely, summer temperature behaviour during the mid-to-late Holocene was mainly driven by changes in insolation. While over northern Europe, temperature evolution was the result of a direct response to changes in insolation, in the South surface processes, such as enhanced surface evapotranspiration as a result of more insolation, were the main drivers of changes.

Model results were consistent with the reconstructions only in some cases. In winter over southern Europe, temporal behaviour and spatial distribution of temperature in the two datasets were comparable. Conversely, the model reproduced generally colder conditions over central and northern continental Europe. This bias was most likely due to a different representation by the model of the expected changes in atmospheric circulation. In summer instead, the model was too sensitive to insolation changes. While over northern Europe the two datasets were in good agreement, for the South a large warm bias was present. According to previous results and to a test-run for present day conditions, we suggested that this bias was most likely due to model deficiencies in the representation of soil-atmosphere heat fluxes over the area.

The results of the RCM simulation were successively used as input for a bioequilibrium model simulation. Our attention focused on the following question:

4. What were the changes in vegetation distribution during the mid-to-late Holocene in Europe? How is the developed experimental framework able to reproduce such changes?

Proxy reconstructions indicated that at the mid-Holocene, temperate forests dominated both northern and southern Europe. Then they progressively retreated, displaced by boreal forests and tundra in the North and by drier vegetation in the South. A qualitatively good agreement between a pollen-based reconstruction database and the simulated results was evident over central Europe, for which both the climate and the bioequilibrium vegetation model presented the best performance. Conversely, in the North, even if the model reproduced a spread of temperate forests towards higher latitudes, this was limited when compared to the northward expansion of temperate forests evinced from the reconstructions. Additionally, in the South, the simulated results were characterized by a major presence of grass and savanna-like biomes at the mid-Holocene with respect to the reconstructions, most likely due to the warm bias of the climate model over this area.

Finally, the results of a mutidisciplinary case study were presented. The question that stimulated our research was:

5. Are there any relationships between the mid-to-late Holocene climate change and societal changes over Europe?

Research focused on a specific case study: the textile revolution in the Pannonian plain between the 7th and the 5th millennium BP. Results have shown that two main fibres were exploited over the region during this period, with three different phases characterized by significant changes in the textile production: the late Eneolithic, the middle Eneolithic and the early Bronze age. While during the first and the latest phases the production was more specialized, with findings suggesting a major use of light and short fibres in the late Eneolithic and heavier and longer fibres in the early Bronze age, the transitional period of the late Eneolithic was characterized by a broad diversification of tools and materials. Research suggested that such behaviour was most likely related, among other factors, to a rapid deterioration of climatic conditions, with a large decrease in summer temperatures and an increase in summer moisture content. The evinced trend in the textile production of the Pannonian Plain during the late Eneolithic was very likely the result of an attempt of the civilizations of the area to adapt to excessive climate stress, with populations inhabiting areas with less favourable conditions induced to the use of alternative resources.

8.2 Perspectives and Future Work

The results evinced from our climate/ecological simulations cannot be considered completely exhaustive with regards to the main research questions that arose, and further work can help in clarifying uncertainties by allowing an improvement of the results.

In order to have a more robust estimation of the possible added value of RCMs for their use in paleoclimate studies, further research should be performed by considering other GCM-RCM couples and a wider number of simulations. Additionally, joint efforts from specialists of different disciplines are still required in order to further clarify proxy uncertainties.

With respect to the study of the temporal evolution of European temperature during the mid-to-late Holocene, the improvement over some aspects of the experimental setup should contribute to more comprehensive results. In particular, further experiments need to be designed in order to test the proposed hypothesis. New simulations should be performed in order to test the effective contribution of soil water content and improved soil properties

on the climate of the Mediterranean region. This could have relevant implications for the study of present and future climate change over the area. Resources for these simulations have already been made available at the supercomputer service of the German weather society.

For the study of the mid-to-late Holocene vegetation evolution, the results of Dynamical Vegetation models should be considered for the evaluation of the results of the bio-equilibrium model employed in this study. Additionally, a better reproduced land cover could be used for the performance of new mid-to-late Holocene climate simulations. Other archaeological case studies have been investigated in this work and further research is ongoing, with focus on different areas and cultural backgrounds.

Acknowledgments

This experience has meant a lot to me. The last three and a half years have represented a period in which I had the chance to grow not only professionally, but also humanly. Facing several challenging difficulties I had the opportunity to better understand the importance of exploiting and cultivating my personal capabilities, not only for the achievement of the academic goals, but for life in general. In this experience I had the opportunity to learn, understand and grow up.

In a first instance, I would like to thank my supervisor Prof. Dr. Ulrich Cubasch, for the great opportunity he has given to me and for his unconditional trust.

A particular acknowledgment goes to my co-supervisor Prof. Dr. Wiebke Bebermeier, for her constructive comments and support at different times of my doctoral studies.

A special thought is for my family, my father and my mother, my brothers and the persons who are not here anymore.

I additionally want to thank the Excellence Cluster TOPOI and the Berlin Graduate School of Ancient Studies, which provided the economic and academic support for the successful accomplishment of this doctoral project.

Among all I want to sincerely express my gratitude to Prof. Dr. Sahar Soudoudi for her support and unconditional trust. Without her, I would have never managed to succeed in this experience.

A special thank goes to all the people that I met or with which I shared part of this experience. From my old friends Chiara, Mario, Gianluca, Rita, Armando, Peppedagata, Peppeangilella, Agnese, Giovanni, Vaipino, Pieggioggio, Peppe Signorelli, Budda, to the new ones Edoardo, Walter, Bijan, Nico, Alexander, Christos, Federica, Rudi, Dagmar, Mustafa, Nicola, Giulia, Marco, Joanne, Ilona and all the colleagues from the meteorological institute of Berlin and the ones with which I shared the graduation studies: Ioulia, Ana, Simona and all the other students from the BerGSAS. A particular thanks goes to Tina, Oul and Elke for their support in academic bureaucracy and the proofreading of the manuscript.

There have been several challenging moments and situations, and I would not have been able to overcome them without the support of all of these people.

Finally, I have to express special gratitude to the city of Berlin. For its spirit, its life, and its uniqueness that have indelibly marked my life forever.

Vielen Dank.

Appendix A

Table A1: *Classification of the different PFTs, as used in the BIOME4 model, according to different bioclimatic limits:* T_c ***min*** *and* T_c ***max*** *represent respectively min. and max. absolute minimum temperature during the year;* T_{min} ***min*** *and* T_{min} ***max*** *are the min. and the max. temperature of the coldest month;* GDD_5 ***min*** *and* GDD_0 ***min*** *are the number of minimum growing degree days above, respectively, 5 and 0 °C.* T_{wm} ***min*** *and* T_{wm} ***max*** *represent the min. and the max. temperature of the warmest month.* ***Snow min*** *is the minimum depth of snow cover.*

Plant Functional Types	T_c min (°C)	T_c max (°C)	T_{min} min (°C)	T_{min} max (°C)	GDD_5 min	GDD_0 min	T_{wm} min (°C)	T_{wm} max (°C)	Snow min (cm)
Tropical Broadleaf			0				10		
Temperate Broadleaf Evergreen			-10	5	1200		10		
Temperate Broadleaf Summergreen	5			-10	1200				
Temperate Needleleaf Evergreen	-2			10	900		10		
Cold Evergreen	-32.5	-2						21	
Cold Deciduous		5		-10				21	
Temperate Grass				0	550				
Tropical Grass			-3				10		
Desert Woody Shrub			-45		500		10		
Tundra Woody Shrub						50		15	15
Cold Herbaceous						50		15	
Cushion-Forb								15	

Acronyms

AGCM Atmospheric General Circulation Model.

AMIP2 Atmospheric Model Intercomparison Project phase 2.

AO Atlantic Oscillation.

AOGCM Atmosphere Ocean General Circulation Model.

BP Before Present.

CCA Canonical Correlation Analysis.

CCLM COSMO model in CLimate Mode.

CDO Climate Data Operators.

CE Common Era.

CF Cost Function.

CMIP5 Coupled Model Intercomparison Project phase 5.

COHMAP Cooperative Holocene Mapping Project.

CRU Climate Research Unit.

DJF December January February.

DVM Dynamical Vegetation Model.

E-OBS European daily high-resolution gridded dataset.

ECMWF European Centre for Medium-Range Weather Forecasts.

EOF Empirical Orthogonal Function.

ERA-Interim ECMWF Interim Reanalysis.

GCM General Circulation Model.

GE Greenhouse Effect.

GHG Greenhouse Gas.

GLDAS Global Land Data Assimilation System.

IPCC Intergovernmental Panel on Climate Change.

JJA June July August.

LAI Leaf Area Index.

LGM Last Glacial Maximum.

LIA Little Ice Age.

LM Local Model.

LOESS LOcal regrESSion.

MSLP Mean Sea Level Pressure.

N North.

NAO North Atlantic Oscillation.

NH Northern Hemisphere.

NPP Net Primary Productivity.

PC Principal Component.

PFT Plant Functional Type.

PMIP3 Paleoclimate Modeling Intercomparison Project phase 3.

RCM Regional Climate Model.

SAM Southern Annular Mode.

SE Standard Error.

SH Southern Hemisphere.

SIC Sea Ice Cover.

SLP Sea Level Pressure.

SST Sea Surface Temperature.

SVAT Soil Atmosphere Vegetation Transfer scheme.

TOA Top Of the Atmosphere.

Abbreviations

$\boldsymbol{CH_4}$ methan.

$\boldsymbol{CO_2}$ carbon dioxide.

$\boldsymbol{N_2O}$ nitrous oxide.

$\boldsymbol{^oC}$ degrees Celsius.

$\boldsymbol{^{14}C}$ carbon-14 isotope.

$\boldsymbol{^{18}O}$ oxygen-18 isotope.

$\boldsymbol{m^2}$ square metre.

a.s.l. above sea level.

e.g. exempli gratia.

Fig. figure.

GDD5 growing degree days above 5 ^oC.

hPa hectopascals.

i.e. id est.

km kilometres.

lat latitude.

lon longitude.

mm millimetres.

ppbv parts per billion by volume.

ppmv parts per million by volume.

rlat latitude in rotated coordinates.

rlat longitude in rotated coordinates.

s seconds.

Sec. section.

T 2M near surface temperature.

Tab. table.

TOT PREC total precipitation.

W watt.

Bibliography

Abe-Ouchi, A., Segawa, T., and Saito, F. Climatic conditions for modelling the northern hemisphere ice sheets throughout the ice age cycle. *Climate of the Past*, 3(3):423–438, 2007.

Ahn, J. and Brook, E.J. Atmospheric co_2 and climate on millennial time scales during the last glacial period. *Science*, 322(5898):83–85, 2008.

Alfaro, C. Étoffes cordées du site néolithique de tell-halula (syrie-viii e millénaire avant j.-c.). *Bulletin du CIETA*, 79:16–25, 2002.

Anderson, P.M., Barnosky, C.W., Bartlein, P.J., Behling, P.J., Brubaker, L., Cushing, E.J., Dodson, J., Dworetsky, B., Guetter, P.J., Harrison, S.P., et al. Climatic changes of the last 18,000 years: Observations and model simulations. *Science*, 241:1043–1052, 1988.

Andersson, E. Textile production at birka: Household needs or organised workshops? In *Northern Archaeological Textiles: NESAT VII: Textile Symposium in Edinburgh, 5th-7th May 1999*, volume 7, page 44. Oxbow Books, 2015.

Andrič, M. and Willis, K.J. The phytogeographical regions of slovenia: a consequence of natural environmental variation or prehistoric human activity? *Journal of Ecology*, 91(5):807–821, 2003.

Anthony, D. The wheel, the horse, and language, 2007.

Barbante, C., Barnola, J.M., Becagli, S., Beer, J., Bigler, M., Boutron, C., Blunier, T., Castellano, E., Cattani, O., Chappellaz, J., et al. One-to-one coupling of glacial climate variability in greenland and antarctica. *Nature*, 444(7116):195–198, 2006.

Barber, E.J.W. *Prehistoric textiles: the development of cloth in the Neolithic and Bronze Ages with special reference to the Aegean*. Princeton University Press, 1991.

Barker, G. *Prehistoric farming in Europe*. CUP Archive, 1985.

Barnett, T.P. and Preisendorfer, R.W. Origins and levels of monthly and seasonal forecast skill for united states surface air temperatures determined by canonical correlation analysis. *Mon. Wea. Rev.*, 115:1825–1850, 1987.

Bartlein, P.J. and Prentice, I.C. Orbital variations, climate and paleoecology. *Trends in ecology & evolution*, 4(7):195–199, 1989.

Bartosiewicz, L. Mammalian bone. *The early Neolithic on the Great Hungarian plain Investigations of the Körös culture site of Ecsegfalva*, 23, 2007.

Benestad, R.E., Hanssen-Bauer, I., and Chen, D. *Empirical-statistical downscaling*. World Scientific, 2008.

Benito-Garzon, M., Sánchez de Dios, R., and Sáinz Ollero, H. Predictive modelling of tree species distributions on the iberian peninsula during the last glacial maximum and mid-holocene. *Ecography*, 30(1):120–134, 2007.

Berger, A. Long-term variations of daily insolation and quaternary climatic changes. *Journal of Atmospheric Science*, 35(12):2362–2367, 1978.

Berger, A. and Loutre, M. Insolation values for the climate of the last 10 million years. *Quaternary Science Reviews*, 10(4):297–317, 1991.

Berger, A. and Loutre, M. An exceptionally long interglacial ahead? *Science*, 297(5585):1287–1288, 2002.

Berglund, B.E. Human impact and climate changes—synchronous events and a causal link? *Quaternary International*, 105(1):7–12, 2003.

Berglund, B.E., Barnekow, L., Hammarlund, D., Sandgren, P., and Snowball, I.F. Holocene forest dynamics and climate changes in the abisko area, northern sweden: the sonesson model of vegetation history reconsidered and confirmed. *Ecological Bulletins*, pages 15–30, 1996.

Bichler, P., Grömer, K., Hofmann-de Keijzer, R., Kern, A., and Reschreiter, H. *Hallstatt textiles: technical analysis, scientific investigation and experiment on Iron Age textiles*. Archaeopress, 2005.

Binford, S.R. and Binford, L.R. *New perspectives in archaeology*. Chicago: Aldine Publishing Company, 1968.

Blunier, T. and Brook, E.J. Timing of millennial-scale climate change in antarctica and greenland during the last glacial period. *Science*, 291(5501): 109–112, 2001.

Bluth, G.J.S., Doiron, S.D., Schnetzler, C.C., Krueger, A.J., and Walter, L.S. Global tracking of the so2 clouds from the june, 1991 mount pinatubo eruptions. *Geophysical Research Letters*, 19(2):151–154, 1992.

Bohnsack, A. Spinnen und weben. *Entwicklung von Technik und Arbeit im Textilgewerbe. Reinbek*, 1981.

Bond, G., Kromer, B., Beer, J., Muscheler, R., Evans, M.N., Showers, W., Hoffmann, S., Lotti-Bond, R., Hajdas, I., and Bonani, G. Persistent solar influence on north atlantic climate during the holocene. *Science*, 294(5549): 2130–2136, 2001.

Bond-Lamberty, B., Gower, S.T., Ahl, D.E., and Thornton, P. Reimplementation of the biome-bgc model to simulate successional change. *Tree Physiology*, 25(4):413–424, 2005.

Bonfils, C., de Noblet-Ducoudré, N., Guiot, J., and Bartlein, P. Some mechanisms of mid-holocene climate change in europe, inferred from comparing pmip models to data. *Climate Dynamics*, 23(1):79–98, 2004.

Braconnot, P., Otto-Bliesner, B., Harrison, S., Joussaume, S., Peterchmitt, J.Y., Abe-Ouchi, A., Crucifix, M., Driesschaert, E., Fichefet, T., Hewitt, C.D., et al. Results of pmip2 coupled simulations of the mid-holocene and last glacial maximum–part 2: feedbacks with emphasis on the location of the itcz and mid-and high latitudes heat budget. *Climate of the Past*, 3 (2):279–296, 2007a.

Braconnot, P., Otto-Bliesner, B., Kageyama, M., Kitoh, A., Laîné, A., Loutre, M.F., Marti, O., Merkel, U., Ramstein, G., Valdes, P., et al. Results of pmip2 coupled simulations of the mid-holocene and last glacial maximum–part 1: experiments and large-scale features. *Climate of the Past*, pages 261–277, 2007b.

Braconnot, P., Harrison, S.P., Otto-Bliesner, B., Abe-Ouchi, A., Jungclaus, J., and Peterschmitt, J.Y. The paleoclimate modeling intercomparison project contribution to cmip5. *Clivar Echanges No. 56*, 16, No.2:15–19, 2011.

Braconnot, P., Harrison, S.P., Kageyama, M., Bartlein, P.J., Masson-Delmotte, V., Abe-Ouchi, A., Otto-Bliesner, B., and Zhao, Y. Evaluation of climate models using palaeoclimatic data. *Nature Climate Change*, 2 (6):417–424, 2012.

Brewer, S., François, L., Cheddadi, R., Laurent, J.M., and Favre, E. Comparison of simulated and observed vegetation for the mid-holocene in europe. *Climate of the Past Discussions*, 5(2):965–1011, 2009.

Brooke, John L. *Climate change and the course of global history: a rough journey*. Cambridge University Press, 2014.

Brunsdon, C., Fotheringham, A.S., and Charlton, M.E. Geographically weighted regression: a method for exploring spatial nonstationarity. *Geographical analysis*, 28(4):281–298, 1996.

Budja, M. Archaeology and rapid climate changes: from the collapse concept to a panarchy interpretative model. *Documenta Praehistorica*, 42:171–184, 2015.

Cain, M.L., Bowman, W.D., and Hacker, S.D. *Ecology*. Sinauer Associates, Incorporated, 2014. ISBN 9780878939084. URL https://books.google.de/books?id=CeSWngEACAAJ.

Canadell, J., Jackson, R.B., Ehleringer, J.B., Mooney, H.A., Sala, O.E., and Schulze, E.D. Maximum rooting depth of vegetation types at the global scale. *Oecologia*, 108(4):583–595, 1996.

Charvát, P. On sheep, sumerians and the early state. *Ancient Near Eastern Studies in Memory of Blahoslav Hruška*, pages 49–60, 2011.

Cheddadi, R. and Bar-Hen, A. Spatial gradient of temperature and potential vegetation feedback across europe during the late quaternary. *Climate Dynamics*, 32(2-3):371–379, 2009.

Cheddadi, R., Yu, G., Guiot, J., Harrison, S.P., and Prentice, I.C. The climate of europe 6000 years ago. *Climate dynamics*, 13(1):1–9, 1996.

Chemikosova, S.B., Pavlencheva, N.V., Gur'yanov, O.P., and Gorshkova, T.A. The effect of soil drought on the phloem fiber development in long-fiber flax. *Russian Journal of Plant Physiology*, 53(5):656–662, 2006.

Chmielewski, T. and Gardyński, L. New frames of archaeometrical description of spindle whorls: a case study of the late eneolithic spindle whorls from the 1c site in grodek, district of hrubieszow, poland. *Archaeometry*, 52(5):869–881, 2010.

Christensen, J.H., Carter, T.R., Rummukainen, M., and Amanatidis, G. Evaluating the performance and utility of regional climate models: the prudence project. *Climatic Change*, 81(1):1–6, 2007.

Christensen, J.H., Boberg, F., Christensen, O.B., and Lucas-Picher, P. On the need for bias correction of regional climate change projections of temperature and precipitation. *Geophysical Research Letters*, 35(20), 2008.

Christensen, O.B. Relaxation of soil variables in a regional climate model. *Tellus A*, 51(5):674–685, 1999.

Cleveland, W.S. and Devlin, S.J. Locally weighted regression: an approach to regression analysis by local fitting. *Journal of the American Statistical Association*, 83(403):596–610, 1988.

Coats, S., Smerdon, J.E., Cook, B.I., and Seager, R. Stationarity of the tropical pacific teleconnection to north america in cmip5/pmip3 model simulations. *Geophysical Research Letters*, 40(18):4927–4932, 2013.

Collins, P.M., Davis, B.A.S., and Kaplan, J.O. The mid-holocene vegetation of the mediterranean region and southern europe, and comparison with the present day. *Journal of Biogeography*, 39(10):1848–1861, 2012.

Craig, O.E., Chapman, J., Heron, C., Willis, L.H., Bartosiewicz, L., Taylor, G., Whittle, A., and Collins, M. Did the first farmers of central and eastern europe produce dairy foods? *ANTIQUITY-OXFORD-*, 79(306):882, 2005.

Cressie, N., Assuncao, R., Holan, S.H., Levine, M., Nicolis, O., Zhang, J., and Zou, J. Dynamical random-set modeling of concentrated precipitation in north america. 2012.

Cressman, G.P. An operational objective analysis system. *Mon. Wea. Rev*, 87(10):367–374, 1959.

Crewe, L. *Spindle whorls: a study of form, function and decoration in prehistoric Bronze Age Cyprus*, volume 149. Coronet Books, 1998.

Cubasch, U. Das klima der nächsten 100 jahre: Szenarienrechnungen mit dem gekoppelten globalen ozean-atmosphärenmodell aus hamburg. *Physikalische Blätter*, 48(2):85–89, 1992.

Cubasch, U., Waszkewitz, J., Hegerl, G., and Perlwitz, J. Regional climate changes as simulated in time-slice experiments. *Climatic Change*, 31(2-4): 273–304, 1995.

Cullen, H.M., Hemming, S., Hemming, G., Brown, F.H., Guilderson, T., Sirocko, F., et al. Climate change and the collapse of the akkadian empire: Evidence from the deep sea. *Geology*, 28(4):379–382, 2000.

Curry, A. Gobekli tepe: The world's first temple? *Smithsonian Magazine*, 3:1–4, 2008.

Cybulska, M. and Maik, J. Archaeological textiles-a need of new methods of analysis and reconstruction. *Fibres & Textiles in Eastern Europe*, 15(5-6): 64–65, 2007.

Damon, P.E. and Jirikowic, J.L. The sun as a low-frequency harmonic oscillator. *Radiocarbon*, 34(2):199–205, 1992.

Davis, B.A.S. and Stevenson, A.C. The 8.2 ka event and early–mid holocene forests, fires and flooding in the central ebro desert, ne spain. *Quaternary Science Reviews*, 26(13):1695–1712, 2007.

Davis, B.A.S., Brewer, S., Stevenson, A.C., and Guiot, J. The temperature of europe during the holocene reconstructed from pollen data. *Quaternary Science Reviews*, 22(15):1701–1716, 2003.

Davis, B.A.S., Collins, P.M., and Kaplan, J.O. The age and post-glacial development of the modern european vegetation: a plant functional approach based on pollen data. *Vegetation history and archaeobotany*, 24(2): 303–317, 2015.

De Castro, M., Gallardo, C., Jylha, K., and Tuomenvirta, H. The use of a climate-type classification for assessing climate change effects in europe from an ensemble of nine regional climate models. *Climatic Change*, 81(1): 329–341, 2007.

de Melo, M.L.D. and Marengo, J.A. The influence of changes in orbital parameters over south american climate using the cptec agcm: simulation of climate during the mid holocene. *The Holocene*, 18(4):501–516, 2008.

Dee, D.P., Uppala, S.M., Simmons, A.J., Berrisford, P., Poli, P., Kobayashi, S., Andrae, U., Balmaseda, M.A., Balsamo, G., Bauer, P., et al. The era-interim reanalysis: Configuration and performance of the data assimilation system. *Quarterly Journal of the Royal Meteorological Society*, 137(656): 553–597, 2011.

Denis, B., Laprise, R., Caya, D., and Côté, J. Downscaling ability of one-way nested regional climate models: the big-brother experiment. *Climate Dynamics*, 18(8):627–646, 2002.

Déqué, M., Marquet, P., and Jones, R.G. Simulation of climate change over europe using a global variable resolution general circulation model. *Climate Dynamics*, 14(3):173–189, 1998.

Di Luca, A., de Elía, R., and Laprise, R. Potential for added value in precipitation simulated by high-resolution nested regional climate models and observations. *Climate Dynamics*, 38(5-6):1229–1247, 2012.

Di Luca, A., de Elía, R., and Laprise, R. Potential for small scale added value of rcm's downscaled climate change signal. *Climate Dynamics*, 40 (3-4):601–618, 2013.

Di Luca, A., de Elía, R., and Laprise, R. Challenges in the quest for added value of regional climate dynamical downscaling. *Current Climate Change Reports*, 1(1):10–21, 2015.

Dimri, A.P. Impact of subgrid scale scheme on topography and landuse for better regional scale simulation of meteorological variables over the western himalayas. *Climate dynamics*, 32(4):565–574, 2009.

Doms, G. and Schättler, U. A description of the nonhydrostatic regional model lm, part ii: Physical parameterization. Technical report, Consortium for Small Scale Modelling (COSMO), 2003.

Doumas, C. *Thera: Pompeii of the Ancient Aegean: Excavations at Akrotiri, 1967-79*. Thames and Hudson, 1983.

Douville, H. Limitations of time-slice experiments for predicting regional climate change over south asia. *Climate Dynamics*, 24(4):373–391, 2005.

Driessen, J. Towards an archaeology of crisis: Defining the long-term impact of the bronze age santorini eruption. *Natural Disasters and Cultural Change*, pages 250–263, 2002.

Elderfield, H., Ferretti, P., Greaves, M., Crowhurst, S., McCave, I.N., Hodell, D., and Piotrowski, A.M. Evolution of ocean temperature and ice volume through the mid-pleistocene climate transition. *Science*, 337(6095):704–709, 2012.

Evershed, R.P., Payne, S., Sherratt, A. G, Copley, M.S., Coolidge, J., Urem-Kotsu, D., Kotsakis, K., Özdoğan, M., Özdoğan, A.E., Nieuwenhuyse, O., et al. Earliest date for milk use in the near east and southeastern europe linked to cattle herding. *Nature*, 455(7212):528–531, 2008.

Fagan, B. *The great warming: Climate change and the rise and fall of civilizations*. Bloomsbury Publishing USA, 2008.

Fallah, B., Sodoudi, S., and Cubasch, U. Westerly jet stream and past millennium climate change in arid central asia simulated by cosmo-clm model. *Theoretical and Applied Climatology*, pages 1–10, 2015.

Faruk, O. and Sain, M. *Biofiber reinforcements in composite materials*. Number 51. Elsevier, 2014.

Feser, F., Rockel, B., von Storch, H., Winterfeldt, J., and Zahn, M. Regional climate models add value to global model data: a review and selected examples. *Bulletin of the American Meteorological Society*, 92(9):1181, 2011.

Fischer, E.M., Seneviratne, S.I., Vidale, P.L., Lüthi, D., and Schär, C. Soil moisture-atmosphere interactions during the 2003 european summer heat wave. *Journal of Climate*, 20(20):5081–5099, 2007.

Fischer, N. and Jungclaus, J.H. Evolution of the seasonal temperature cycle in a transient holocene simulation: orbital forcing and sea-ice. *Climate of the Past*, 7:1139–1148, 2011.

Flato, G., Marotzke, J., Abiodun, B., Braconnot, P., Chou, S.C., Collins, W.J., Cox, P., Driouech, F., Emori, S., Eyring, V., et al. Evaluation of climate models. in: Climate change 2013: The physical science basis. contribution of working group i to the fifth assessment report of the intergovernmental panel on climate change. *Climate Change 2013*, 5:741–866, 2013.

Fleitmann, D., Burns, S.J., Mudelsee, M., Neff, U., Kramers, J., Mangini, A., and Matter, A. Holocene forcing of the indian monsoon recorded in a stalagmite from southern oman. *Science*, 300(5626):1737–1739, 2003.

Flückiger, J., Monnin, E., Stauffer, B., Schwander, J., Stocker, T.F., Chappellaz, J., Raynaud, D., and Barnola, J.M. High-resolution holocene n2o ice core record and its relationship with ch4 and co2. *Global Biogeochemical Cycles*, 16(1), 2002.

Folland, C., Knight, J., Linderholm, H., Fereday, D., Ineson, S., and Hurrell, J. The summer north atlantic oscillation: Past, present, and future. *Journal of Climate*, 22:1082–1103, 2009.

Foster, K.P., Ritner, R.K., and Foster, B.R. Texts, storms, and the thera eruption. *Journal of Near Eastern Studies*, 55(1):1–14, 1996.

François, L.M., Delire, C., Warnant, P., and Munhoven, G. Modelling the glacial–interglacial changes in the continental biosphere. *Global and Planetary Change*, 16:37–52, 1998.

François, L.M., Goddéris, Y., Warnant, P., Ramstein, G., de Noblet, N., and Lorenz, S. Carbon stocks and isotopic budgets of the terrestrial biosphere at mid-holocene and last glacial maximum times. *Chemical geology*, 159 (1):163–189, 1999.

Fröhlich, C. and Lean, J. Solar radiative output and its variability: evidence and mechanisms. *The Astronomy and Astrophysics Review*, 12(4):273–320, 2004.

Fyfe, R.M., Brown, A.G., and Rippon, S.J. Mid-to-late holocene vegetation history of greater exmoor, uk: estimating the spatial extent of human-induced vegetation change. *Vegetation History and Archaeobotany*, 12(4): 215–232, 2003.

Gachet, S., Brewer, S., Cheddadi, R., Davis, B., Gritti, E., and Guiot, J. A probabilistic approach to the use of pollen indicators for plant attributes and biomes: an application to european vegetation at 0 and 6 ka. *Global Ecology and Biogeography*, 12(2):103–118, 2003.

Gaillard, M.J., Sugita, S., Mazier, F., Trondman, A.K., Brostrom, A., Hickler, T., Kaplan, J.O., Kjellström, E., Kokfelt, U., Kunes, P., et al. Holocene land-cover reconstructions for studies on land cover-climate feedbacks. *Climate of the Past*, 6:483–499, 2010.

Gaillard-Lemdahl, M.J. and Berglund, B.E. Quantification of land surfaces cleared of forest during the holocene. 1998.

Gajewski, K., Viau, A.E., Sawada, M., Atkinson, D.E., and Fines, P. Synchronicity in climate and vegetation transitions between europe and north america during the holocene. *Climatic change*, 78(2-4):341–361, 2006.

Gallimore, R., Jacob, R., and Kutzbach, J. Coupled atmosphere-ocean-vegetation simulations for modern and mid-holocene climates: role of extratropical vegetation cover feedbacks. *Climate Dynamics*, 25(7-8):755–776, 2005.

Ganopolski, A. and Calov, R. The role of orbital forcing, carbon dioxide and regolith in 100 kyr glacial cycles. *Climate of the Past*, 7(4):1415–1425, 2011.

Gao, Y., Vano, J.A., Zhu, C., and Lettenmaier, D.P. Evaluating climate change over the colorado river basin using regional climate models. *Journal of Geophysical Research: Atmospheres*, 116(D13), 2011.

Giorgi, F. Regional climate modeling: Status and perspectives. In *Journal de Physique IV (Proceedings)*, volume 139, pages 101–118. EDP sciences, 2006.

Giorgi, F., Mearns, L.O., Shields, C., and McDaniel, L. Regional nested model simulations of present day and 2× co2 climate over the central plains of the us. *Climatic Change*, 40(3-4):457–493, 1998.

Gleba, M. and Mannering, U. Textiles and textile production in europe from prehistory to ad 400. 2012.

Gliemeroth, A.K. Paläoökologische aspekte der einwanderungsgeschichte einiger baumgattungen während des holozäns nach europa. *Angewandte Botanik*, 71(1-2):54–61, 1997.

Goldewijk, K.K. Estimating global land use change over the past 300 years: the hyde database. *Global Biogeochemical Cycles*, 15(2):417–433, 2001.

Gómez-Navarro, J.J., Montávez, J.P., Jerez, S., Jiménez-Guerrero, P., Lorente-Plazas, R., González-Rouco, J.F., and Zorita, E. A regional climate simulation over the iberian peninsula for the last millennium. 2011.

Gómez-Navarro, J.J., Montávez, J.P., Jiménez-Guerrero, P., Jerez, S., Lorente-Plazas, R., González-Rouco, J.F., and Zorita, E. Internal and external variability in regional simulations of the iberian peninsula climate over the last millennium. *Climate of the Past*, 8(1):25–36, 2012.

Gómez-Navarro, J.J., Montávez, J.P., Wagner, S., and Zorita, E. A regional climate palaeosimulation for europe in the period 1500–1990–part 1: Model validation. *Climate of the Past*, 9(4):1667–1682, 2013.

Gómez-Navarro, J.J., Bothe, O., Wagner, S., Zorita, E., Werner, J.P., Luterbacher, J., Raible, C.C., and Montávez, J.P. A regional climate paleosimulation for europe in the period 1500-1990-part2: Shortcomings and strengths of models and reconstructions. *Climate of the Past*, 11:1077–1095, 2015.

Goosse, H., Renssen, H., Timmermann, A., Bradley, R.S., and Mann, M.E. Using paleoclimate proxy-data to select optimal realisations in an ensemble of simulations of the climate of the past millennium. *Climate Dynamics*, 27(2-3):165–184, 2006.

Goosse, H., Crespin, E., Dubinkina, S., Loutre, M., Mann, M.E., Renssen, H., Sallaz-Damaz, Y., and Shindell, D. The role of forcing and internal dynamics in explaining the "medieval climate anomaly". *Climate dynamics*, 39(12):2847–2866, 2012.

Grabundzija, A. and Russo, E. Tools tell tales - climate trends changing threads in the praehistoric pannonian plain. *Documenta Praehistorica*, XLIII:301–326, 2016.

Grasselt, R., Schüttemeyer, D., Warrach-Sagi, K., Ament, F., and Simmer, C. Validation of terra-ml with discharge measurements. *Meteorologische Zeitschrift*, 17(6):763–773, 2008.

Grattan, J. Aspects of armageddon: an exploration of the role of volcanic eruptions in human history and civilization. *Quaternary International*, 151 (1):10–18, 2006.

Greenfield, H.J. A reconsideration of the secondary products revolution in south-eastern europe: on the origins and use of domestic animals for milk, wool, and traction in the central balkans. *The zooarchaeology of fats, oils, milk and dairying*, pages 14–31, 2005.

Greenfield, H.J., Chapman, J., Clason, A.T., Gilbert, A.S., Hesse, B., and Milisauskas, S. The origins of milk and wool production in the old world: a zooarchaeological perspective from the central balkans [and comments]. *Journal of Consumer Research*, 29(4):573–593, 1988.

Griggs, D.J. and Noguer, M. Climate change 2001: the scientific basis. contribution of working group i to the third assessment report of the intergovernmental panel on climate change. *Weather*, 57(8):267–269, 2002.

Gronenborn, D., Strien, H.C., Dietrich, S., and Sirocko, F. 'adaptive cycles' and climate fluctuations: a case study from linear pottery culture in western central europe. *Journal of Archaeological Science*, 51:73–83, 2014.

Hagemann, S., Machenhauer, B., Jones, R., Christensen, O.B., Déqué, M., Jacob, D., and Vidale, P.L. Evaluation of water and energy budgets in regional climate models applied over europe. *Climate Dynamics*, 23(5): 547–567, 2004.

Hansen, J., Lacis, A., Rind, D., Russell, G., Stone, P., Fung, I., Ruedy, R., and Lerner, J. Climate sensitivity: Analysis of feedback mechanisms. *Climate processes and climate sensitivity*, pages 130–163, 1984.

Härdle, W. and Simar, L. *Applied multivariate statistical analysis*, volume 22007. Springer, 2007.

Harris, I.P., Jones, P.D., Osborn, T.J., and Lister, D.H. Updated high-resolution grids of monthly climatic observations–the cru ts3. 10 dataset. *International Journal of Climatology*, 34(3):623–642, 2014.

Harrison, S.P. and Prentice, C.I. Climate and co_2 controls on global vegetation distribution at the last glacial maximum: analysis based on palaeovegetation data, biome modelling and palaeoclimate simulations. *Global Change Biology*, 9(7):983–1004, 2003.

Harrison, S.P., Bartlein, P.J., Izumi, K., Li, G., Annan, J., Hargreaves, J., Braconnot, P., and Kageyama, M. Evaluation of cmip5 palaeo-simulations to improve climate projections. *Nat. Clim. Change*, 5:735–743, 2015.

Haug, G.H., Günther, D., Peterson, L.C., Sigman, D.M., Hughen, K.A., and Aeschlimann, B. Climate and the collapse of maya civilization. *Science*, 299(5613):1731–1735, 2003.

Haxeltine, A. and Prentice, I.C. Biome3: An equilibrium terrestrial biosphere model based on ecophysiological constraints, resource availability, and competition among plant functional types. *Global Biogeochemical Cycles*, 10(4):693–709, 1996.

Haylock, M.R., Hofstra, N., Klein Tank, A.M.G., Klok, E.J., Jones, P.D., and New, M. European daily high-resolution gridded dataset of surface temperature and precipitation for 1950- 2006. *Journal of Atmospheric Science*, 112:D20119, 2008.

Hays, J.D., Imbrie, J., Shackleton, N.J., et al. Variations in the earth's orbit: pacemaker of the ice ages. American Association for the Advancement of Science, 1976.

Haywood, A.M., Valdes, P.J., Francis, J.E., and Sellwood, B.W. Global middle pliocene biome reconstruction: A data/model synthesis. *Geochemistry, Geophysics, Geosystems*, 3(12):1–18, 2002. ISSN 1525-2027. doi: 10.1029/2002GC000358. URL http://dx.doi.org/10.1029/2002GC000358. 1072.

Helbaek, H. *Notes on Evolution and History of Linum*. Jysk Arkaeologisk Selskab, 1959.

Helbaek, H. Textiles from catal huyuk. *Archaeology*, pages 39–46, 1963.

Herbert, T.D., Peterson, L.C., Lawrence, K.T., and Liu, Z. Tropical ocean temperatures over the past 3.5 million years. *Science*, 328(5985):1530–1534, 2010.

Herbig, C. and Maier, U. Flax for oil or fibre? morphometric analysis of flax seeds and new aspects of flax cultivation in late neolithic wetland settlements in southwest germany. *Vegetation history and archaeobotany*, 20(6):527–533, 2011.

Hochberg, B. *Spin span spun: fact and folklore for spinners*. B & B Hochberg, 1979.

Holden, P.B. and Edwards, N.R. Dimensionally reduced emulation of an aogcm for application to integrated assessment modelling. *Geophysical Research Letters*, 37(21), 2010.

Hollweg, H.D., Böhm, U., Fast, I., Hennemuth, B., Keuler, K., Keup-Thiel, E., Lautenschlager, M., Legutke, S., Radtke, K., Rockel, B., et al. Ensemble simulations over europe with the regional climate model clm forced with ipcc ar4 global scenarios. *M & D Technical Report*, 3:2008, 2008.

Horváth, T., Gherdán, K., Kulcsár, G., Sipos, G., and Tóth, M. An enigmatic funnel find of the somogyvár-vinkovci culture from balatonőszöd-temetői dűlő in transdanubia, hungary. *Interdisciplinaria Archaeologica. Natural Sciences in Archaeology*, 4(1):23–38, 2013.

Hoskins, B.J. and Simmons, A.J. A multi-layer spectral model and the semi-implicit method. *Quarterly Journal of the Royal Meteorological Society*, 101(429):637–655, 1975.

Hotelling, H. Canonical correlation analysis (cca). *Journal of Educational Psychology*, 1935.

Huebener, H. and Körper, J. Changes in regional potential vegetation in response to an ambitious mitigation scenario. *Journal of Environmental Protection*, 4(08):16, 2013.

Huntley, B. European vegetation history: Palaeovegetation maps from pollen data-13 000 yr bp to present. *Journal of Quaternary Science*, 5(2):103–122, 1990.

Huntley, B. and Birks, H.J.B. An atlas of past and present pollen maps for europe, 0-13,000 years ago. 1983.

Huntley, B. and Prentice, I.C. July temperatures in europe from pollen data, 6000 years before present. *Science*, 241(4866):687–690, 1988.

Huntley, B., Bartlein, P.J., and Prentice, I.C. Climatic control of the distribution and abundance of beech (fagus l.) in europe and north america. *Journal of Biogeography*, pages 551–560, 1989.

Huntley, B., Prentice, I.C., et al. Holocene vegetation and climates of europe. *Global climates since the last glacial maximum*, pages 136–168, 1993.

Hurrell, J.W. Decadal trends in the north-atlantic oscillation regional temperatures and precipitation. *Science*, 269:676–679, 1995.

Hurrell, J.W., Kushnir, Y., Ottersen, G., and Visbeck, M. An overview of the north atlantic oscillation. *Geophys. Monogr.*, 134:1–35, 2003.

Imbrie, J., Boyle, E.A., Clemens, S.C., Duffy, A., Howard, W.R., Kukla, G., Kutzbach, J., Martinson, D.G., McIntyre, A., Mix, A.C., et al. On the structure and origin of major glaciation cycles 1. linear responses to milankovitch forcing. *Paleoceanography*, 7(6):701–738, 1992.

Ineson, S., Scaife, A.A., Knight, J.R., Manners, J.C., Dunstone, N.J., Gray, L.J., and Haigh, J.D. Solar forcing of winter climate variability in the northern hemisphere. *Nature Geoscience*, 4(11):753–757, 2011.

Jackson, R.B., Canadell, J., Ehleringer, J.R., Mooney, H.A., Sala, O.E., and Schulze, E.D. A global analysis of root distributions for terrestrial biomes. *Oecologia*, 108(3):389–411, 1996.

Jacob, D., Kotlarski, S., and Kröner, N. Euro-cordex: New high resolution climate change projections for europe impact research. *Regional Environmental Change*, 14-2:563–578, 2014.

Jalut, G., Dedoubat, J.J., Fontugne, M., and Otto, T. Holocene circum-mediterranean vegetation changes: climate forcing and human impact. *Quaternary international*, 200(1):4–18, 2009.

Jansen, E., Overpeck, J., Briffa, K.R., Duplessy, J.C., Joos, F., Masson-Delmotte, V., Olago, D., Otto-Bliesner, B., Peltier, W.R., Rahmstorf, S., et al. Paleoclimate. *Climate Change 2007: The Physical Science Basis. Working Contribution of Working Group I to the Fourth Assessment Report of the Intergovernmental Panel on Climate Change*, 2007.

Jerez, S., Montavez, J.P., Gomez-Navarro, J.J., Jimenez-Guerrero, P., Jimenez, J., and Gonzalez-Rouco, J.F. Temperature sensitivity to the land-surface model in mm5 climate simulations over the iberian peninsula. *Meteorologische Zeitschrift*, 19(4):363–374, 2010.

Jerez, S., Montavez, J.P., Gomez-Navarro, J.J., Jimenez, P.A., Jimenez-Guerrero, P., Lorente, R., and Gonzalez-Rouco, J.F. The role of the land-surface model for climate change projections over the iberian peninsula. *Journal of Geophysical Research: Atmospheres*, 117(D1), 2012.

Jiang, D. and Zhang, Z. Paleoclimate modelling at the institute of atmospheric physics, chinese academy of sciences. *Advances in Atmospheric Sciences*, 23:1040–1049, 2006.

Joussaume, S. and Taylor, K.E. Status of the paleoclimate modeling intercomparison project (pmip). 92, 1995.

Jouzel, J., Masson, V., Cattani, O., Falourd, S., Stievenard, M., Stenni, B., Longinelli, A., Johnsen, S.J., Steffenssen, J.P., Petit, J.R., et al. A new 27 ky high resolution east antarctic climate record. *Geophysical Research Letters*, 28(16):3199–3202, 2001.

Jouzel, J., Masson-Delmotte, V., Cattani, O., Dreyfus, G., Falourd, S., Hoffmann, G., Minster, B., Nouet, J., Barnola, J.M., Chappellaz, J., et al. Orbital and millennial antarctic climate variability over the past 800,000 years. *science*, 317(5839):793–796, 2007.

Kaplan, J.O. Geophysical applications of vegetation modeling. Technical report, Lund University, 2001.

Kaplan, J.O., Bigelow, N.H., Prentice, I.C., Harrison, S.P., Bartlein, P.J., Christensen, T.R., Cramer, W., Matveyeva, N.V., McGuire, A.D., Murray, D.F., et al. Climate change and arctic ecosystems: 2. modeling, paleodata-model comparisons, and future projections. *Journal of Geophysical Research: Atmospheres*, 108(D19), 2003.

Karlén, W. and Kuylenstierna, J. On solar forcing of holocene climate: evidence from scandinavia. *The Holocene*, 6(3):359–365, 1996.

Keith, K. Spindle whorls, gender, and ethnicity at late chalcolithic hacinebi tepe. *Journal of Field Archaeology*, 25(4):497–515, 1998.

Kimbrough, C.K. *Spindle Whorls, Ethnoarchaeology, and the Study of Textile Production in Third Millennium BCE Northern Mesopotamia: A Methodological Approach.* ProQuest, 2006.

Kleinen, T., Brovkin, V., von Bloh, W., Archer, D., and Munhoven, G. Holocene carbon cycle dynamics. *Geophysical Research Letters*, 37(2), 2010.

Kohfeld, K.E. and Harrison, S.P. How well can we simulate past climates? evaluating the models using global palaeoenvironmental datasets. *Quaternary Science Reviews*, 19(1):321–346, 2000.

Körper, J., Wagner, S., and Cubasch, U. Downscaling a transient simulation of the Holocene with a time-slice technique. *AGU Fall Meeting Abstracts*, December 2009.

Kotlarski, S., Keuler, K., Christensen, O.B., Colette, A., Déqué, M., Gobiet, A., Goergen, K., Jacob, D., Lüthi, D., van Meijgaard, E., et al. Regional climate modeling on european scales: a joint standard evaluation of the euro-cordex rcm ensemble. *Geoscientific Model Development*, 7(4):1297–1333, 2014.

Kotova, N. and Makhortykh, S. Human adaptation to past climate changes in the northern pontic steppe. *Quaternary International*, 220(1):88–94, 2010.

Laurito, R., Lemorini, C., and Perilli, A. Making textiles at arslantepe, turkey, in the 4th and 3rd millennia bc. archaeological data and experimental archaeology. *Wool Economy in the Ancient Near East*, 17:151, 2014.

Lean, J., Rottman, G., Harder, J., and Kopp, G. Sorce contributions to new understanding of global change and solar variability. In *The Solar Radiation and Climate Experiment (SORCE)*, pages 27–53. Springer, 2005.

Leary, J. *Past mobilities: archaeological approaches to movement and mobility*. Ashgate Publishing, Ltd., 2014.

Lee, J. and Hong, S. Potential for added value to downscaled climate extremes over korea by increased resolution of a regional climate model. *Theoretical and applied climatology*, 117(3-4):667–677, 2014.

Legutke, S., Voss, R., and Klimarechenzentrum, Deutsches. Echo-g. *The Hamburg atmosphere-ocean coupled circulation model, DKRZ-Report*, (18), 1999.

Leung, L.R., Mearns, L.O., Giorgi, F., and Wilby, R.L. Regional climate research: needs and opportunities. *Bulletin of the American Meteorological Society*, 84(1):89, 2003.

Li, F., Zeng, X., Song, X., Tian, D., Shao, P., and Zhang, D. Impact of spin-up forcing on vegetation states simulated by a dynamic global vegetation model coupled with a land surface model. *Advances in Atmospheric Sciences*, 28:775–788, 2011.

Liou, K. Radiation and cloud processes in the atmosphere. theory, observation, and modeling. 1992.

Lisiecki, L.E. and Raymo, M.E. A pliocene-pleistocene stack of 57 globally distributed benthic δ18o records. *Paleoceanography*, 20(1), 2005.

Lohmann, G., Schneider, R., Jungclaus, J.H., Leduc, G., Fischer, N., Pfeiffer, M., and Laepple, T. Evaluation of eemian and holocene climate trends: Combining marine archives with climate modelling. In *Integrated Analysis of Interglacial Climate Dynamics (INTERDYNAMIC)*, pages 31–35. Springer, 2015.

Lotter, A.F. Late-glacial and holocene vegetation history and dynamics as shown by pollen and plant macrofossil analyses in annually laminated sediments from soppensee, central switzerland. *Vegetation History and Archaeobotany*, 8(3):165–184, 1999.

Loughran-Delahunt, I. A functional analysis of northwest coast spindle whorls. Master's thesis, Western Washington University, 1996.

Loutre, M. and Berger, A. Marine isotope stage 11 as an analogue for the present interglacial. *Global and planetary change*, 36(3):209–217, 2003.

Lüthi, D., Le Floch, M., Bereiter, B., Blunier, T., Barnola, J.M., Siegenthaler, U., Raynaud, D., Jouzel, J., Fischer, H., Kawamura, K., et al. High-resolution carbon dioxide concentration record 650,000–800,000 years before present. *Nature*, 453(7193):379–382, 2008.

Magny, M. and Haas, J.N. A major widespread climatic change around 5300 cal. yr bp at the time of the alpine iceman. *Journal of Quaternary Science*, 19(5):423–430, 2004.

Magny, M., Bégeot, C., Guiot, J., Marguet, A., and Billaud, Y. Reconstruction and palaeoclimatic interpretation of mid-holocene vegetation and lake-level changes at saint-jorioz, lake annecy, french pre-alps. *The Holocene*, 13(2):265–275, 2003.

Magny, M., Peyron, O., Sadori, L., Ortu, E., Zanchetta, G., Vannière, B., and Tinner, W. Contrasting patterns of precipitation seasonality during

the holocene in the south-and north-central mediterranean. *Journal of Quaternary Science*, 27(3):290–296, 2012.

Magny, M., Combourieu-Nebout, N., De Beaulieu, J.L., Bout-Roumazeilles, V., Colombaroli, D., Desprat, S., Francke, A., Joannin, S., Peyron, O., Revel, M., et al. North-south palaeohydrological contrasts in the central mediterranean during the holocene: tentative synthesis and working hypotheses. *Climate of the Past*, 9:1901–1967, 2013.

Maier, U. and Schlichtherle, H. Flax cultivation and textile production in neolithic wetland settlements on lake constance and in upper swabia (southwest germany). *Vegetation history and archaeobotany*, 20(6):567–578, 2011.

Mårtensson, L., Andersson, E.B., Nosch, M.B., and Batzer, A. Technical report, experimental archaeology, part 1, 2005-2006. 2006.

Martin-Puertas, C., Matthes, K., Brauer, A., Muscheler, R., Hansen, F., Petrick, C., Aldahan, A., Possnert, G., and van Geel, B. Regional atmospheric circulation shifts induced by a grand solar minimum. *Nature Geoscience*, 5(6):397–401, 2012.

Masson, V., Cheddadi, R., Braconnot, P., Joussaume, S., Texier, D., et al. Mid-holocene climate in europe: what can we infer from pmip model-data comparisons? *Climate Dynamics*, 15(3):163–182, 1999.

Masson-Delmotte, V., Schulz, M., Abe-Ouchi, A., Beer, J., Ganopolski, A., González Rouco, J.F., Jansen, E., Lambeck, K., Luterbacher, J., Naish, T., et al. Information from paleoclimate archives. *Climate Change 2013: The Physical Science Basis. Contribution of Working Group I to the Fifth Assessment Report of the Intergovernmental Panel on Climate change*, 2013.

Maurer, E.P., Brekke, L., Pruitt, T., and Duffy, P.B. Fine-resolution climate projections enhance regional climate change impact studies. *Eos, Transactions American Geophysical Union*, 88(47):504–504, 2007.

Mauri, A., Davis, B.A.S., Collins, P.M., and Kaplan, J.O. The influence of atmospheric circulation on the mid-holocene climate of europe: a data–model comparison. *Climate of the Past*, 10(5):1925–1938, 2014.

Mauri, A., Davis, B.A.S., Collins, P.M., and Kaplan, J.O. The climate of europe during the holocene: a gridded pollen-based reconstruction and its multi-proxy evaluation. *Quaternary Science Reviews*, 112:109–127, 2015.

May, W. and Roeckner, E. A time-slice experiment with the echam4 agcm at high resolution: the impact of horizontal resolution on annual mean climate change. *Climate Dynamics*, 17(5-6):407–420, 2001.

Mayer, S., Maule, C.F., Sobolowski, S., Christensen, O.B., Sørup, H.J.D., Sunyer, M.A., Arnbjerg-Nielsen, K., and Barstad, I. Identifying added value in high-resolution climate simulations over scandinavia. *Tellus A*, 67, 2015.

Mayewski, P.A., Rohling, E.E., Stager, J.C., Karlén, W., Maasch, K.A., Meeker, L.D., Meyerson, E.A., Gasse, F., van Kreveld, S., Holmgren, K., et al. Holocene climate variability. *Quaternary research*, 62(3):243–255, 2004.

Mazăre, P. Investigating neolithic and copper age textile production in transylvania (romania). applied methods and results. *Prehistoric, Ancient Near Eastern & Aegean Textiles and Dress*, page 1, 2014.

McCorriston, J. Textile extensification, alienation, and social stratification in ancient mesopotamia 1. *Current anthropology*, 38(4):517–535, 1997.

McCoy, F.W., Heiken, G., et al. The late-bronze age explosive eruption of thera (santorini), greece: regional and local effects. *SPECIAL PAPERS-GEOLOGICAL SOCIETY OF AMERICA*, pages 43–70, 2000.

McGuffie, K. and Henderson-Sellers, A. *A climate modelling primer*. John Wiley & Sons, 2005.

Médard, F. *Les activités de filage au Néolithique sur le Plateau suisse: analyse technique, économique et sociale*. CNRS éd., 2006.

Mercuri, A.M., Mazzanti, M.B., Torri, P., Vigliotti, L., Bosi, G., Florenzano, A., Olmi, L., and N'siala, I.M. A marine/terrestrial integration for mid-late holocene vegetation history and the development of the cultural landscape in the po valley as a result of human impact and climate change. *Vegetation History and Archaeobotany*, 21(4-5):353–372, 2012.

Milanković, M. *Kanon der Erdbestrahlung und seine Anwendung auf das Eiszeitenproblem*. na, 1941.

Miller, G.H., Geirsdóttir, Á., Zhong, Y., Larsen, D.J., Otto-Bliesner, B.L., Holland, M.M., Bailey, D.A., Refsnider, K.A., Lehman, S.J., Southon, J.R., et al. Abrupt onset of the little ice age triggered by volcanism and sustained by sea-ice/ocean feedbacks. *Geophysical Research Letters*, 39(2), 2012.

Minoura, K., Imamura, F., Kuran, U., Nakamura, T., Papadopoulos, G.A., Takahashi, T., and Yalciner, A.C. Discovery of minoan tsunami deposits. *Geology*, 28(1):59–62, 2000.

Nosch, M.L. and Michel, C. *Textile Terminologies in the Ancient Near East and Mediterranean from the third to the first millennia BC*. Citeseer, 2010.

Noti, R., van Leeuwen, J.F.N., Colombaroli, D., Vescovi, E., Pasta, S., La Mantia, T., and Tinner, W. Mid- and late-holocene vegetation and fire history at biviere di gela, a coastal lake in southern sicily, italy. *Vegetation History and Archaeobotany*, 18(5):371–387, 2009.

Odgaard, B.V. and Rasmussen, P. Origin and temporal development of macro-scale vegetation patterns in the cultural landscape of denmark. *Journal of Ecology*, 88(5):733–748, 2000.

Osborne, C.P., Mitchell, P.L., Sheehy, J.E., and Woodward, F.I. Modelling the recent historical impacts of atmospheric co2 and climate change on mediterranean vegetation. *Global Change Biology*, 6(4):445–458, 2000.

Pearson, C.L., Dale, D.S., Brewer, P.W., Kuniholm, P.I., Lipton, J., and Manning, S.W. Dendrochemical analysis of a tree-ring growth anomaly associated with the late bronze age eruption of thera. *Journal of Archaeological Science*, 36(6):1206–1214, 2009.

Pearson, R.G. and Dawson, T.P. Predicting the impacts of climate change on the distribution of species: are bioclimate envelope models useful? *Global ecology and biogeography*, 12(5):361–371, 2003.

Pérez-Obiol, R., Jalut, G., Julià, R., Pèlachs, A., Iriarte, M.J., Otto, T., and Hernández-Beloqui, B. Mid-holocene vegetation and climatic history of the iberian peninsula. *The Holocene*, 21(1):75–93, 2011.

Petit, J.R., Jouzel, J., Raynaud, D., Barkov, N.I., Barnola, J.M., Basile, I., Bender, M., Chappellaz, J., Davis, M., Delaygue, G., et al. Climate and atmospheric history of the past 420,000 years from the vostok ice core, antarctica. *Nature*, 399(6735):429–436, 1999.

Petrova, V.N. *Textile Production in the Bronze and early Iron Age in the North Balkan Region*. PhD dissertation, Sofia University, 2011.

Peyron, O., Magny, M., Goring, S., Joannin, S., Beaulieu, J.L. de, Brugiapaglia, E., Sadori, L., Garfi, G., Kouli, K., Ioakim, C., et al. Contrasting

patterns of climatic changes during the holocene across the italian peninsula reconstructed from pollen data. *Climate of the Past*, 9(3):1233–1252, 2013.

Pichler, Hans and Schiering, Wolfgang. The thera eruption and late minoan-ib destructions on crete. *Nature*, 267(5614):819–822, 1977.

Prentice, C., Guiot, J., Huntley, B., Jolly, D., and Cheddadi, R. Reconstructing biomes from palaeoecological data: a general method and its application to european pollen data at 0 and 6 ka. *Climate Dynamics*, 12 (3):185–194, 1996.

Prentice, I.C. Vegetation responses to past climatic variation. *Vegetatio*, 67 (2):131–141, 1986.

Prentice, I.C. and Jolly, D. Mid-holocene and glacial-maximum vegetation geography of the northern continents and africa. *Journal of Biogeography*, 27(3):507–519, 2000.

Prentice, I.C. and Webb III, T. Biome 6000: Reconstructing global mid-holocene vegetation patterns from palaeoecological records. *Journal of Biogeography*, 25(6):997–1005, 1998.

Prentice, I.C., Cramer, W., Harrison, S.P., Leemans, R., Monserud, R.A., and Solomon, A.M. Special paper: a global biome model based on plant physiology and dominance, soil properties and climate. *Journal of biogeography*, pages 117–134, 1992.

Prentice, I.C., Sykes, M.T., Lautenschlager, M., Harrison, S.P., Denissenko, O., and Bartlein, P. Modelling global vegetation patterns and terrestrial carbon storage at the last glacial maximum. *Global Ecology and Biogeography Letters*, pages 67–76, 1993.

Prentice, I.C., Harrison, S.P., Jolly, D., and Guiot, J. The climate and biomes of europe at 6000yr bp: comparison of model simulations and pollen-based reconstructions. *Quaternary Science Reviews*, 17(6):659–668, 1998.

Prentice, I.C., Harrison, S.P., and Bartlein, P.J. Global vegetation and terrestrial carbon cycle changes after the last ice age. *New Phytologist*, 189 (4):988–998, 2011.

Prömmel, K., Geyer, B., Jones, J.M., and Widmann, M. Evaluation of the skill and added value of a reanalysis-driven regional simulation for alpine temperature. *International Journal of Climatology*, 30(5):760–773, 2010.

Prömmel, K., Cubasch, U., and Kaspar, F. A regional climate model study of the impact of tectonic and orbital forcing on african precipitation and vegetation. *Palaeogeography, Palaeoclimatology, Palaeoecology*, 369:154–162, 2013.

Ramaswamy, V., Boucher, O., Haigh, J., Hauglustaine, D., Haywood, J., Myhre, G., Nakajima, T., Shi, G., Solomon, S., Betts, R.E., et al. Radiative forcing of climate change. Technical report, Pacific Northwest National Laboratory (PNNL), Richland, WA (US), 2001.

Rampino, M.R. and Self, S. Historic eruptions of tambora (1815), krakatau (1883), and agung (1963), their stratospheric aerosols, and climatic impact. *Quaternary Research*, 18(2):127–143, 1982.

Randall, D.A., Wood, R.A., Bony, S., Colman, R., Fichefet, T., Fyfe, J., Kattsov, V., Pitman, A., Shukla, J., Srinivasan, J., et al. Climate models and their evaluation. In *Climate change 2007: The physical science basis. Contribution of Working Group I to the Fourth Assessment Report of the IPCC (FAR)*, pages 589–662. Cambridge University Press, 2007.

Rast-Eicher, A. Bast before wool: the first textiles. *Hallstatt Textiles: Technical Analysis, Scientific Investigation and Experiment on Iron Age Textiles*, pages 117–131, 2005.

Reed, K. Agricultural change in copper age croatia (ca. 4500-2500 cal bc)? *Archaeological and Anthropological Sciences*, pages 1–21, 2016.

Renssen, H., Isarin, R.F.B., Jacob, D., Podzun, R., and Vandenberghe, J. Simulation of the younger dryas climate in europe using a regional climate model nested in an agcm: preliminary results. *Global and Planetary Change*, 30(1):41–57, 2001.

Riede, F. Climate models: use archaeology record. *Nature*, 513(7518):315–315, 2014.

Rind, D., Shindell, D., Perlwitz, J., Lerner, J., Lonergan, P., Lean, J., and McLinden, C. The relative importance of solar and anthropogenic forcing of climate change between the maunder minimum and the present. *Journal of Climate*, 17(5):906–929, 2004.

Ritter, B. and Geleyn, J.F. A comprehensive radiation scheme for numerical weather prediction models with potential applications in climate simulations. *Monthly Weather Review*, 120(2):303–325, 1992.

Ritz, S.P., Stocker, T.F., and Joos, F. A coupled dynamical ocean-energy balance atmosphere model for paleoclimate studies. *Journal of Climate*, 24(2):349–375, 2011.

Roberts, N., Eastwood, W.J., Kuzucuoğlu, C., Fiorentino, G., and Caracuta, V. Climatic, vegetation and cultural change in the eastern mediterranean during the mid-holocene environmental transition. *The Holocene*, 21(1): 147–162, 2011.

Rockel, B. and Geyer, B. The performance of the regional climate model clm in different climate regions, based on the example of precipitation. *Meteorologische Zeitschrift*, 17(4):487–498, 2008.

Rockner, E., Arpe, K., Bengtsson, L., Christoph, M., Claussen, M., DÜMENIL, L., Esch, M., Giorgetta, M., Schlese, U., and Schulzweida, U. The atmospheric general circulation model echam-4: Model description and simulation of present day climate, mpireport no. 218, mpi für meteorologie, hamburg, 1996.

Roeckner, E., Bäuml, G., Bonaventura, L., Brokopf, R., Esch, M., Giorgetta, M., Hagemann, S., Kirchner, I., Kornblueh, L., Manzini, E., et al. The atmospheric general circulation model echam 5. part i: Model description. 2003.

Rohling, E.J., Braun, K., Grant, K., Kucera, M., Roberts, A.P., Siddall, M., and Trommer, G. Comparison between holocene and marine isotope stage-11 sea-level histories. *Earth and Planetary Science Letters*, 291(1):97–105, 2010.

Rokou, V. *Ta vyrsodepseia tōn Iōanninōn: apo to ergastērio sto ergostasio tēs viotechnikēs polēs*. Hellēnika Grammata, 2004.

Ruddiman, W.F. The anthropogenic greenhouse era began thousands of years ago. *Climatic change*, 61(3):261–293, 2003.

Rummukainen, M. Added value in regional climate modeling. *Wiley Interdisciplinary Reviews: Climate Change*, 7(1):145–159, 2016.

Russo, E. and Cubasch, U. Mid-to-late holocene temperature evolution and atmospheric dynamics over europe in regional model simulations. *Climate of the Past*, 12(8):1645–1662, 2016.

Sakamoto, K., Tsujino, H., Nishikawa, S., Nakano, H., and Motoi, T. Dynamics of the coastal oyashio and its seasonal variation in a high-resolution

western north pacific ocean model. *Journal of Physical Oceanography*, 40 (6):1283–1301, 2010.

Salzmann, U., Haywood, A.M., Lunt, D.J., Valdes, P.J., and Hill, D.J. A new global biome reconstruction and data-model comparison for the middle pliocene. *Global Ecology and Biogeography*, 17(3):432–447, 2008.

Schibler, J., Jacomet, S., Hüster-Plogmann, H., and Brombacher, C. Economic crash in the 37th and 36th centuries cal. bc in neolithic lake shore sites in switzerland: Postpalaeolithic europe i. *Anthropozoologica*, (25-26): 553–570, 1997.

Schick, T. Nahal hemar cave: cordage, basketry and fabrics. *Atiqot*, 18: 31–43, 1988.

Schimanke, S., Meier, H.E.M., Kjellström, E., Strandberg, G., and Hordoir, R. The climate in the baltic sea region during the last millennium simulated with a regional climate model. *Climate of the Past*, 8(5):1419–1433, 2012.

Seneviratne, S.I., Lüthi, D., Litschi, M., and Schär, C. Land–atmosphere coupling and climate change in europe. *Nature*, 443(7108):205–209, 2006.

Seneviratne, S.I., Corti, T., Davin, E.L., Hirschi, M., Jaeger, E.B., Lehner, I., Orlowsky, B., and Teuling, A.J. Investigating soil moisture–climate interactions in a changing climate: A review. *Earth-Science Reviews*, 99 (3):125–161, 2010.

Shakun, J.D., Clark, P.U., He, F., Marcott, S.A., Mix, A.C., Liu, Z., Otto-Bliesner, B., Schmittner, A., and Bard, E. Global warming preceded by increasing carbon dioxide concentrations during the last deglaciation. *Nature*, 484(7392):49–54, 2012.

Sherratt, A. *Plough and pastoralism: aspects of the secondary products revolution*. Cambrdge University Press, 1981.

Sherratt, A. *Economy and society in prehistoric Europe: changing perspectives*. Edinburgh University Press Edinburgh, 1997.

Sherratt, A. La traction animale et la transformation de l'europe néolithique. *Premiers Chariots, Premiers Araires. La Traction Animale En Europe Pendant Les Ive Et Iiie Millénaires Avant Notre Ére*, pages 329–360, 2006.

Siegenthaler, U., Monnin, E., Kawamura, K., Spahni, R., Schwander, J., Stauffer, B., Stocker, T.F., Barnola, J., and Fischer, H. Supporting evidence from the epica dronning maud land ice core for atmospheric co2 changes during the past millennium. *Tellus B*, 57(1):51–57, 2005.

Solanki, S.K., Usoskin, I.G., Kromer, B., Schüssler, M., and Beer, J. Unusual activity of the sun during recent decades compared to the previous 11,000 years. *Nature*, 431(7012):1084–1087, 2004.

Solomon, S. *Climate change 2007-the physical science basis: Working group I contribution to the fourth assessment report of the IPCC*, volume 4. Cambridge University Press, 2007.

Starz, M., Lohmann, G., and Knorr, G. Dynamic soil feedbacks on the climate of the mid-holocene and the last glacial maximum. *Climate of the Past*, 9:2717–2730, 2013.

Stenni, B., Buiron, D., Frezzotti, M., Albani, S., Barbante, C., Bard, E., Barnola, J.M., Baroni, M., Baumgartner, M., Bonazza, M., et al. Expression of the bipolar see-saw in antarctic climate records during the last deglaciation. *Nature Geoscience*, 4(1):46–49, 2011.

Stephenson, D.B. and Held, I.M. Gcm response of northern winter stationary waves and storm tracks to increasing amounts of carbon dioxide. *Journal of climate*, 6(10):1859–1870, 1993.

Stocker, T.F., Qin, D., Plattner, G.K., Tignor, M., Allen, S.K., Boschung, J., Nauels, A., Xia, Y., Bex, V., and Midgley, P.M. Climate change 2013: The physical science basis. Technical report, 2013.

Stothers, R.B. Volcanic eruptions and climate change. In *Encyclopedia of Paleoclimatology and Ancient Environments*, pages 976–979. Springer, 2009.

Strandberg, G., Kjellström, E., Poska, A., Wagner, S., Gaillard, M.J., Trondman, A.K., Mauri, A., Kaplan, J.O., Birks, H.J.B., Bjune, A.E., et al. Regional climate model simulations for europe at 6 and 0.2 k bp: sensitivity to changes in anthropogenic deforestation. *Climate of the Past*, (10): 661–680, 2014.

Tanţău, I., Feurdean, A., de Beaulieu, J.L., Reille, M., and Fărcaş, S. Holocene vegetation history in the upper forest belt of the eastern romanian carpathians. *Palaeogeography, Palaeoclimatology, Palaeoecology*, 309 (3):281–290, 2011.

Tapiador, F.J. and Sánchez, E. Changes in the european precipitation climatologies as derived by an ensemble of regional models. *Journal of Climate*, 21(11):2540–2557, 2008.

Tapiador, F.J., Angelis, C.F., Viltard, N., Cuartero, F., and De Castro, M. On the suitability of regional climate models for reconstructing climatologies. *Atmospheric Research*, 101(3):739–751, 2011.

Texier, D., De Noblet, N., Harrison, S.P., Haxeltine, A., Jolly, D., Joussaume, S., Laarif, F., Prentice, I.C., and Tarasov, P. Quantifying the role of biosphere-atmosphere feedbacks in climate change: coupled model simulations for 6000 years bp and comparison with palaeodata for northern eurasia and northern africa. *Climate Dynamics*, 13(12):865–881, 1997.

Tiedtke, M. A comprehensive mass flux scheme for cumulus parameterization in large-scale models. *Monthly Weather Review*, 117(8):1779–1800, 1989.

Torma, C., Giorgi, F., and Coppola, E. Added value of regional climate modeling over areas characterized by complex terrain—precipitation over the alps. *Journal of Geophysical Research: Atmospheres*, 120(9):3957–3972, 2015.

Tóth, M., Magyari, E.K., Brooks, S.J., Braun, M., Buczkó, K., Bálint, M., and Heiri, O. A chironomid-based reconstruction of late glacial summer temperatures in the southern carpathians (romania). *Quaternary Research*, 77(1):122–131, 2012.

Trondman, A.K., Gaillard, M.J., Mazier, F., Sugita, S., Fyfe, R., Nielsen, A.B., Twiddle, C., Barratt, P., Birks, H.J.B., Bjune, A.E., et al. Pollen-based quantitative reconstructions of holocene regional vegetation cover (plant-functional types and land-cover types) in europe suitable for climate modelling. *Global change biology*, 21(2):676–697, 2015.

Tselioudis, G., Douvis, C., and Zerefos, C. Does dynamical downscaling introduce novel information in climate model simulations of precipitation change over a complex topography region? *International Journal of Climatology*, 32(10):1572–1578, 2012.

Vakirtzi, S., Koukouli-Chryssanthaki, C., and Papadopoulos, S. Spindle whorls from two prehistoric settlements on thassos, north aegean. *Prehistoric, Ancient Near Eastern & Aegean Textiles and Dress*, page 43, 2014.

Vallinheimo, V. *Das Spinnen in Finnland unter besonderer Berücksichtigung finnischer Tradition*, volume 11. Suomen muinaismuistoyhdistys, 1956.

Van de Noort, R. Conceptualising climate change archaeology. *Antiquity*, 85 (329):1039–1048, 2011.

Varekamp, J.C., Luhr, J.F., and Prestegaard, K.L. The 1982 eruptions of el chichón volcano (chiapas, mexico): character of the eruptions, ash-fall deposits, and gasphase. *Journal of Volcanology and Geothermal Research*, 23(1):39–68, 1984.

Verhecken, A. The moment of inertia: a parameter for the functional classification of worldwide spindle-whorls from all periods. In *North European Symposium for Archaeological Textiles X, Oxford–Oakville: Oxbow Books*, pages 257–270, 2010.

Vigne, J.D. and Helmer, D. Was milk a "secondary product" in the old world neolithisation process? its role in the domestication of cattle, sheep and goats. *Anthropozoologica*, 42(2):9–40, 2007.

von Storch, H. and Zwiers, F.W. *Statistical Analysis in Climate Research*. Cambridge University Press, 1995.

Von Storch, H., Zorita, E., Jones, J.M., Dimitriev, Y., González-Rouco, F., and Tett, S.F.B. Reconstructing past climate from noisy data. *Science*, 306(5696):679–682, 2004.

Wagner, S., Widmann, M., Jones, J., Haberzettl, T., Lücke, A., Mayr, C., Ohlendorf, C., Schäbitz, F., and Zolitschka, B. Transient simulations, empirical reconstructions and forcing mechanisms for the mid-holocene hydrological climate in southern patagonia. *Climate Dynamics*, 29(4):333–355, 2007.

Wagner, S., Fast, I., and Kaspar, F. Comparison of 20th century and preindustrial climate over south america in regional model simulations. *Climate of the Past*, 8(5):1599–1620, 2012.

Wang, Y.M., Lean, J.L., and Sheeley Jr, N.R. Modeling the sun's magnetic field and irradiance since 1713. *The Astrophysical Journal*, 625(1):522, 2005.

Wanner, H., Beer, J., Bütikofer, J., Crowley, T.J., Cubasch, U., Flückiger, J., Goosse, H., Grosjean, M., Joos, F., Kaplan, J.O., et al. Mid-to late holocene climate change: an overview. *Quaternary Science Reviews*, 27 (19):1791–1828, 2008.

Wanner, H., Solomina, O., Grosjean, M., Ritz, S.P., and Jetel, M. Structure and origin of holocene cold events. *Quaternary Science Reviews*, 30(21): 3109–3123, 2011.

Watanabe, O., Jouzel, J., Johnsen, S., Parrenin, F., Shoji, H., and Yoshida, N. Homogeneous climate variability across east antarctica over the past three glacial cycles. *Nature*, 422(6931):509–512, 2003.

Watterson, I.G., Bathols, J., and Heady, C. What influences the skill of climate models over the continents? *Bulletin of the American Meteorological Society*, 95(5):689–700, 2014.

Webb III, T. Is vegetation in equilibrium with climate? how to interpret late-quaternary pollen data. *Vegetatio*, 67(2):75–91, 1986.

Weiss, H. Late third millennium abrupt climate change and social collapse in west asia and egypt. In *Third millennium BC climate change and Old World collapse*, pages 711–723. Springer, 1997.

Weiss, H. and Bradley, R.S. What drives societal collapse? *Science*, 291 (5504):609–610, 2001.

Weninger, B., Clare, L., Rohling, E.J., Bar-Yosef, O., Böhner, U., Budja, M., Bundschuh, M., Feurdean, A., Gebel, H., Jöris, O., et al. The impact of rapid climate change on prehistoric societies during the holocene in the eastern mediterranean. *Documenta praehistorica*, 36(7):59, 2009.

Wigley, T.M.L., Ingram, M.J., and Farmer, G. *Climate and history: studies in past climates and their impact on man*. CUP Archive, 1985.

Wilby, R.L., Wigley, T.M.L., Conway, D., Jones, P.D., Hewitson, B.C., Main, J., and Wilks, D.S. Statistical downscaling of general circulation model output: a comparison of methods. *Water resources research*, 34(11):2995–3008, 1998.

Wilby, R.L., Charles, S.P., Zorita, E., Timbal, B., Whetton, P., and Mearns, L.O. Guidelines for use of climate scenarios developed from statistical downscaling methods. 2004.

Wilks, D.S. *Statistical Methods in the Atmospheric Sciences*. International Geophysics Series, Academic Press, 1995.

Wohlfahrt, J., Harrison, S.P., and Braconnot, P. Synergistic feedbacks between ocean and vegetation on mid-and high-latitude climates during the mid-holocene. *Climate Dynamics*, 22(2-3):223–238, 2004.

Wolff, J., Maier-Reimer, E., and Legutke, S. The hamburg primitive equation model hope. In *Technical Report No. 8*. Germany Climate Computer Centre (DKRZ) Hamburg, 1997.

Zhang, D.D., Brecke, P., Lee, H.F., He, Y., and Zhang, J. Global climate change, war, and population decline in recent human history. *Proceedings of the National Academy of Sciences*, 104(49):19214–19219, 2007.

Zhang, Q., Sundqvist, H., Moberg, A., Körnich, H., Nilsson, J., and Holmgren, K. Climate change between the mid and late holocene in northern high latitudes: part 2: model-data comparisons. *Climate of the Past*, 6: 609–626, 2010.

Zhao, D. Performance of regional integrated environment modeling system (riems) in precipitation simulations over east asia. *Climate dynamics*, 40 (7-8):1767–1787, 2013.

Zveryeav, I. and Allan, R. Summertime precipitation variability over europe and its links to atmospheric dynamics and evaporation. *Journal of Geophysical Research*, 115:D12102, 2010.